Habilitationsschrift
zur
Erlangung der Venia legendi
für das Fach Physik
der
Ruprecht–Karls–Universität
Heidelberg

vorgelegt von
Werner Rodejohann
aus Erwitte

2021

New Neutrino Interactions in New and Old Experiments

Habilitation summary
by
Werner Rodejohann

October 2021

Contents

Chapter 1

Introduction

The present habilitation summary deals with effects of **new neutrino physics** in existing and planed experiments. While neutrinos are an established fact of the Standard Model of particle physics (SM), the discovery that they are massive remains the only physics beyond the Standard Model (BSM) that is testable in the lab, or put differently, the only laboratory-based proof of BSM physics.

Neutrinos are very special particles which have led again and again to surprising and important discoveries, a number of which were recognized with Noble prizes. Neutrinos were theoretically invented in 1930 by Pauli to preserve energy-momentum conservation and their first experimental detection occurred in 1956. Later it was found that three versions (flavors) exist, which was again a major discovery. Next, solar and atmospheric neutrinos showed oscillations, which is a quantum mechanical effect on truly macroscopic scales, something usually only relevant on atomic scales. Neutrinos were found to have very tiny masses, which is so far the only solid evidence for particle physics beyond the Standard Model and has important consequences for theory, the dynamics of stars, or the Universe as a whole. There are numerous other topics where it is already known that neutrinos play an important role, but there are also very good reasons and maybe even indications that more surprising results may show up in the future.

While neutrino physics has entered the precision era, the values of all its standard parameters, its nature under self-conjugacy, the origin of its mass, its flavor distribution and its interactions with SM and BSM particles is far from settled or even completely unknown. Moreover, new windows open up in the field, the most recent example being coherent elastic neutrino-nucleus scattering, allowing completely new studies. The focus of this work lies on economical scenarios of new neutrino physics, which denotes the introduction of a single new particle. This particle can be either a scalar, a vector or a fermion. Illustrative examples for each case are given, including always an extension to the quark sector. Such new physics can be tested with a variety of experimental approaches, from low to high energy. Pure neutrino experiments can be used, or facilities with other main goals. Different flavors are used, and the time scale of searches is current, intermediate or far future. Moreover, as neutrinos are crucial for many astrophysical and cosmological processes, constraints arise from those sources. This richness and broadness of phenomenology is connected to the richness and broadness of neutrino physics.

Parameter	Main method(s)	Source(s)	Status
θ_{12}	Oscillations	solar, reactor	known
θ_{23}	Oscillations	atmospheric, accelerator	known
θ_{13}	Oscillations	reactor, accelerator	known
δ_{CP}	Oscillations	accelerator	hints
α, β	Rare processes	double beta decay	unknown
Δm^2_{21}	Oscillations	reactor, solar	known
$\lvert\Delta m^2_{31}\rvert$	Oscillations	reactor, accelerator, atmospheric	known
Ordering (sgn Δm^2_{31})	Oscillations	reactor, accelerator, atmospheric	hints
$m_{1,2,3}$	Kinematics	β decay, cosmology	limits

Table 1.1: Standard neutrino parameters, the main method(s) to determine them, the most important source(s) for the determination and the current status. Except the phases α and β (for the case of Majorana neutrinos), all unknown parameters are expected to be determined within the next 10 years.

1.1 Neutrino Physics

More often than not, the particles considered here are present in scenarios related to neutrino physics, or BSM frameworks in general:

- New scalars may be connected to mass generation of neutrinos, which is expected to be different from the one of the other SM fermions. Examples are additional Higgs multiplets or (Pseudo)Goldstone bosons of global symmetries related to neutrinos;
- New vectors may be connected to new flavor-dependent or -independent gauge symmetries related to the masses and flavor structure of neutrinos and other particles of and beyond the SM. Examples are $B - L$ or $L_\mu - L_\tau$;
- New fermions may be related to neutrino mass generation, and may be part of Dark Matter (DM) in addition to that. Examples are keV-scale fermions as warm dark matter, or TeV-scale Weakly Interacting Massive Particle (WIMP)-like stable sterile neutrinos.

The last 25 years saw the establishment of a standard paradigm: 3 massive neutrinos mixing with each other. As all SM fermions, neutrinos come in three generations, that is, there are three flavor states ν_e, ν_μ and ν_τ, which live together with their charged lepton counterparts e^-, μ^- and τ^- in weak interaction doublets. The neutrinos have well-defined quantum numbers under the SM gauge symmetries, which fix their interactions with the W and Z bosons of the electroweak interactions. Diagonalising the mass matrices of leptons and neutrinos yields the three known charged lepton masses. In addition to those, three neutrino masses $m_{1,2,3}$ are present, corresponding to the mass states $\nu_{1,2,3}$. Another consequence of diagonalisation is the existence of the PMNS matrix denoted here by U, which is the analogue of the CKM matrix in the quark sector; U implies, for instance,

	$T^{0\nu}_{1/2}$ ($\times 10^{25}$ yr)	$m_{\beta\beta}$ (eV)	**Experiment**
^{76}Ge	> 18	$< 0.08 - 0.18$	GERDA [1]
	> 2.7	$< 0.20 - 0.43$	Majorana Demonstrator [2]
^{82}Se	$> 3.5 \times 10^{-1}$	$< 0.31 - 0.64$	CUPID-0 [3]
^{100}Mo	$> 1.5 \times 10^{-1}$	$< 0.31 - 0.54$	CUPID-Mo [4]
^{130}Te	> 2.2	$< 0.09 - 0.31$	CUORE [5]
^{136}Xe	> 10.7	$< 0.06 - 0.17$	KamLAND-Zen [6]
	> 3.5	$< 0.09 - 0.29$	EXO-200 [7]
^{3}H	β-endpoint measurement	$m_\beta < 0.8$	KATRIN [8]
	cosmology	$\Sigma < 0.12 - 0.54$	Planck [9]

Table 1.2: Comparison of current limits on neutrino mass from the main approaches double beta decay (90% C.L.), beta decay (90% C.L.) and cosmology (95% C.L.). For the latter, mass bounds from two data set combinations ("Planck TT+lowE" and "Planck TT,TE,EE+lowE +lensing+BAO") are given.

that the electron-neutrino is a linear combination of the three mass states, $\nu_e = U_{ei}\nu_i$:

$$U = \begin{pmatrix} 1 & 0 & 0 \\ 0 & c_{23} & s_{23} \\ 0 & -s_{23} & c_{23} \end{pmatrix} \begin{pmatrix} c_{13} & 0 & s_{13}e^{-i\delta_{\mathrm{CP}}} \\ 0 & 1 & 0 \\ -s_{13}e^{i\delta_{\mathrm{CP}}} & 0 & c_{13} \end{pmatrix} \begin{pmatrix} c_{12} & s_{12} & 0 \\ -s_{12} & c_{12} & 0 \\ 0 & 0 & 1 \end{pmatrix}. \tag{1.1}$$

Here $c_{ij} = \cos\theta_{ij}$ and $s_{ij} = \sin\theta_{ij}$. For vanishing neutrino masses the PMNS matrix would be the identity matrix. The PMNS matrix contains three mixing angles, θ_{12}, θ_{13} and θ_{23}, plus a phase δ_{CP} responsible for CP violation. In case neutrinos are their own antiparticles, i.e. if they are Majorana fermions, two additional phases exist (denoted for instance by α and β), which only appear in lepton-number violating processes, and in particular do not influence neutrino oscillations. They can be included via multiplying U with $P = \mathrm{diag}(e^{i\alpha}, e^{i\beta}, 1)$ from the right. The standard parameters are summarized in Tab. 1.1, together with the main methods and neutrino sources to determine them. The current knowledge on the parameters of neutrino physics is shown in Tabs. 1.2 and 1.3, as well as Fig. 1.1.

One subtlety exists here, namely it is not clear whether the mass state that is mostly composed of the first-generation electron neutrino state is the heaviest or the lightest one. This is the question of the mass ordering, which can be normal or inverted. In the established notation of the field the normal mass ordering corresponds to $m_3 > m_2 > m_1$, or $\Delta m^2_{31} > 0$, while the inverted mass ordering corresponds to $m_2 > m_1 > m_3$, or $\Delta m^2_{31} < 0$. Here the notation normal and inverted compares the situation to the quark sector, in which the mass state which is mostly composed of the first-generation up-quark

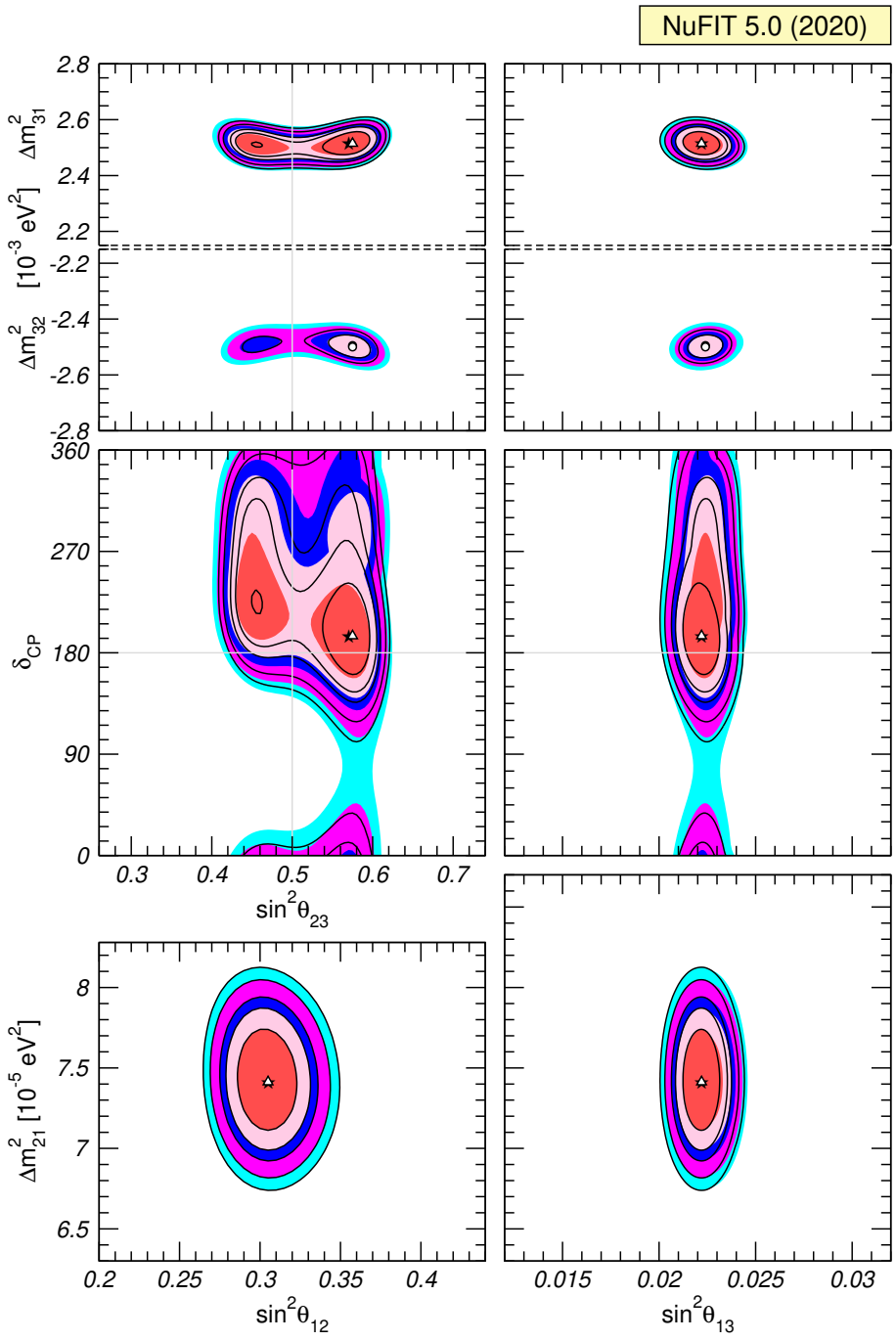

Figure 1.1: Allowed values of the oscillation parameters at 1σ, 90%, 2σ, 99%, 3σ C.L. (2 dof). Each panel shows the two-dimensional projection after marginalisation with respect to the undisplayed parameters. In the lower 4 panels, the results are minimized with respect to the mass ordering. Colored regions (black contour curves) do not (do) include Super-Kamiokande atmospheric neutrino data. Taken from [10, 11].

NuFIT 5.0 (2020)

		Normal Ordering (best fit)		Inverted Ordering ($\Delta\chi^2 = 2.7$)	
		bfp $\pm 1\sigma$	3σ range	bfp $\pm 1\sigma$	3σ range
without SK atmospheric data	$\sin^2\theta_{12}$	$0.304^{+0.013}_{-0.012}$	$0.269 \to 0.343$	$0.304^{+0.013}_{-0.012}$	$0.269 \to 0.343$
	$\theta_{12}/^\circ$	$33.44^{+0.78}_{-0.75}$	$31.27 \to 35.86$	$33.45^{+0.78}_{-0.75}$	$31.27 \to 35.87$
	$\sin^2\theta_{23}$	$0.570^{+0.018}_{-0.024}$	$0.407 \to 0.618$	$0.575^{+0.017}_{-0.021}$	$0.411 \to 0.621$
	$\theta_{23}/^\circ$	$49.0^{+1.1}_{-1.4}$	$39.6 \to 51.8$	$49.3^{+1.0}_{-1.2}$	$39.9 \to 52.0$
	$\sin^2\theta_{13}$	$0.02221^{+0.00068}_{-0.00062}$	$0.02034 \to 0.02430$	$0.02240^{+0.00062}_{-0.00062}$	$0.02053 \to 0.02436$
	$\theta_{13}/^\circ$	$8.57^{+0.13}_{-0.12}$	$8.20 \to 8.97$	$8.61^{+0.12}_{-0.12}$	$8.24 \to 8.98$
	$\delta_{\rm CP}/^\circ$	195^{+51}_{-25}	$107 \to 403$	286^{+27}_{-32}	$192 \to 360$
	$\frac{\Delta m^2_{21}}{10^{-5}\ \text{eV}^2}$	$7.42^{+0.21}_{-0.20}$	$6.82 \to 8.04$	$7.42^{+0.21}_{-0.20}$	$6.82 \to 8.04$
	$\frac{\Delta m^2_{3\ell}}{10^{-3}\ \text{eV}^2}$	$+2.514^{+0.028}_{-0.027}$	$+2.431 \to +2.598$	$-2.497^{+0.028}_{-0.028}$	$-2.583 \to -2.412$
		Normal Ordering (best fit)		Inverted Ordering ($\Delta\chi^2 = 7.1$)	
		bfp $\pm 1\sigma$	3σ range	bfp $\pm 1\sigma$	3σ range
with SK atmospheric data	$\sin^2\theta_{12}$	$0.304^{+0.012}_{-0.012}$	$0.269 \to 0.343$	$0.304^{+0.013}_{-0.012}$	$0.269 \to 0.343$
	$\theta_{12}/^\circ$	$33.44^{+0.77}_{-0.74}$	$31.27 \to 35.86$	$33.45^{+0.78}_{-0.75}$	$31.27 \to 35.87$
	$\sin^2\theta_{23}$	$0.573^{+0.016}_{-0.020}$	$0.415 \to 0.616$	$0.575^{+0.016}_{-0.019}$	$0.419 \to 0.617$
	$\theta_{23}/^\circ$	$49.2^{+0.9}_{-1.2}$	$40.1 \to 51.7$	$49.3^{+0.9}_{-1.1}$	$40.3 \to 51.8$
	$\sin^2\theta_{13}$	$0.02219^{+0.00062}_{-0.00063}$	$0.02032 \to 0.02410$	$0.02238^{+0.00063}_{-0.00062}$	$0.02052 \to 0.02428$
	$\theta_{13}/^\circ$	$8.57^{+0.12}_{-0.12}$	$8.20 \to 8.93$	$8.60^{+0.12}_{-0.12}$	$8.24 \to 8.96$
	$\delta_{\rm CP}/^\circ$	197^{+27}_{-24}	$120 \to 369$	282^{+26}_{-30}	$193 \to 352$
	$\frac{\Delta m^2_{21}}{10^{-5}\ \text{eV}^2}$	$7.42^{+0.21}_{-0.20}$	$6.82 \to 8.04$	$7.42^{+0.21}_{-0.20}$	$6.82 \to 8.04$
	$\frac{\Delta m^2_{3\ell}}{10^{-3}\ \text{eV}^2}$	$+2.517^{+0.026}_{-0.028}$	$+2.435 \to +2.598$	$-2.498^{+0.028}_{-0.028}$	$-2.581 \to -2.414$

Table 1.3: Oscillation parameters from a fit of the global data as of July 2020, version NuFit-5.0. The results in the lower (upper) sections are obtained (without) including atmospheric neutrino data from Super-Kamiokande. Note that $\Delta m^2_{3\ell} = \Delta m^2_{31} > 0$ for NO and $\Delta m^2_{3\ell} = \Delta m^2_{32} < 0$ for IO. Taken from Ref. [10, 11].

is the lightest one.

Apart from this standard paradigm of three massive (Majorana) neutrinos mixing with each other, more neutrino states may exist, which must be sterile, i.e. not participating in SM interactions except for via mixing with the active states. Additional parameters such as magnetic moments may exist, or neutrinos may participate in new interactions beyond the SM. Furthermore, the mechanism that generates neutrino mass may come with new particles, energy states and parameters, whose main methods of determination needs to be discussed for each model individually. The presence of such particles is what this thesis is about.

Regarding neutrino masses, we have two options, Dirac or Majorana neutrinos. The former imply the conservation of lepton number, which in the SM is an accidental global symmetry. Typically, additional symmetries are necessary in theories beyond the SM to keep lepton number conserved. The situation resembles that for dark matter, where often a symmetry that stabilises the dark matter particle needs to be introduced. In general, the violation of lepton and/or baryon number is crucial for our ideas for the generation of the baryon asymmetry of the Universe. Moreover, Grand Unified Theories do generically predict Majorana neutrinos, e.g. the violation of lepton number. This is on equal footing with the prediction of baryon number violation (that is, proton decay); therefore, baryon number and lepton number violation are not separate questions. The Majorana nature of light neutrinos necessarily implies further terms in the overall particle physics Lagrangian, and in particular implies new particles, parameters and energy scales. Determining those, also with the help of experiments beyond pure neutrino physics, such as direct searches at colliders or via lepton flavor violating processes, may teach us valuable lessons on the correct BSM approach. Eventually, the question of the neutrino nature needs to be answered experimentally, via observation (or perhaps non-observation) of neutrinoless double beta decay ($0\nu\beta\beta$).

1.2 Neutrinos and New Particles

Where do tiny neutrino masses come from? The most simple possibility would be to add right-handed neutrinos to the SM particle content, and thus create a Dirac mass term m_D for neutrinos in analogy to all other fermions of the SM. The corresponding Yukawa coupling would be at least six orders of magnitude smaller than the one for the electron. While this is the same hierarchy as for the third-generation top quark and the first-generation electron Yukawa, the point is that this strong hierarchy affects particles in the same $SU(2)_L$ doublet, for each generation: up- and down quarks have only a mild, if any, mass hierarchy, while electrons and electron neutrinos have a mass ratio of 10^{-6} or below.

Therefore, some universal suppression mechanism is required. Connected to that, the gauge symmetries of the SM allow a bare mass term for the right-handed neutrinos, M_R. "Bare" denotes here a mass term not connected to the SM Higgs mechanism, which gives mass to all other particles in the SM. This mass term is thus not bounded from above by perturbativity of couplings, thus can be arbitrarily high. Moreover, it is a Majorana mass term. Via the coupling of the right-handed neutrinos with the left-handed ones through the Dirac mass, the Majorana character is passed to the light neutrinos. In addition, light neutrinos have a mass given by m_D^2/M_R and thus are suppressed for all three generations. This is the type I seesaw mechanism [12–16]. The lessons of this most simple mechanism are that

(i) new particles exist, in this case, right-handed neutrinos.

(ii) a new energy scale exists. Recall that the SM possesses only a single energy scale.

(iii) a new property exists, in this case the violation of lepton number due to the Majorana nature of the light neutrinos.

(iv) the mass of the light neutrinos is inversely proportional to the energy scale related to their origin.

These lessons are almost generic for the countless mechanisms that have been proposed to generate neutrino mass. These features allows testing and distinguishing the mechanisms. In addition, the new particles often come with additional interactions of their own, for instance caused by a gauge symmetry related to the difference of baryon minus lepton number ($B-L$), $L_\mu - L_\tau$, left-right symmetry, etc. Theories that gauge the difference of baryon and lepton number $B-L$ are attractive as this charge is exactly conserved in the SM [17–22]. The symmetry is anomaly-free and can thus be consistently gauged, if three right-handed neutrinos are added to the particle content, providing therefore motivation for the seesaw mechanism. The difference $B-L$ is also part of many other BSM theories, for instance in left-right symmetric models [16, 23–28]. Another anomaly-free example in the presence of right-handed neutrinos is difference of muon and tau flavors [29–32], $L_\mu - L_\tau$, which provides automatically an attractive flavor scheme for the lepton sector.

For the type I seesaw, the naive picture implies that $M_R \sim m_D^2/m_\nu \sim v^2/m_\nu \gtrsim 10^{14}$ GeV, and a mixing of the right-handed neutrinos with the charged current of order $m_D/M_R \simeq \sqrt{m_\nu/M_R}$, which implies little hope of testability. However, m_D and M_R are matrices, allowing for cancellations. Motivational values for lower scales are keV for warm dark matter or TeV for cold dark matter. In addition, simple variants and modifications of the type I seesaw exist, that allow even more flexibility. For instance the type II [17, 28, 33–36] or III mechanisms [37] are other options, which introduce scalar and fermion triplets, respectively. More involved scenarios such as inverse [38–40] or linear [41–43] seesaws have additional singlet fermions and more than one new energy scale.

Loop mechanisms are the second-most popular way to generate neutrino masses. Examples are the Zee model [44] or the "scotogenic" model [45], which work at one-loop, or the Zee-Babu model [46, 47] at two-loop order. Again, new particles are introduced, mostly scalars, but also fermions. The loop-suppression of neutrino mass allows for more easily testable scenarios at colliders or using lepton flavor violating processes, Higgs physics or anomalous magnetic moments of charged leptons.

Thus, there are various ways for testable neutrino mass generation mechanisms. They can be distinguished by their different particle content, energy scales, couplings to SM particles and predictions for neutrino parameters. Identifying them will be of crucial importance to understand particle physics beyond the SM. In this document we will study generic examples on new particles coupling to neutrinos. We will show how very different processes constrain the scenarios and this broad set of probes is necessary to disentangle models. This broadness maps the broadness of neutrino physics.

Chapter 2

Phenomenology of new Scalars

In this chapter we discuss examples on the phenomenology of new scalar particles coupling to neutrinos.

2.1 Generics

New scalars may couple to neutrinos. Such particles maybe part of a new Higgs doublet or SM singlets, with this difference playing a big role in determining their phenomenology. An example for the latter kind is a Majoron, the (Pseudo-)Goldstone boson of spontaneously broken global lepton number. This is of particular interest in the form of neutrino self-interactions, which are used to explain the current discrepancy in local and global determinations of the Hubble parameter.

We consider a scalar field denoted by ϕ which couples to neutrinos. There are two possibilities for the coupling, namely lepton number violating (LNV) and conserving (LNC) couplings. The latter possibility requires the presence of right-handed neutrinos:

$$\mathcal{L}_{\text{LNC}} \equiv g_\phi \phi \bar{\nu}_R \nu_L + h.c. \tag{2.1}$$

For simplicity, we implicitly assume that ϕ is a real field but most of the discussion remains valid for a complex ϕ as well. Flavor indices are suppressed for clarity. The lepton number violating form of the interaction can be written in analogy as

$$\mathcal{L}_{\text{LNV}} \equiv \frac{g_\phi}{2} \phi \bar{\nu}^c_L \nu_L + h.c. = \frac{g_\phi}{2} \phi \nu^T_L C \nu_L + h.c. \tag{2.2}$$

Such couplings induce neutrino self-interactions (νSI), with an effective coupling constant $G_S = g^2_\phi / m^2_\phi$:

$$\mathcal{L}^{\text{LNC}}_{\nu\text{SI}} = G_S (\nu_\gamma \nu_\delta)(\overline{\nu}_\alpha \overline{\nu}_\beta), \quad \text{or} \quad \mathcal{L}^{\text{LNV}}_{\nu\text{SI}} = G_S (\nu_\gamma \nu_\delta)(\nu_\alpha \nu_\beta). \tag{2.3}$$

This coupling has been used to explain the discrepancy between Cosmic Microwave Background (CMB) and local measurements of the Hubble constant, known as the Hubble

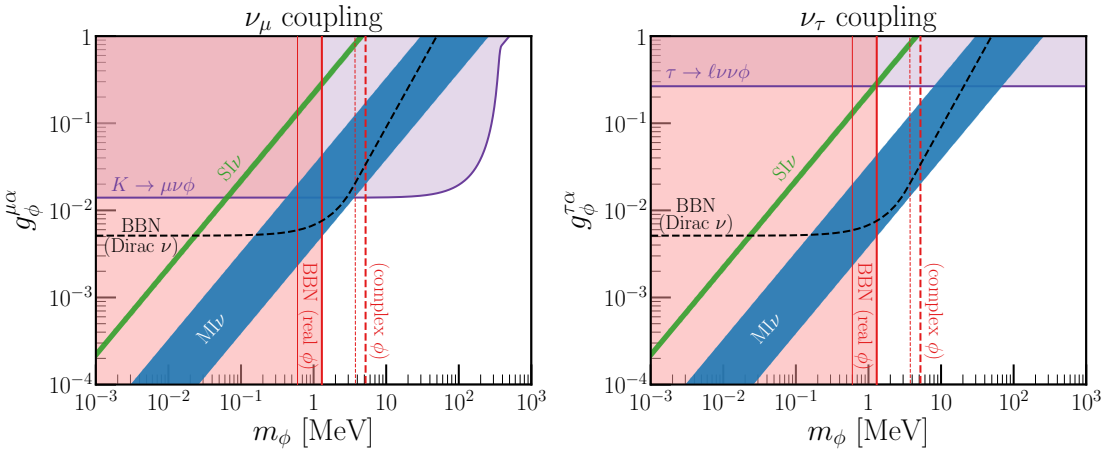

Figure 2.1: Limits on a scalar coupling to muon (left) and tau (right) neutrinos. The parameter space explaining the Hubble tension is shown in green and blue, corresponding to the strongly and moderately interacting regime. Taken from [62].

tension. This tension has grown to about 4σ [48–52], see Ref. [53] for a recent review. While no proposed particle physics solution can fully be in accordance with all cosmological data [53], among the many proposed particle-physics scenarios to explain the problem, νSI are interesting to us and in general, because laboratory tests are possible.

Scenarios of νSI to explain the Hubble tension actually need extra radiation in addition, corresponding to $\Delta N_{\rm eff} \simeq 1$. Using the strong positive correlation between the Hubble parameter and extra radiation, $\Delta N_{\rm eff} = N_{\rm eff} - 3.046$, in the early Universe implies that the increased $N_{\rm eff}$ delays matter-radiation equality and thus modifies the CMB power spectrum. This, in turn, is compensated by introducing non-standard neutrino self-interactions during recombination [54, 55], which inhibits neutrino free-streaming. The required strength of νSI needs to be much larger than Fermi interactions [54–58]: there is the strongly interacting regime with $G_S = 3.83^{+1.22}_{-0.54} \times 10^9\, G_F$ and the moderately interacting regime with $1.3 \times 10^6 < G_S/G_F < 1.1 \times 10^8$ [55]. Such strong νSI have drawn considerable attention [59–69], but in general they are difficult to probe in laboratory experiments because only neutrinos are involved. Nevertheless, Fig. 2.1 from Ref. [62] shows constraints. Comparing the various astrophysical, cosmological and laboratory constraints on the scenario leaves only coupling to tau neutrinos allowed.

In this chapter we will discuss the only existing direct bound on the 4-neutrino self-interaction and demonstrate how the large value of $\Delta N_{\rm eff}$ can be made compatible with Big Bang Nucleosynthesis. Leaving the Hubble tension we also show how models that let the scalar couple to quarks as well can be tested in coherent elastic neutrino-nucleus scattering.

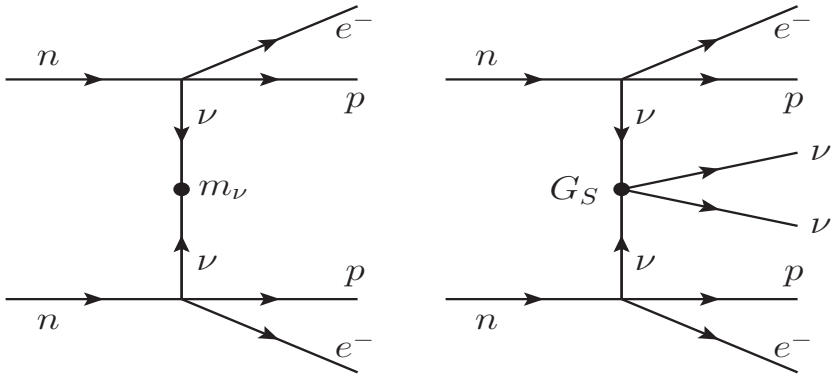

Figure 2.2: Neutrinoless double beta decay via Majorana neutrino exchange ($0\nu\beta\beta$) and double beta decay induced by νSI ($2\nu\text{SI}\beta\beta$).

2.2 Direct Constraints from Double Beta Decay Experiments

All constraints in Fig. 2.1 are either indirect or use only the coupling of a single line of neutrinos with the scalar, instead of the effective 4-neutrino interaction in Eq. (2.3). Ref. [70] provided the currently only direct constraint on the effective νSI operator without any assumption on its origin, using 2-neutrino double beta decay ($2\nu\beta\beta$). The Feynman-diagram is shown in Fig. 2.2 together with the diagram of light Majorana neutrino exchange for neutrinoless double beta decay ($0\nu\beta\beta$). While this lepton-number violating process has not been observed so far [71], the many experiments looking for it have data on the SM-allowed $2\nu\beta\beta$. This will be used in what follows to constrain νSI.

Using that the momenta of leptonic final states (of order $Q = \mathcal{O}(1)$ MeV) are negligible compared to the momenta of the neutrino propagators ($\mathcal{O}(100)$ MeV), it can be shown that the two processes in Fig. 2.2 share the same nuclear matrix elements (NMEs) [70]. Consequently, we can compute the decay rate of $2\nu_{\text{SI}}\beta\beta$ using the NME of $0\nu\beta\beta$:

$$\Gamma_{\nu\text{SI}} = \left|\frac{G_S m_e}{2R}\right|^2 \mathcal{G}_{\nu\text{SI}} |\mathcal{M}_{0\nu}|^2. \tag{2.4}$$

Ignoring interference, the total decay rate is

$$\Gamma_{2\nu} + \Gamma_{\nu\text{SI}} \simeq \left(|\mathcal{M}_{2\nu}|^2 + \left|\frac{G_S m_e}{2R}\right|^2 \frac{|\mathcal{M}_{0\nu}|^2}{4\pi^2}\right) \mathcal{G}_{2\nu}. \tag{2.5}$$

Here m_e is the electron mass, $R = 1.2A^{1/3}$ fm is the radius of the nucleus with nucleon number A, and the structure of the $0\nu\beta\beta$ NME $\mathcal{M}_{0\nu}$ is explained in Ref. [70]. The quantity $\mathcal{G}_{\nu\text{SI}}$ is the $2\nu_{\text{SI}}\beta\beta$ phase space factor; neglecting the final state lepton momenta, the phase space factors are related as $\mathcal{G}_{\nu\text{SI}} = \mathcal{G}_{2\nu}/(4\pi)^2$. In the NME ratio $|\mathcal{M}_{0\nu}|^2/|\mathcal{M}_{2\nu}|^2$ many of the nuclear uncertainties are expected to drop out.

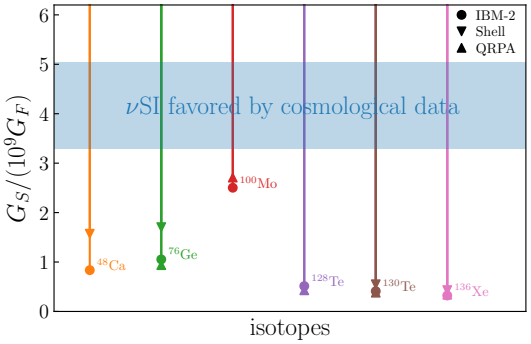

Figure 2.3: Constraint on the νSI coupling G_S from $2\nu\beta\beta$ decay data for several isotopes and NMEs. The blue band corresponds to the strongly interacting regime $G_S = 3.83^{+1.22}_{-0.54} \times 10^9\, G_F$ favored by cosmological data. Taken from Ref. [70].

Requiring the rates of $2\nu\text{SI}\beta\beta$ and $2\nu\beta\beta$ to obey $\Gamma_{\nu\text{SI}}/\Gamma^{\text{ex}}_{2\nu} < 1$ gives limits on G_S, which are shown in Fig. 2.3 for three sets of NME calculations (IBM-2 [72], Shell Model [73] and QRPA [74]). The strongly interacting regime, assuming that two ν_e are involved in the decay, is ruled out by data from $2\nu\beta\beta$.

We can also consider possible distortions of the electron energy and angular distributions arising from the νSI-induced contribution. While for a contact interaction the electron spectra are identical [70], if an s- or t-channel diagram is responsible for G_S, there is an effect. In these cases,

$$G_S = \frac{-m_\phi^2}{s - m_\phi^2} G_S^0 \quad (s\text{-channel}), \tag{2.6}$$

$$G_S = \frac{m_\phi^2}{t + m_\phi^2} G_S^0 \quad (t\text{-channel}), \tag{2.7}$$

where $G_S^0 = g_\phi^2/m_\phi^2$. Using the easiest case of s-channel mediation, one finds [70]

$$\frac{d\Gamma_{\nu\text{SI}}}{dp_1 dp_2 d\cos\theta_{12}} \propto |G_S^0|^2 p_1^2 p_2^2 I_s(T_{12})\,(1 - \beta_1\beta_2\cos\theta_{12})\,. \tag{2.8}$$

Here θ_{12} is the angle between the two emitted electrons and $\beta_i = p_i/E_i$ are the electron velocities. The function

$$I_s(T_{12}) = \frac{Q - T_{12}}{4(2\pi)^4}\left(\xi\frac{2 + \cos\xi}{\sin\xi} - 3\right), \tag{2.9}$$

where $\xi = 2\arcsin((Q - T_{12})/m_\phi)$, quantifies the effect of ϕ. It is a function of the total electron kinetic energy T_{12}. In the limit $m_\phi \to \infty$ we recover the known effective operator results, in particular $I_s(T_{12}) \propto (Q - T_{12})^5$. From Eq. (2.8) we can obtain the energy and angular distributions. While all experiments [71] measure $d\Gamma_{\nu\text{SI}}/dT_{12}$, only the past NEMO and the potential future SuperNEMO experiments have sensitivity on the angular distributions. Assuming $m_\phi = Q + 0.1 m_e$, slightly above the kinematic threshold,

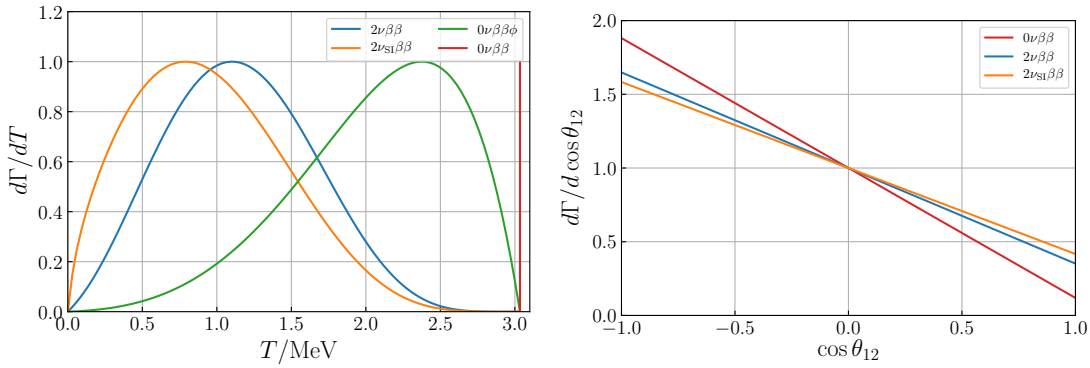

Figure 2.4: Electron energy and angular distribution of the two emitted electrons for neutrinoless double beta decay ($0\nu\beta\beta$), νSI-induced double beta decay (2νSI$\beta\beta$), double beta decay with Majoron emission ($0\nu\beta\beta\phi$) and 2-neutrino double beta decay ($2\nu\beta\beta$), all using ^{100}Mo. The energy spectra are normalized to the same maximal height and the angular distributions to the value 1 at $\cos\theta_{12} = 0$. Taken from Ref. [70].

Fig. 2.4 displays the electron energy distributions of $2\nu_{\rm SI}\beta\beta$ and $2\nu\beta\beta$ decay, together with the ones for $0\nu\beta\beta$ decay and for Majoron emission ($0\nu\beta\beta\phi$) [75]. A χ^2-fit to NEMO-3 data [76] for the quantity r in $\Gamma_{\nu\rm SI} = r^2\Gamma_{2\nu}$ yields $r = 16\%$. If the spectral distortion is taken into account, the bound on G_S can thus be approximately improved by one order of magnitude. The sensitivity will decrease for larger masses m_ϕ. Including in addition the angular distribution yields $r < 29\%$ at 3σ. Therefore the angular distribution is less sensitive than the energy distribution, which is interesting as only SuperNEMO could measure this.

All in all, the results of this section imply a new test of neutrino self-interactions and demonstrate that double beta decay experiments have interesting physics potential beyond their main goal of determining lepton number violation.

2.3 What about Big Bang Nucleosynthesis?

As mentioned above, neutrino self-interactions are needed in addition to a sizable amount of $\Delta N_{\rm eff} \simeq 1$ in the early Universe. In this respect, Big Bang Nucleosynthesis (BBN) data implies [77]

$$N_{\rm eff} = 2.88 \pm 0.27\,, \tag{2.10}$$

or $\Delta N_{\rm eff} < 0.42$ at 2σ. How can this be made compatible with the the presence of $\Delta N_{\rm eff} \simeq 1$ in order to explain the Hubble tension?

In this section we take the LNV interaction in Eq. (2.3), in which ϕ could be a Majoron, the Pseudo-Goldstone boson of spontaneously broken global lepton number. This scalar increases $N_{\rm eff}$, if in thermal equilibrium with the neutrino plasma, by $\Delta N_{\rm eff} = 1/2 \cdot 8/7 \simeq$

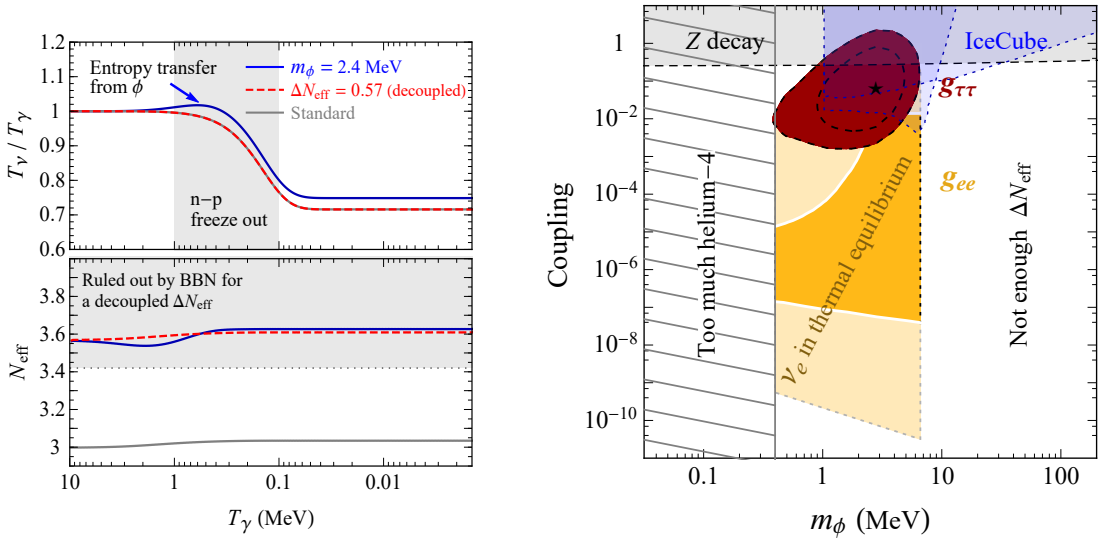

Figure 2.5: Left: The temperature ratio for neutrinos and photons T_ν/T_γ (upper panel) and $N_{\rm eff}$ (lower panel) with respect to the photon temperature. The blue curves assume $m_\phi = 2.4$ MeV in thermal equilibrium with neutrinos, while the red curves is for $\Delta N_{\rm eff} = 0.57$. Right: Fit result of the Majoron scenario at 90% and 68% C.L., using BBN, CMB, the moderately self-interacting case and the local value of H_0 [79]. Taken from Ref. [78].

0.57 for $m_\phi \ll T_\nu$, where T_ν is the plasma temperature. For $m_\phi \gtrsim 1$ MeV, the neutrino temperature will increase with respect to the photon one due to $\phi \leftrightarrow \nu + \overline{\nu}$ reactions. The rise in the neutrino temperature (increasing the neutron burning rate in BBN) will cancel the effect caused by a larger $N_{\rm eff}$ (increasing the expansion rate), such that the final neutron-to-proton ratio n/p remains almost the same as in the standard case.

In Fig. 2.5 we see this quantitatively. Shortly after $T_\gamma < m_\phi$, entropy is transferred o the neutrinos, increasing their temperature by 4.6%. In contrast, if only $\Delta N_{\rm eff}$ is added to the framework (decoupled scenario), the ratio T_ν/T_γ is essentially constant. One can show [78] that $\delta T_\nu/T_\nu = 4.6\%$ implies $\delta\Gamma/\Gamma_{{\rm n}\nu_e} \simeq 13.8\%$ for the neutron burning rate. With the Hubble rate $H \propto T^2 \propto 1/t$ the time interval between two temperatures goes as $\delta t/t \simeq -4.9\%$. This reduces the time for neutron burning, and thus compensates the effect of $\Delta N_{\rm eff}$.

Adopting the `AlterBBN` code [80, 81] to calculate the light element abundances and assuming the scalar only coupling with[1] $g_{\tau\tau}$ gives Fig. 2.5. The best-fit point is $m_\phi = 2.8$ MeV and $g_{\tau\tau} = 0.07$. Various other limits exist, see the previous section. Noteworthy is a bound on $g_{\tau\tau}$ from Z decays due to its enhancement of the invisible decay rate of Z. Our best-fit would imply $N_\nu = 3.0012$ [82]. The parameter $g_{\tau\tau}$ may also lead to a dip in the spectrum of ultra-high energy neutrinos observed at IceCube by scattering off the

[1]Actually, $g_{ee} \gtrsim 2.2 \times 10^{-10}({\rm MeV}/m_\phi)$ in order for ν_e to stay in equilibrium with ϕ during the BBN era [60].

relic neutrinos [83]. For $m_\nu = 0.1$ eV, the dip occurs at $E_\nu = m_\phi^2/(2m_\nu) \simeq 78$ TeV, see the blue curves in Fig. 2.5, partly covering our 1σ range.

Therefore, we have shown here how a typical solution to the Hubble tension, that usually incorporates a sizable $\Delta N_{\rm eff}$, can be made compatible with strong constraints on $N_{\rm eff}$ from BBN.

2.4 Dirac Neutrinos and $N_{\rm eff}$

We have seen that the number of relativistic degrees of freedom, $N_{\rm eff}$, can have important impact on model parameter space. In connection to neutrino physics, the right-handed neutrino counterpart comes to mind as a potential contribution to $N_{\rm eff}$. This only makes sense for Dirac neutrinos, for Majorana neutrinos the right-handed neutrinos are connected to the left-handed ones and do not count as additional degrees of freedom. The only interaction of right-handed neutrinos is via the Yukawa interaction $\bar{L}\tilde{\Phi}\nu_R$, with L the lepton and Φ the Higgs doublet. The smallness of neutrino mass implies tiny Yukawa couplings and thus the right-handed neutrinos never enter equilibrium and do not contribute to $N_{\rm eff}$ in significant amounts, see below. However, new interactions can equilibrate the right-handed species, and constraints on such scenarios arise from measurements of $N_{\rm eff}$ [84]. In general, we can assume that ν_R couples to a chiral fermion F and a scalar boson B:

$$\mathcal{L} \supset g_\nu B \overline{F} \nu_R + h.c. \tag{2.11}$$

Assuming B and F are heavy, they will not contribute to $N_{\rm eff}$, but the above interaction may put ν_R in equilibrium with the thermal plasma in the early Universe. The case of massless F could correspond to SM neutrinos coupling to a new scalar.

The ν_R energy density, ρ_{ν_R}, enters a Boltzmann equation [85] with a collision term C_{ν_R}

$$\dot{\rho}_{\nu_R} + 4H\rho_{\nu_R} = C_{\nu_R}, \tag{2.12}$$

which is calculated as

$$\begin{aligned} C_{\nu_R} \;\equiv\; & N_{\nu_R} \int E_{\nu_R} d\Pi_1 d\Pi_2 d\Pi_3 d\Pi_4 (2\pi)^4 \delta^4(p_1 + p_2 - p_3 - p_4) \\ & \times S|\mathcal{M}|^2 \left[f_1 f_2 (1 \pm f_3)(1 \pm f_4) - f_3 f_4 (1 \pm f_1)(1 \pm f_2) \right], \end{aligned} \tag{2.13}$$

$$d\Pi_i \equiv \frac{1}{(2\pi)^3} \frac{d^3 p_i}{2E_i}, \quad f_i \equiv \frac{1}{\exp\left(E_i/T_i\right) \mp 1}, \quad (i = 1,\, 2,\, 3,\, 4). \tag{2.14}$$

Here $N_{\nu_R} = 6$ (including ν and $\overline{\nu}$ of three flavors); E_{ν_R} is the energy of ν_R, S is the symmetry factor, $|\mathcal{M}|^2$ is the squared amplitude of the process; p_i, E_i, and T_i denote the momentum, energy, and temperature of the i-th particle in the process. If energy is injected to the ν_R, the SM particles are governed by

$$\dot{\rho}_{\rm SM} + 3H(\rho_{\rm SM} + P_{\rm SM}) = -C_{\nu_R}, \tag{2.15}$$

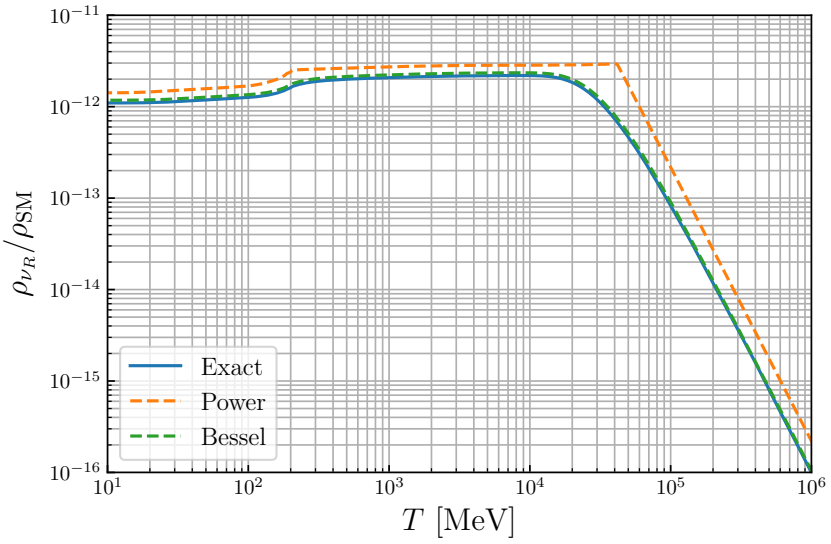

Figure 2.6: The SM Higgs as an example: $\Delta N_{\rm eff} \simeq 7.5 \times 10^{-12}$. We show an exact numerical computation, as well as various approximate analytical approaches, see [87] for details.

where $\rho_{\rm SM}$ and $P_{\rm SM}$ are the energy density and pressure of SM particles. Solving Eqs. (2.12) gives

$$\Delta N_{\rm eff} = \frac{4}{7} g_{\star,\rm dec}^{(\rho)} \left[\frac{10.75}{g_{\star,\rm dec}^{(s)}}\right]^{4/3} \frac{\rho_{\nu_R,\rm dec}}{\rho_{\rm SM,dec}} \simeq N_\nu \left(\frac{T_{\nu_R,\rm low}}{T_{\rm low}}\right)^4 , \tag{2.16}$$

where the subscript "dec" denotes any moment after ν_R is fully decoupled from the SM plasma, $N_\nu = 3$ and the subscript "low" denotes generally any moment at which the approximation $g_\star^{(\rho)} \simeq g_\star^{(s)} \simeq 10.75$ is valid [86].

Details of the calculations can be found in Ref. [87]. As a simple example, we assume Dirac masses generated by the SM Higgs, i.e. $Y_\nu \overline{L}\tilde{\Phi}\nu_R$, with $Y_\nu = \sqrt{2}\frac{m_\nu}{v} = 5.7 \times 10^{-13} \left(\frac{m_\nu}{0.1 \text{ eV}}\right)$. Taking the low-temperature value of the blue curve in Fig. 2.6 and using Eq. (2.16), we obtain

$$\Delta N_{\rm eff} \simeq 7.5 \times 10^{-12} \left(\frac{m_\nu}{0.1 \text{ eV}}\right)^2 . \tag{2.17}$$

This is a precise result on $\Delta N_{\rm eff}$ that originates from the SM Higgs interaction with Dirac neutrinos.

Another example in the spirit of this chapter is assuming $m_F = 0$, which corresponds to a ν_L-ν_R coupling with a new scalar boson. Fig. 2.7 shows the outcome of a numerical analysis for different values of the new scalar mass. The left panel displays the process $B \to F\nu_R$, that is, F and B are in equilibrium. The right panel is for the t-channel process $FF \to \nu_R\nu_R$ mediated by B, i.e., F is in equilibrium while B is not. The same cases for $m_F = m_B/2$ are also given. We confront the results with current and future experimental bounds on $\Delta N_{\rm eff}$ from Planck 2018 [51, 88], the Simons Observatory (SO) [89], the South Pole Telescope (SPT-3G) [90], and CMB-S4 [91, 92]. The Planck 2018 measurement gives

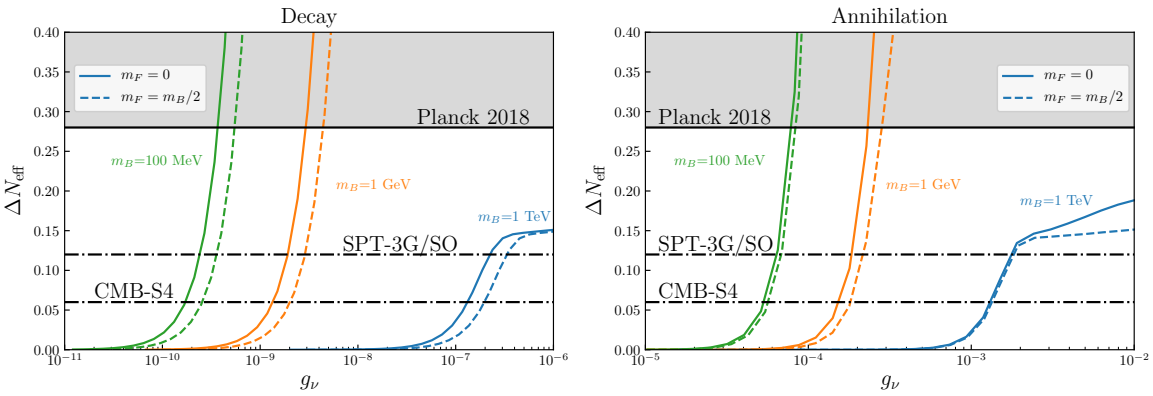

Figure 2.7: Contributions of ν_R to $N_{\rm eff}$ for varying g_ν. The left panel displays the process $B \to F\nu_R$, that is, F and B are in equilibrium. The right panel is for the t-channel process $FF \to \nu_R\nu_R$ mediated by B, i.e., F is in equilibrium while B is not. The same cases for $m_F = m_B/2$ are also given. Taken from Ref. [87].

$\Delta N_{\rm eff} < 0.285$ at 2σ. The SO and SPT-3G sensitivities are similar ($\Delta N_{\rm eff} < 0.12$), while the future CMB-S4 limit is expected to reach 0.06, all numbers at 2σ.

Thus, we have shown that decay or scattering of new particles with Dirac neutrinos can give sizable contributions to $N_{\rm eff}$, and limits on the new coupling constants of order 10^{-4} (10^{-9}) can be set if the new particles are around TeV (GeV). Similar considerations could be done for new vector bosons. As a byproduct, we have obtained the contribution of the SM contribution from a possible Higgs mechanism of neutrinos: $\Delta N_{\rm eff}^{\rm SM} \simeq 7.5 \times 10^{-12}\,(m_\nu/(0.1\,{\rm eV}))^2$.

2.5 Extension to the Quark Sector

Scalar fields could also couple to quarks. This is of particular interest when a relatively new process to probe neutrino features is discussed: coherent elastic neutrino-nucleus scattering (CEνNS). In the Standard Model, the neutral current (NC) interaction enables low energy neutrinos with $E_\nu \lesssim 50$ MeV (corresponding to length scales of $\gtrsim 10^{-14}$ m) to interact coherently with protons and neutrons in a nucleus, which significantly enhances the cross section for a large nucleus [93–95]:

$$\frac{d\sigma}{dT} = \frac{\sigma_0^{\rm SM}}{M}\left(1 - \frac{T}{T_{\rm max}}\right), \tag{2.18}$$

where $\sigma_0^{\rm SM}$ is defined as

$$\sigma_0^{\rm SM} \equiv \frac{G_F^2\left[N - (1-4s_W^2)Z\right]^2 F^2(q^2) M^2}{4\pi}. \tag{2.19}$$

Here G_F, $s_W = \sin\theta_W$, and M are the Fermi constant, the Weinberg angle, and the mass of the nucleus, respectively. The cross section is dominated by the neutron number N; $F(q^2)$ is the form factor of the nucleus. The maximal recoil energy T of the nucleus depends on the initial neutrino energy E_ν:

$$T_{\max}(E_\nu) = \frac{2E_\nu^2}{M + 2E_\nu}\,. \tag{2.20}$$

We consider here a new scalar coupling to neutrinos and nucleons. The Lagrangian on the nuclear level is

$$\mathcal{L}_{N\phi} \equiv \overline{\psi_N}\Gamma_{N\phi}\psi_N\phi, \tag{2.21}$$

where ψ_N is the Dirac spinor of the nucleus[2] $N = n, p$. With $\Gamma_{N\phi} \equiv C_N + D_N i\gamma^5$, only C_N is important, as the contribution of D_N is very much suppressed. For scalar interactions there is no interference with the SM contribution:

$$\frac{d\sigma}{dT} = \frac{d\sigma_{\rm SM}}{dT} + \frac{d\sigma_\phi}{dT}. \tag{2.22}$$

Coherent scattering mediated by the light scalar, independent of whether the new scalar interaction is of the LNC or LNV form, has a cross section of [97]

$$\frac{d\sigma_\phi}{dT} = \frac{MY^4A^2}{4\pi(2MT + m_\phi^2)^2}\left[\frac{MT}{E_\nu^2} + \mathcal{O}\left(\frac{T^2}{E_\nu^2}\right)\right], \tag{2.23}$$

where we have defined

$$Y^4 \equiv \frac{C_N^2}{A^2}|y_\nu|^2. \tag{2.24}$$

The effective couplings C_N and D_N originate from fundamental couplings of ϕ with the quarks and require knowing the scalar form factors of quarks in the nuclei. Using results from Refs. [98–103], and rewriting Y in Eq. (2.24) in terms of the fundamental couplings as

$$Y \equiv \sqrt{\frac{|C_N y_\nu|}{A}} = \sqrt{\left|\left(\frac{A-Z}{A}\,C_n + \frac{Z}{A}\,C_p\right)y_\nu\right|}, \tag{2.25}$$

we obtain [97]

$$Y_{\rm Ge} \simeq \sqrt{|(0.56\,C_n + 0.44\,C_p)y_\nu|}\,, \tag{2.26}$$

$$Y_{\rm CsI} \simeq \sqrt{|(0.58\,C_n + 0.42\,C_p)y_\nu|}\,. \tag{2.27}$$

When comparing the sensitivities of CEνNS experiments using different targets, we will ignore the small difference and assume $Y_{\rm Ge} \simeq Y_{\rm CsI}$.

Bounds on C_n, y_ν or on their product come from various observations and experiments other than coherent scattering, such as neutron-nucleus scattering, meson decays, double beta decay, BBN, CMB, as well as supernova considerations, and detailed discussions can

[2]The appendix of [96] demonstrates that there is hardly an effect of the nucleon spin.

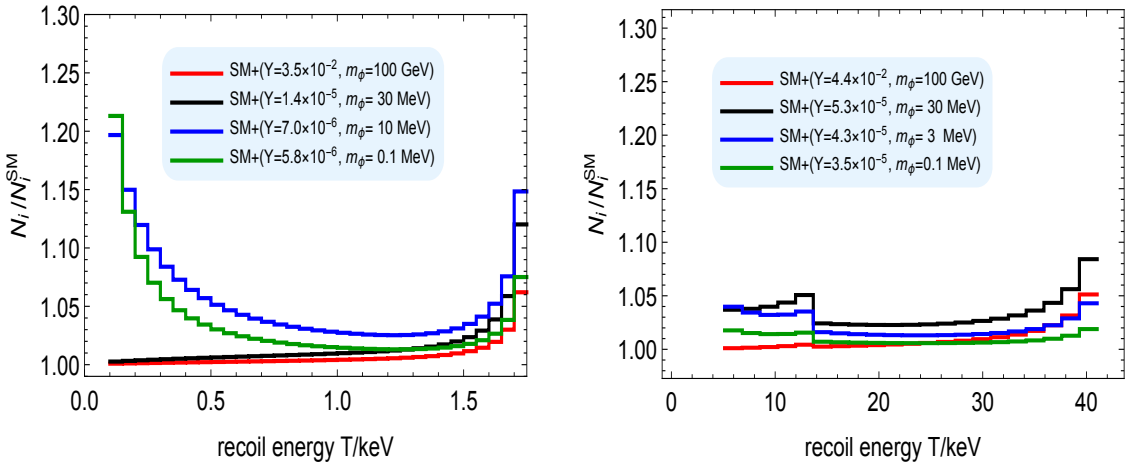

Figure 2.8: Event excess caused by light scalar bosons in CONUS (left) and COHERENT (right). The effective coupling Y is defined in Eq. (2.25). Taken from Ref. [97].

be found in Ref. [97]. Let us discuss the impact on supernova cooling in a bit of detail. In total we can have three effects: (1) change of equation of state in case of LNV interaction ("SN core EOS"); (2) new cooling modes because of right-handed (anti)neutrino emission in case of LNC interaction ("SN energy loss" and "SN ν_R trapping"); (3) prolonging the duration of neutrino emission (R^2/λ) because of a shorter mean free path λ ("SN ν diffusion"). There are differences depending on whether the interaction is LNC or LNV. For instance, converting ν_e into $\bar{\nu}_e$ would produce strongly interacting e^+ in the SN core, while converting ν_L into sterile ν_R produces sterile particles that take away energy. We will present in what follows limits for a typical neutrino temperature of 30 MeV. Regarding constraints from BBN and CMB, the contributions from the LNC and LNV cases to the additional number of relativistic degrees of freedom ($\Delta N_{\rm eff}$) will also be quite different, as we can understand from the previous sections.

Having summarized the current constraints on our scenario, we continue with setting limits using coherent elastic neutrino-nucleus scattering with existing COHERENT and future CONUS data. These experiments will also be used later in this document. COHERENT has observed CEνNS [104] on a CsI target (with a recent improved measurement [105] and a limit on the cross section using an Ar target [106]), which allows to set definite limits on new physics scenarios. The COHERENT experiment uses a CsI scintillator to detect neutrinos produced by π^+ and μ^+ decay at rest. There are three types of neutrinos in the neutrino flux, ν_μ, $\overline{\nu}_\mu$, and ν_e. The first is produced in the decay $\pi^+ \to \mu^+ + \nu_\mu$ while the second and the third are produced in the subsequent decay $\mu^+ \to e^+ + \overline{\nu}_\mu + \nu_e$. CONUS will be used as a prototype future precision, large-statistics experiment. It uses a very low threshold Germanium detector at the Brokdorf nuclear power plant. The flux contains electron electron antineutrinos, and the energy range is such that the fully coherent regime is realized. We note that limits on CEνNS have been set by CONUS [107], and interesting constraints on new physics have been obtained [108]. For definiteness, the CsI results of COHERENT and expected limits from CONUS will

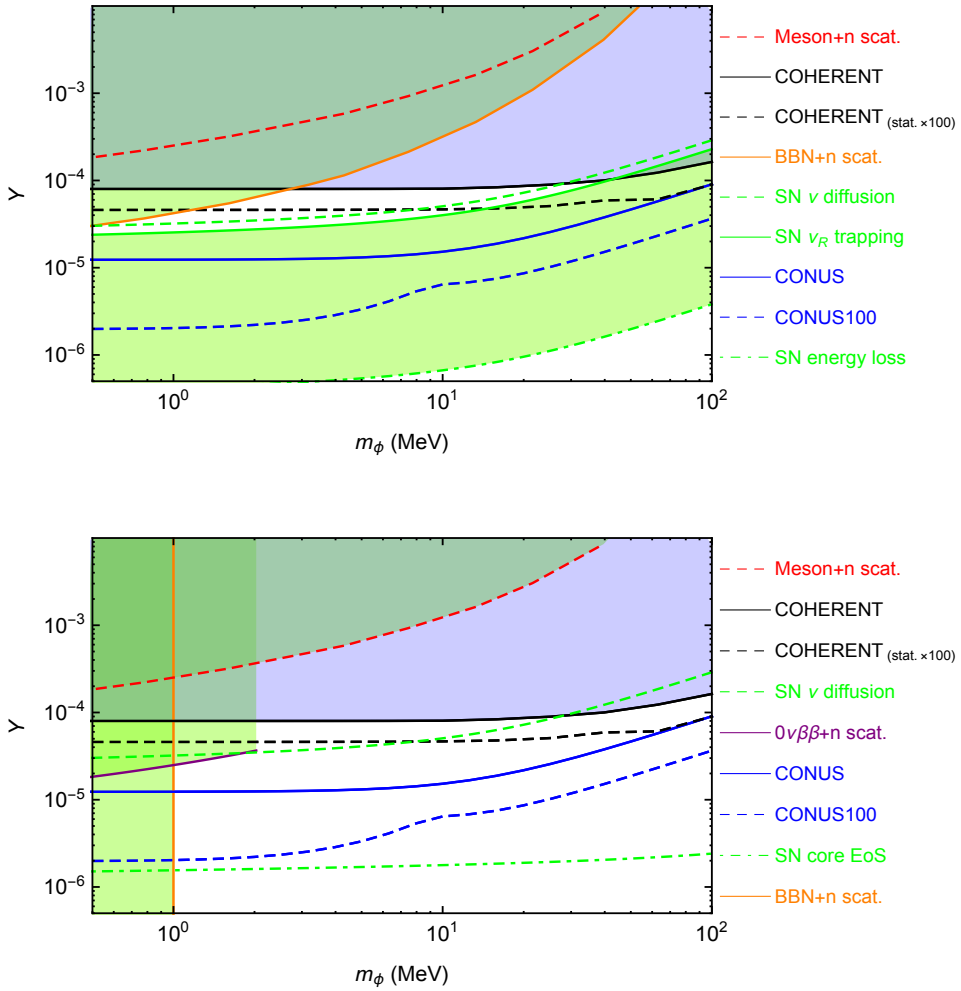

Figure 2.9: The upper (lower) plot shows constraints from CEνNS experiments on (Y, m_ϕ) for a lepton number conserving (violating) interaction. The black, dashed black, blue, and dashed blue curves correspond to the 95% C.L. constraint from COHERENT data [104], the sensitivities of future COHERENT, CONUS 4 kg×1 year, and CONUS 100 kg×5 years (light-blue) respectively. Taken from Ref. [97].

be used. In the near future, other upcoming experiments including ν-cleus [109], CONNIE [110], MINER [111], TEXONO [112], νGEN [113] and Ricochet [114] will also be able to measure the CEνNS process.

Examples on the event spectra in these two experiments can be found in Fig. 2.8, for details see Ref. [97]. We fit the COHERENT data from Ref. [104], and for CONUS we assume 1 year of data taking with a 4 kg detector and 1.2 keV threshold. Future limits are illustrated by assuming again that CONUS runs for 5 years with 100 kg Ge, an improved threshold of 0.1 keV and theoretical flux uncertainties being one half of those today. COHERENT statistics will be assumed to be improved by a factor of 100 and

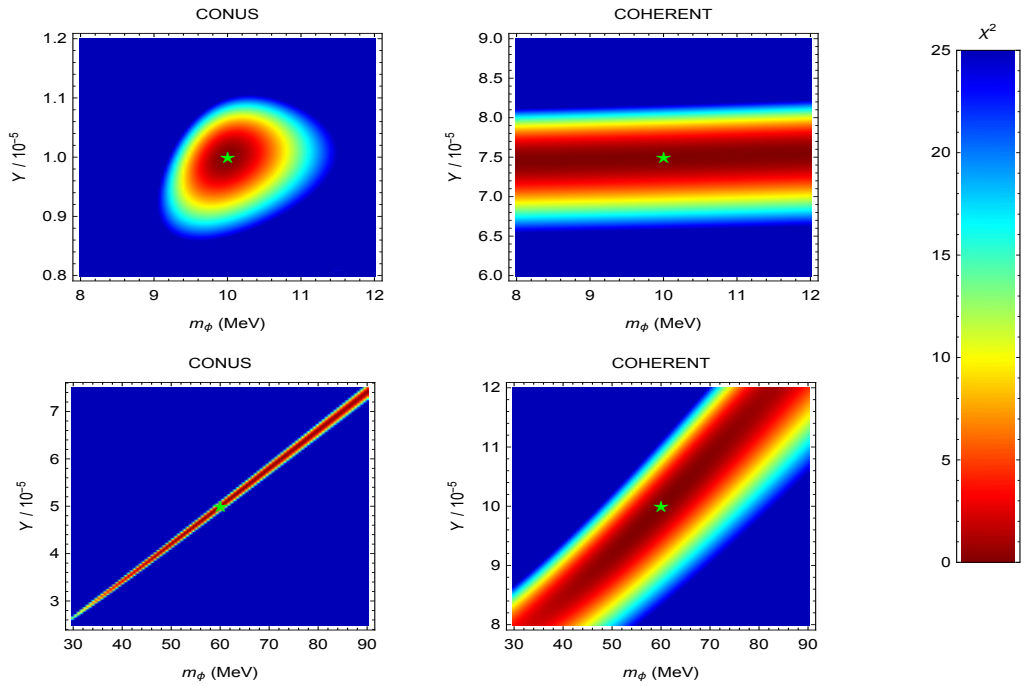

Figure 2.10: Measurements of the mass m_ϕ and coupling Y with future CONUS and COHERENT data, assuming the presence of a scalar boson, with the true values indicated by the green stars. Taken from Ref. [97].

the overall uncertainty reduced by 10. One can see from the figure that the shape of the spectrum when we include the scalar contribution can be dramatically different, in particular for low values of m_ϕ. A statistical analysis [97] ends up in Fig. 2.9 for the LNC and LNV cases. Both existing and prospective future limits are used. Fig. 2.10 gives the potential of CONUS100 for determining the mass and coupling of the ϕ particle assuming two characteristic examples.

Thus, new scalar interactions of neutrinos and quarks can have observable consequences in coherent scattering while still being in accordance with other limits. For instance, a positive signal for the effects of ϕ with a value of Y below the green solid line in Fig. 2.9 implies from supernova cooling bounds that the interaction can not be lepton number conserving. If ϕ turns out to have a mass around 2 MeV, double beta experiments may see it. If they do not, one might have $(y_\nu)_{ee} \ll (y_\nu)_{e\mu}, (y_\nu)_{e\tau}$, thus gaining information on the flavor structure of the new interaction.

Chapter 3

Phenomenology of new Vectors

This section deals with new vector bosons coupling in particular to neutrinos, or being motivated by neutrinos. Since we are interested in gauge theories, there is most of the times also coupling to other particles, providing further constraints.

3.1 Generics

In addition to the direct coupling of the new $U(1)'$ gauge boson to SM fermions we will also allow for mixing between the Z' and the Z and start with the most general Lagrangian describing the mixing. The formalism for Z-Z' mixing [115, 116] has been frequently discussed in the literature:

$$\begin{aligned}
\mathcal{L}_{\text{SM}} &= -\frac{1}{4}\hat{B}_{\mu\nu}\hat{B}^{\mu\nu} - \frac{1}{4}\hat{W}^a_{\mu\nu}\hat{W}^{a\mu\nu} + \frac{1}{2}\hat{M}_Z^2\hat{Z}_\mu\hat{Z}^\mu - \frac{\hat{e}}{\hat{c}_W}j_Y^\mu\hat{B}_\mu - \frac{\hat{e}}{\hat{s}_W}j_W^{a\,\mu}\hat{W}^a_\mu\,, \\
\mathcal{L}_{Z'} &= -\frac{1}{4}\hat{Z}'_{\mu\nu}\hat{Z}'^{\mu\nu} + \frac{1}{2}\hat{M}_Z'^2\hat{Z}'_\mu\hat{Z}'^\mu - \hat{g}'j'^\mu\hat{Z}'_\mu\,, \\
\mathcal{L}_{\text{mix}} &= -\frac{\sin\chi}{2}\hat{Z}'^{\mu\nu}\hat{B}_{\mu\nu} + \delta\hat{M}^2\hat{Z}'_\mu\hat{Z}^\mu\,.
\end{aligned} \tag{3.1}$$

Hatted fields indicate here that those fields have neither canonical kinetic nor mass terms. Even if zero at some scale, kinetic mixing governed by χ is generated at loop level if there are particles charged under hypercharge and $U(1)'$ [116]. Tree-level mass mixing via the term $\delta\hat{M}^2\hat{Z}'_\mu\hat{Z}^\mu$ requires that there is a scalar with a nonzero vacuum expectation value charged under the SM and $U(1)'$.

The new neutral current j' of the $U(1)'$ is left unspecified, but has for our purposes to be flavor *non-universal*:

$$j'_\mu \supset \sum_{\alpha,\beta} q_{\alpha\beta}\overline{\nu}_\alpha\gamma_\mu P_L\nu_\beta\,, \tag{3.2}$$

with $q \neq \mathbb{1}$. After diagonalization, the physical massive gauge bosons $Z_{1,2}$ and the massless photon couple to a linear combination of j', as well as the textbook QED and neutral

currents:

$$\mathcal{L}_{\text{int}} = -\left(\; e j_{\text{EM}}, \;\; \tfrac{e}{2\hat{s}_W \hat{c}_W} j_{\text{NC}}, \;\; g' j' \; \right) \begin{pmatrix} 1 & a_1 & a_2 \\ 0 & b_1 & b_2 \\ 0 & d_1 & d_2 \end{pmatrix} \begin{pmatrix} A \\ Z_1 \\ Z_2 \end{pmatrix} . \tag{3.3}$$

with parameters

$$\begin{aligned} a_1 &= -\hat{c}_W \sin\xi \tan\chi \,, \quad b_1 = \cos\xi + \hat{s}_W \sin\xi \tan\chi \,, \quad d_1 = \frac{\sin\xi}{\cos\chi} \,, \\ a_2 &= -\hat{c}_W \cos\xi \tan\chi \,, \quad b_2 = \hat{s}_W \cos\xi \tan\chi - \sin\xi \,, \quad d_2 = \frac{\cos\xi}{\cos\chi} \,. \end{aligned} \tag{3.4}$$

In particular,

$$\begin{pmatrix} \cos\xi & \sin\xi \\ -\sin\xi & \cos\xi \end{pmatrix} \begin{pmatrix} a & b \\ b & c \end{pmatrix} \begin{pmatrix} \cos\xi & -\sin\xi \\ \sin\xi & \cos\xi \end{pmatrix} = \begin{pmatrix} M_1^2 & 0 \\ 0 & M_2^2 \end{pmatrix} \equiv \begin{pmatrix} M_Z^2 & 0 \\ 0 & M_{Z'}^2 \end{pmatrix}, \tag{3.5}$$

where

$$\tan 2\xi = \frac{2b}{a-c} \text{ with } \begin{cases} a = \hat{M}_Z^2 \,, \\ b = \hat{s}_W \tan\chi \hat{M}_Z^2 + \frac{\delta\hat{M}^2}{\cos\chi} \,, \\ c = \frac{1}{\cos^2\chi} \left(\hat{M}_Z^2 \hat{s}_W^2 \sin^2\chi + 2\hat{s}_W \sin\chi \delta\hat{M}^2 + \hat{M}_{Z'}^2 \right) . \end{cases} \tag{3.6}$$

Having set the formalism of the Z' physics, we may wonder what to gauge. With the introduction of right-handed neutrinos one can promote $U(1)_{B-L} \times U(1)_{L_\mu - L_\tau} \times U(1)_{L_\mu - L_e}$ or any subgroup thereof to a local gauge symmetry [117]. Hence, an anomaly free and UV-complete gauge group will couple to [118]

$$X = r_{BL}(B-L) + r_{\mu\tau}(L_\mu - L_\tau) + r_{\mu e}(L_\mu - L_e) \tag{3.7}$$

for arbitrary real coefficients r_x [117] (see also Refs. [119–123]), potentially including Z-Z' mixing. We stress here one particular example, namely $L_\mu - L_\tau$ [29–31], whose experimental constraints are relatively loose due to the absence of electron coupling at tree level. Moreover, the flavor structure $L_\mu - L_\tau$ generates attractive parameters in the neutrino sector, namely vanishing θ_{13}, maximal θ_{23}, large θ_{12} and neutrino masses without a strong hierarchy [124, 125]. More interestingly, the Z' can explain the anomalous muon magnetic moment $a_\mu \equiv (g_\mu - 2)/2$, which very recently was shown to have a 4.2σ discrepancy with the SM prediction [126], when combined with the final result from the E821 experiment at Brookhaven National Laboratory in 2006 [127]. While there are also new calculations [128] that reduce the significance, active theory work addressed potential solutions to this anomaly [129]. A Z' coupling to muons is a good and economic guess. An additional motivation of $L_\mu - L_\tau$ came from long-standing anomalies in neutral current B meson decays $B \to K^* \mu^+ \mu^-$ and the ratio of $B \to K \mu^+ \mu^-$ and $B \to K e^+ e^-$, see e.g. [130–132]. In general, a Z' is constrained by a variety of processes. Fig. 3.1 shows an example.

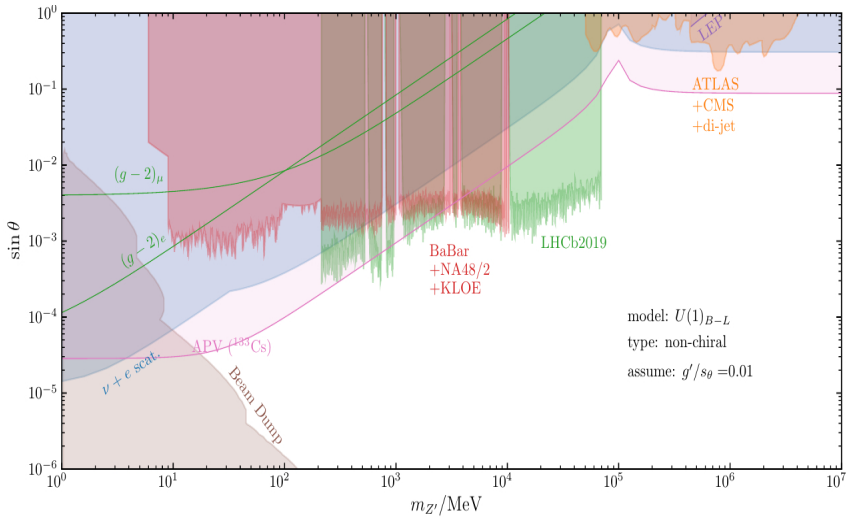

Figure 3.1: Limits on the Z' boson of gauged $B-L$ for $g'/\sin\theta = 0.01$, where $\tan\theta = \delta\hat{M}^2/(m_{Z'}^2 - m_Z^2)$.

In what follows we will discuss aspects of flavor-dependent $U(1)'$ models, namely the generation of so-called NSI operators which are of great interest to the neutrino community. Moreover, focusing on $L_\mu - L_\tau$, we will show the sensitivity of potential muon colliders to probe the parameter space that is responsible for the anomalous muon magnetic moment. As an extension to the quark sector, we deal with a Z' that explains the B meson anomalies, i.e. couples to muon and bs pairs.

3.2 Non-Standard Neutrino Interactions and Neutral Gauge Bosons

The precision era of neutrino physics implies that small effects beyond the standard paradigm of three massive neutrinos may be detected. There are many possibilities for such effects, the most popular one are Non-Standard neutrino Interactions (NSI), which modify neutrino oscillation probabilities in matter and may spoil the determination of unknown neutrino parameters in running and future experiments, see e.g. Refs. [133–139]. NSI stem from an effective Lagrangian [140–143]:

$$\mathcal{L}_{\text{eff}} = -2\sqrt{2}G_F\,\epsilon_{\alpha\beta}^{f\,X}\,(\bar{\nu}_\alpha\gamma_\mu P_L\nu_\beta)\left(\bar{f}\gamma^\mu P_X f\right) \quad \text{with } f = e, u, d. \tag{3.8}$$

We assume here the presence of a flavor-sensitive[1] gauged $U(1)'$ as origin of this effective Lagrangian [144]. In these theories the Z' belonging to the $U(1)'$ is integrated out and generates the effective NSI Lagrangian Eq. (3.8).

NSI relevant for neutrino propagation in matter should be vector-like

$$\epsilon_{\alpha\beta}^{f} \equiv \epsilon_{\alpha\beta}^{f\,L} + \epsilon_{\alpha\beta}^{f\,R}\,. \tag{3.9}$$

[1]Note that $\epsilon \propto \mathbb{1}$ leaves neutrino oscillations unaffected.

Those NSI induce an additional matter term in the Hamiltonian,

$$H_{\text{mat}} = \sqrt{2} G_F N_e(x) \begin{pmatrix} 1+\epsilon_{ee}(x) & \epsilon_{e\mu}(x) & \epsilon_{e\tau}(x) \\ \epsilon^*_{e\mu}(x) & \epsilon_{\mu\mu}(x) & \epsilon_{\mu\tau}(x) \\ \epsilon^*_{e\tau}(x) & \epsilon^*_{\mu\tau}(x) & \epsilon_{\tau\tau}(x) \end{pmatrix}, \tag{3.10}$$

with $\epsilon_{\alpha\beta} = \sum_f \frac{N_f(x)}{N_e(x)} \epsilon^f_{\alpha\beta}$ and number densities $N_f(x)$. Two diagonal entries, $\epsilon_{ee} - \epsilon_{\mu\mu}$ and $\epsilon_{\tau\tau} - \epsilon_{\mu\mu}$ can be constrained with neutrino oscillations. Limits on the diagonal NSI from oscillation data are given in Ref. [145]; they are somewhere between order 1 and 0.01. NSI mediated by a new neutral vector boson Z' with coupling strength g' and mass $M_{Z'}$ are generically of the form $\epsilon \sim (2\sqrt{2}G_F)^{-1}(g'/M_{Z'})^2$, even if the Z' mass is tiny. The limits thus correspond to $M_{Z'}/g'$ from 140 GeV to 2.5 TeV. One needs to confront those limits with other constraints, e.g. from collider or meson decays. Neutrino scattering with electrons [146, 147] or nucleons [148] is also very relevant. Interestingly, oscillations probe zero-momentum forward scattering, while neutrino scattering with quarks and electrons requires a non-vanishing momentum transfer. This can be used to disentangle g' and $M_{Z'}$, as well as studying if the new interaction is flavor-diagonal or not. CEνNS is also a very good recent probe in this respect. The cross section in the presence of NSI depends on

$$\tilde{Q}^2_{i,\alpha} \equiv \left[N_i \left(-\frac{1}{2} + \epsilon^n_{\alpha\alpha} \right) + Z_i \left(\frac{1}{2} - 2s^2_W + \epsilon^p_{\alpha\alpha} \right) \right]^2 + \sum_{\beta \neq \alpha} \left[N_i \epsilon^n_{\alpha\beta} + Z_i \epsilon^p_{\alpha\beta} \right]^2 . \tag{3.11}$$

This expression is only valid for $M_{Z'} \gg q \simeq 10\,\text{MeV}$, otherwise a suppression $\epsilon \to \epsilon M^2_{Z'}/q^2$ occurs [149].

Obtaining the effective NSI Lagrangian by integrating out the Z and Z' gauge boson yields

$$\mathcal{L}_{\text{eff}} = -\sum_{i=1,2} \frac{1}{2M_i^2} \left(e j_{\text{EM}}\, a_i + \frac{e}{2\hat{s}_W \hat{c}_W} j_{\text{NC}}\, b_i + g' j'\, d_i \right)^2 . \tag{3.12}$$

The final result for the NSI parameters is then:

$$\begin{aligned}
\epsilon^e_{\alpha\beta} &= \sum_{i=1,2} q_{\alpha\beta} \frac{g' d_i}{\sqrt{2} M_i^2 G_F} \left(-e a_i + \frac{e b_i}{2 s_W c_W} \left(-\frac{1}{2} + 2 s^2_W \right) + g' d_i \frac{\partial j'_\alpha}{\partial \overline{e} \gamma_\alpha e} \right), \\
\epsilon^u_{\alpha\beta} &= \sum_{i=1,2} q_{\alpha\beta} \frac{g' d_i}{\sqrt{2} M_i^2 G_F} \left(\frac{2}{3} e a_i + \frac{e b_i}{2 s_W c_W} \left(\frac{1}{2} - \frac{4}{3} s^2_W \right) + g' d_i \frac{\partial j'_\alpha}{\partial \overline{u} \gamma_\alpha u} \right), \\
\epsilon^d_{\alpha\beta} &= \sum_{i=1,2} q_{\alpha\beta} \frac{g' d_i}{\sqrt{2} M_i^2 G_F} \left(-\frac{1}{3} e a_i + \frac{e b_i}{2 s_W c_W} \left(-\frac{1}{2} + \frac{2}{3} s^2_W \right) + g' d_i \frac{\partial j'_\alpha}{\partial \overline{d} \gamma_\alpha d} \right).
\end{aligned} \tag{3.13}$$

The terms d_i take into account the possibility that the Z' might couple to first generation charged particles. As we will show, the results depend on whether there is Z-Z' mixing, and also on the type of mixing.

$U(1)_X$	$\epsilon_{ee}^{p+n} - \epsilon_{\mu\mu}^{p+n}$	$\epsilon_{\tau\tau}^{p+n} - \epsilon_{\mu\mu}^{p+n}$	$M_{Z'}/\lvert g'\rvert$
$B - 3L_\tau$	0	$-\frac{3(g')^2}{\sqrt{2}G_F M_{Z'}^2}$	$> 4.8\,\text{TeV}$
$B - \frac{3}{2}(L_\mu + L_\tau)$	$+\frac{3(g')^2}{2\sqrt{2}G_F M_{Z'}^2}$	0	$> 360\,\text{GeV}$
$B - 3L_\mu$	$+\frac{3(g')^2}{\sqrt{2}G_F M_{Z'}^2}$	$+\frac{3(g')^2}{\sqrt{2}G_F M_{Z'}^2}$	$> 1.0\,\text{TeV}$

Table 3.1: Examples for NSI from electrophobic anomaly-free $U(1)_X$ without Z-Z' mass mixing, as well as the NSI limit on the Z' mass and coupling. See Fig. 3.2 for additional limits on the parameter space.

Vanishing Z-Z' mixing

Assuming negligible Z-Z' mixing, one finds

$$\epsilon_{ee}^{p,n} - \epsilon_{\mu\mu}^{p,n} = -\frac{(g')^2}{2\sqrt{2}G_F M_{Z'}^2} r_{BL}(2r_{\mu e} + r_{\mu\tau})\,, \tag{3.14}$$

$$\epsilon_{\tau\tau}^{p,n} - \epsilon_{\mu\mu}^{p,n} = -\frac{(g')^2}{2\sqrt{2}G_F M_{Z'}^2} r_{BL}(2r_{\mu\tau} + r_{\mu e})\,, \tag{3.15}$$

$$\epsilon_{ee}^{e} - \epsilon_{\mu\mu}^{e} = +\frac{(g')^2}{2\sqrt{2}G_F M_{Z'}^2} (r_{BL} + r_{\mu e})(2r_{\mu e} + r_{\mu\tau})\,, \tag{3.16}$$

$$\epsilon_{\tau\tau}^{e} - \epsilon_{\mu\mu}^{e} = +\frac{(g')^2}{2\sqrt{2}G_F M_{Z'}^2} (r_{BL} + r_{\mu e})(2r_{\mu\tau} + r_{\mu e})\,. \tag{3.17}$$

Neutral matter implies that the sum $\epsilon^p + \epsilon^e$ is crucial:

$$(\epsilon_{ee}^{p} + \epsilon_{ee}^{e}) - (\epsilon_{\mu\mu}^{p} + \epsilon_{\mu\mu}^{e}) = +\frac{(g')^2}{2\sqrt{2}G_F M_{Z'}^2} r_{\mu e}(2r_{\mu e} + r_{\mu\tau})\,, \tag{3.18}$$

$$(\epsilon_{\tau\tau}^{p} + \epsilon_{\tau\tau}^{e}) - (\epsilon_{\mu\mu}^{p} + \epsilon_{\mu\mu}^{e}) = +\frac{(g')^2}{2\sqrt{2}G_F M_{Z'}^2} r_{\mu e}(2r_{\mu\tau} + r_{\mu e})\,. \tag{3.19}$$

Non-vanishing NSI in oscillations without Z-Z' mixing thus require either $r_{BL} \neq 0$ or $r_{\mu e} \neq 0$. Fig. 3.2 shows constraints on some examples, together with various other limits. If muons are involved, the Z' contributes to the anomalous magnetic moment of the muon. We also give the limits in Tab. 3.1. In all cases neutrino oscillations provide the strongest limits for light Z', $M_{Z'} = \mathcal{O}(1 - 100)$ MeV, and NSI with a strength that might impair future neutrino oscillation experiments can not be excluded. Also, coherent scattering is very relevant here.

Moving on from the electrophobic NSI to Z' scenarios with electron couplings, limits are given in Tab. 3.2. In particular, positron-electron collisions apply here, see Fig. 3.3. An interesting limit is $r_{\mu e} \simeq +r_{BL} \neq 0$, i.e. there are no NSI in the Earth, but one could still have effects in solar neutrino oscillations. This corresponds to the case $\eta \simeq -44^\circ$ analyzed in Ref. [145], where it was shown that this scenario indeed severely weakens NSI constraints. Analogously, one can easily imagine a scenario with non-vanishing NSI inside

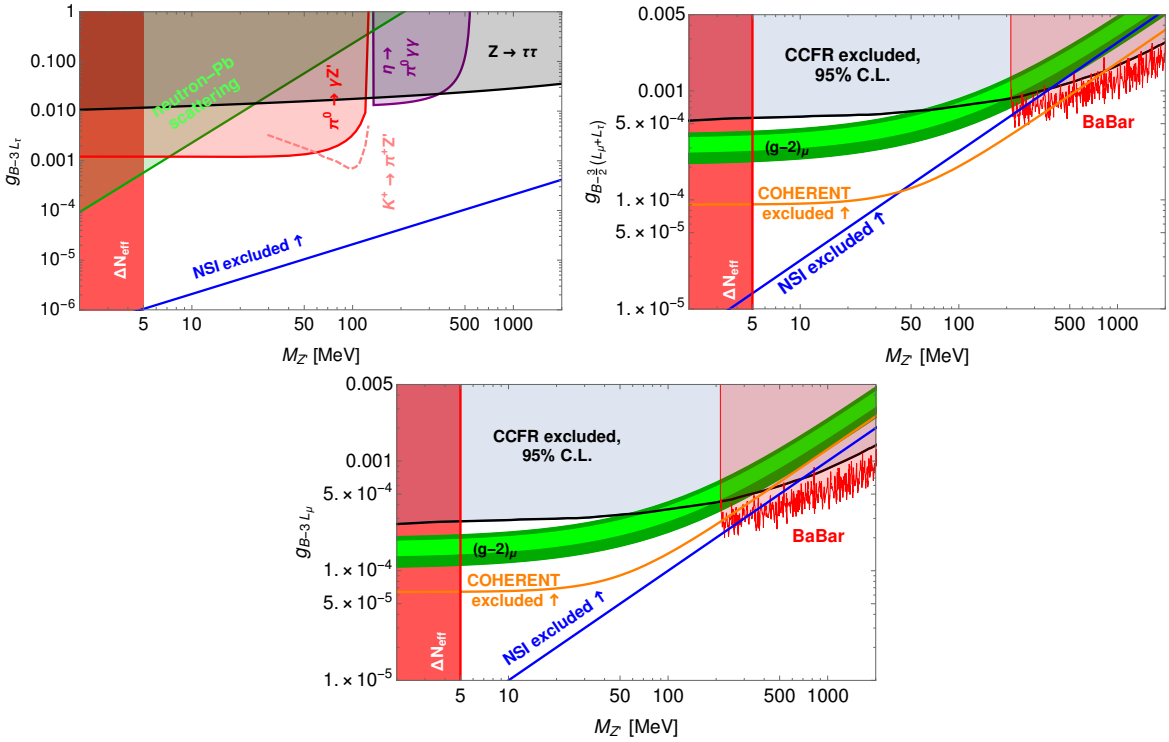

Figure 3.2: Limits on gauge coupling and Z' mass on various electrophobic Z' models without Z-Z' mass mixing. Taken from Ref. [144].

Earth but with $\epsilon \simeq 0$ at one specific radius inside the Sun. This again weakens the NSI bounds and makes other experimental probes, such as neutrino scattering off electrons and nucleons, more important.

Non-vanishing Z-Z' mixing

To see the effect of Z-Z' mixing, let us consider a simple $U(1)_X$ under which no matter particles are charged. This singles out $U(1)_{L_\mu - L_\tau}$ [29–31]. In this case we find for protons, neutrons and electrons that

$$\begin{aligned}
\epsilon^n_{\alpha\beta} &= \sum_{i=1,2} q_{\alpha\beta} \frac{e g' d_i}{\sqrt{2} M_i^2 G_F} \frac{b_i}{2 s_W c_W} \left(-\frac{1}{2}\right), \\
\epsilon^p_{\alpha\beta} &= \sum_{i=1,2} q_{\alpha\beta} \frac{e g' d_i}{\sqrt{2} M_i^2 G_F} \left(a_i + \frac{b_i}{2 s_W c_W} \left(\frac{1}{2} - 2 s_W^2\right)\right), \\
\epsilon^e_{\alpha\beta} &= \sum_{i=1,2} q_{\alpha\beta} \frac{e g' d_i}{\sqrt{2} M_i^2 G_F} \left(-a_i - \frac{b_i}{2 s_W c_W} \left(\frac{1}{2} - 2 s_W^2\right)\right),
\end{aligned} \tag{3.20}$$

where now $q = \mathrm{diag}(0, 1, -1)$. From these expressions one sees that in electrically neutral matter

$$\epsilon^p_{\alpha\beta} + \epsilon^e_{\alpha\beta} = 0 \tag{3.21}$$

$U(1)_X$	$\epsilon_{ee}^{e+p} - \epsilon_{\mu\mu}^{e+p}$	$\epsilon_{ee}^{n} - \epsilon_{\mu\mu}^{n}$	$M_{Z'}/\lvert g'\rvert$ (TEXONO)	$M_{Z'}/\lvert g'\rvert$ (NSI)
$B - 3L_e$	$+\frac{3(g')^2}{\sqrt{2}G_F M_{Z'}^2}$	$-\frac{3(g')^2}{2\sqrt{2}G_F M_{Z'}^2}$	$> 2\,\text{TeV}$	$> 0.2\,\text{TeV}$
$U(1)_X$	$\epsilon_{ee}^{e} - \epsilon_{\mu\mu}^{e}$	$\epsilon_{\tau\tau}^{e} - \epsilon_{\mu\mu}^{e}$	$M_{Z'}/\lvert g'\rvert$ (TEXONO)	$M_{Z'}/\lvert g'\rvert$ (NSI)
$L_e - L_\mu$	$+\frac{(g')^2}{\sqrt{2}G_F M_{Z'}^2}$	$+\frac{(g')^2}{2\sqrt{2}G_F M_{Z'}^2}$	$> 0.7\,\text{TeV}$	$> 0.3\,\text{TeV}$
$L_e - L_\tau$	$+\frac{(g')^2}{2\sqrt{2}G_F M_{Z'}^2}$	$-\frac{(g')^2}{2\sqrt{2}G_F M_{Z'}^2}$	$> 0.7\,\text{TeV}$	$> 1.4\,\text{TeV}$

Table 3.2: Examples for NSI from electrophilic anomaly-free $U(1)_X$ without Z-Z' mass mixing, as well as the TEXONO e-ν-scattering limit [150] on the Z' mass and coupling and approximate NSI constraints.

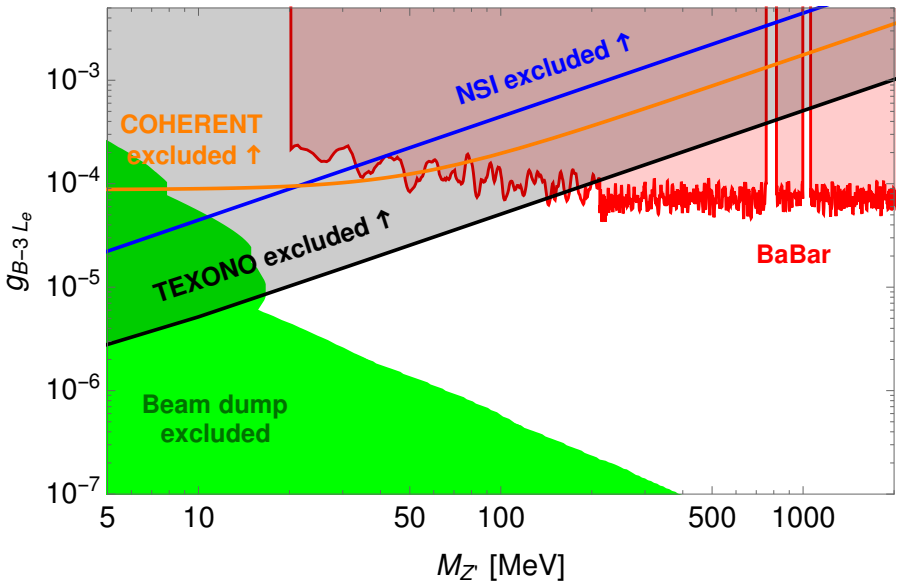

Figure 3.3: Constraints on $U(1)_{B-3L_e}$. Taken from Ref. [144].

holds, that is, only NSI with neutrons are important. Note that this result only needs an $U(1)'$ model with Z-Z' mixing and no coupling to electrons, up- or down-quarks, i.e., it is not unique to $L_\mu - L_\tau$.

Using Eqs. (3.3-3.5) to calculate the neutron part, we find:

$$\begin{aligned}\sum_{i=1,2} \frac{d_i b_i}{M_i^2} &= \frac{1}{c_\chi}\left[c_\xi s_\xi \left(\frac{1}{M_1^2} - \frac{1}{M_2^2}\right) + s_W t_\chi \left(\frac{s_\xi^2}{M_1^2} + \frac{c_\xi^2}{M_2^2}\right)\right] \\ &= \frac{\delta\hat{M}^2}{(\delta\hat{M}^2)^2 - \hat{M}_{Z'}^2\hat{M}_Z^2} = -\frac{\delta\hat{M}^2}{M_1^2 M_2^2 c_\chi^2}.\end{aligned} \tag{3.22}$$

Therefore, without mass mixing $\delta\hat{M}^2$, NSI effects are absent in neutrino oscillations. Mass mixing is required, which is model-building-wise a larger problem. Effects in neutrino scattering experiments are of course still present in case of kinetic mixing. For $L_\mu - L_\tau$

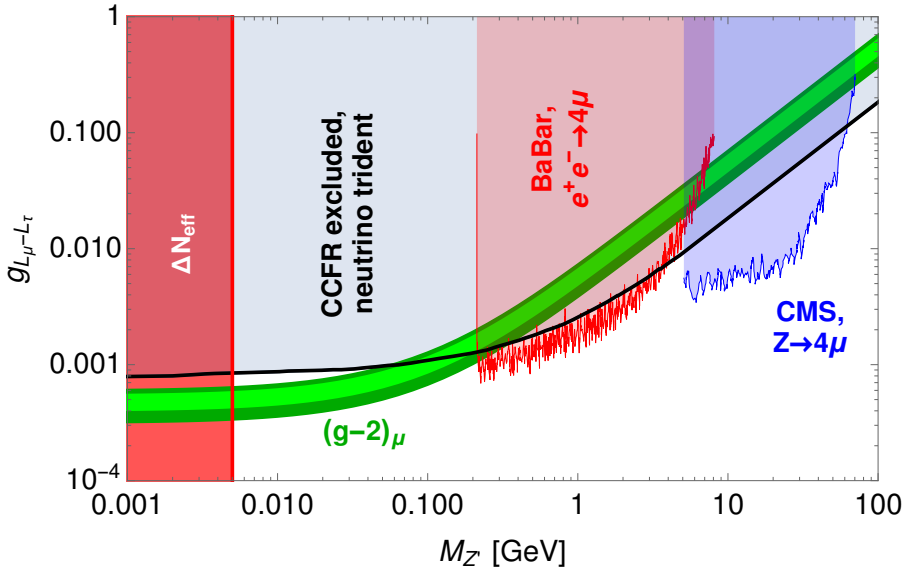

Figure 3.4: Constraints on $U(1)_{L_\mu - L_\tau}$ without any Z-Z' mixing. Taken from Ref. [144].

and only mass mixing, the result is

$$\epsilon^n_{\tau\tau} - \epsilon^n_{\mu\mu} = 2(\epsilon^n_{ee} - \epsilon^n_{\mu\mu}) = -2\frac{eg'}{4\sqrt{2}G_F s_W c_W}\frac{\delta\hat{M}^2}{M_Z^2 M_{Z'}^2 c_\chi^2}\,, \tag{3.23}$$

where we denote $M_{1,2} \to M_{Z,Z'}$.

To sum up, the origin of NSI may be a flavor-sensitive $U(1)'$. There is an interesting interplay of scattering and oscillation experiments, which can disentangle the effects of coupling and new gauge boson mass. In case there is no direct coupling of the Z' to first generation matter particles, the type of Z-Z' mixing is crucial. Mass mixing alone can not generate a NSI effect in oscillations. This is interesting, as mass mixing requires a scalar multiplet charged under the SM and the new $U(1)'$ symmetries. For $L_\mu - L_\tau$ the simplest example would be a doublet ϕ' with charge $q_{\phi'}$, leading to

$$\epsilon^n_{\tau\tau} - \epsilon^n_{\mu\mu} = 2(\epsilon^n_{ee} - \epsilon^n_{\mu\mu}) = -\frac{1}{2\sqrt{2}G_F}\left(\frac{eg'}{s_W c_W}\right)^2 \frac{q_{\phi'}\langle\phi'\rangle^2}{M_Z^2 M_{Z'}^2 c_\chi^2}\,. \tag{3.24}$$

Such a particle would lead to off-diagonal terms in the charged lepton mass matrix and thus LFV decays. With additional parameters, it influences the phenomenology of the SM Higgs.

Thus, the typically only effectively treated NSI effects in neutrino oscillations require a broad approach to identify their origin, with a broad portfolio of flavor, scattering and other probes.

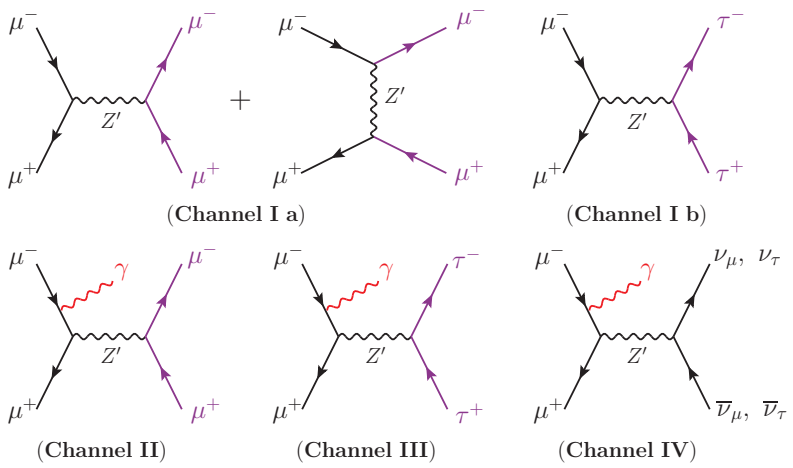

Figure 3.5: Feynman diagrams to probe gauged $L_\mu - L_\tau$ at a muon collider. Detectable final states are in purple and red.

3.3 Gauged $L_\mu - L_\tau$ at a Muon Collider

The previous section dealt with flavor-dependent $U(1)'$ gauge symmetries, including the arguably best-motivated case of $L_\mu - L_\tau$. If the mass of the Z' is large, collider constraints are much weaker than the ones for Z' coupling to first-generation particles. Hence, a muon collider is an attractive facility to probe this parameter space. Muon colliders [151–154] have recently received again attention as a powerful new machine to test the SM and BSM theories [155–164]. In particular muon-specific models are easy to test, and it was found in particular that a "reasonable" machine is guaranteed to probe any new physics solution to the anomalous magnetic moment of the muon [161]. Moreover, the extension of $L_\mu - L_\tau$ to the quark sector is equally interesting to study at future muon colliders, as the long-standing B anomalies may be probed, see Sec. 3.4.

The gauge interactions with the new boson Z' are

$$\mathcal{L} \supset g' \left(\overline{L} q \gamma^\mu L + \overline{\ell_{\mathrm{R}}} q \gamma^\mu \ell_{\mathrm{R}} \right) Z'_\mu \,, \tag{3.25}$$

where g' is the coupling constant, $L \equiv (\nu_L, \ell_L)^{\mathrm{T}}$ is the lepton doublet with ν and ℓ being the neutrino and charged lepton fields, respectively, and $q = \mathrm{Diag}(0, 1, -1)$ denotes the charge in the flavor basis of (e, μ, τ). Loop-level induced γ-Z' mixing is of order $10^{-6}\, g' \,(100 \text{ GeV}/M_{Z'})^2$ and thus negligible. Relevant production channels for a muon collider are given in Fig. 3.5. Taking a muon collider setup with $\sqrt{s} = 3$ TeV and $L = 1$ ab^{-1} luminosity is motivated by presentations of the Muon Collider Working Group [153]. For the $2 \to 2$ processes $\mu^+\mu^- \to \ell^+\ell^-$ we can write the amplitude as a sum of different mediators:

$$\mathcal{M} = \mathcal{M}_\gamma + \mathcal{M}_Z + \mathcal{M}_{Z'} \,. \tag{3.26}$$

For instance, in the tau-channel we have

$$\left(\frac{\mathrm{d}\sigma}{\mathrm{d}\Omega}\right)_{\gamma Z'} = \frac{e^2 g'^2}{16\pi^2 s} \frac{(s - M_{Z'}^2)(t^2 + u^2)}{s[(s - M_{Z'}^2)^2 + \Gamma_{Z'}^2 s^2/M_{Z'}^2]} \,, \tag{3.27}$$

which dominates the new physics contribution for small g'. If $\sqrt{s} \simeq M_{Z'}$ the Breit-Wigner resonance dominates:

$$\left(\frac{\mathrm{d}\sigma}{\mathrm{d}\Omega}\right)_{Z'} = \frac{g'^4}{32\pi^2 s} \frac{(t^2 + u^2)}{(s - M_{Z'}^2)^2 + \Gamma_{Z'}^2 s^2/M_{Z'}^2} \,, \tag{3.28}$$

Here the width of the Z' is

$$\Gamma_{Z'} = \frac{g'^2 M_{Z'}}{4\pi}. \tag{3.29}$$

Besides this resonance in $\mu^+ + \mu^- \to \ell^+ + \ell^-$, the radiative return [165, 166] process of photon emission from an initial leg is in particular sensitive to values $M_{Z'} < \sqrt{s}$.

Using `CalcHEP` [167–169] we perform an analysis of the processes, details can be found in Ref. [170]. We will assume the efficiency of dimuon detection to be 100% [171,172] and that for ditau detection to be conservatively 70% [173]. In the chi-square function

$$\chi^2_{\mathrm{I}} = \sum_i \frac{(N_i - \widetilde{N}_i)^2}{N_i + \epsilon^2 \cdot N_i^2} \,, \tag{3.30}$$

where ϵ denotes the systematic uncertainty of 0.1% [158], we sum over polar angle bins of $\Delta \cos\theta = 0.1$; N_i is the expected total event number of signal and background, $\widetilde{N}_i$ is the assumed event number. The signal from $\mu^+ + \mu^- \to \ell + \overline{\ell} + \gamma$ is a bump above the background in the invariant mass ($m_{\ell\overline{\ell}}$) spectrum of the dileptons, smeared by energy resolution. The values are $\Delta m_{\mu^+\mu^-} \simeq 5 \times 10^{-5}$ GeV$^{-1} \cdot s$ [174] and for photons we assume [175]:

$$\frac{\Delta E_\gamma}{E_\gamma} = \sqrt{\left(\frac{2.8\%}{\sqrt{E_\gamma}}\right)^2 + \left(\frac{0.12}{E_\gamma}\right)^2 + (0.3\%)^2} \,. \tag{3.31}$$

which can be translated in a superior $m_{\mu^+\mu^-}$ resolution via $E_\gamma = (s - m_{\ell\overline{\ell}}^2)/(2\sqrt{s})$. Note that initial state radiation has an $\ln(\sqrt{s}/p_\gamma^{\mathrm{T,cut}})$ enhancement for $p_\gamma^{\mathrm{T,cut}}$ being the transverse momentum of the photon within the detector acceptance.

Our analysis yields Fig. 3.6. Existing bounds on $L_\mu - L_\tau$ span a wide range of masses, see Ref. [170] for a summary. The parameter spaces explaining the $(g-2)_\mu$ and B anomalies (taken from [132]) are given as the yellow and blue bands, respectively. Note that these B parameters do not take any coupling to bs quarks into account. For $M_{Z'} > 100$ GeV, the parameter space favored by the B anomalies is entirely covered by the projection of muon collider. If a Z' signal was found, one may wonder if it is indeed a gauged $L_\mu - L_\tau$

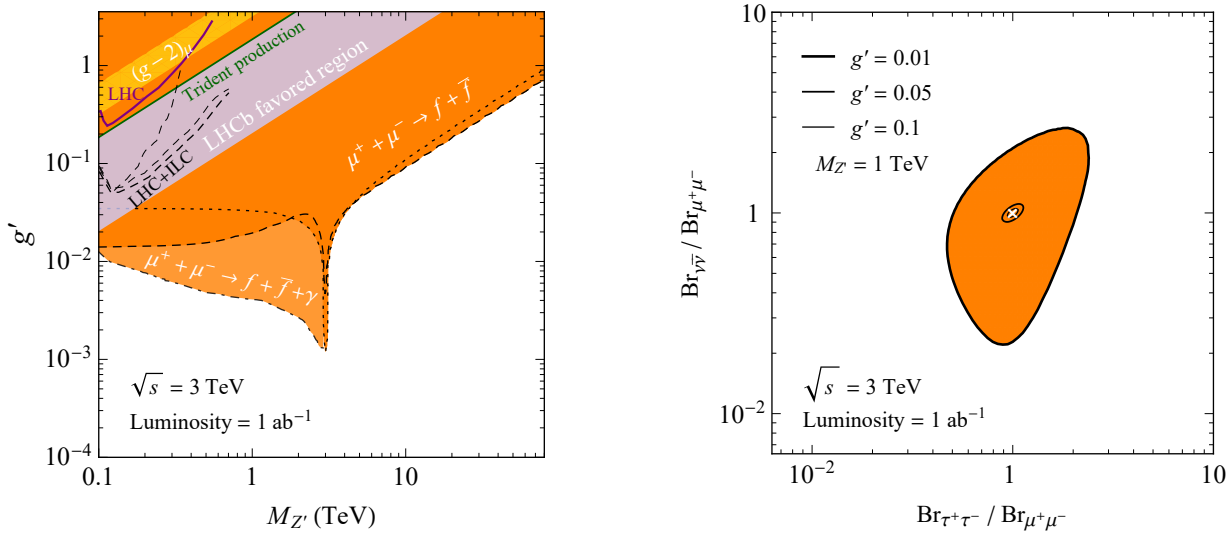

Figure 3.6: The sensitivity of the muon collider with a center-of-mass energy $\sqrt{s} = 3$ TeV and luminosity 1 ab^{-1} with and without a Z' signal. In the left plot, the darker orange region is obtained from $\mu^+ + \mu^- \to \ell^+ + \ell^-$, and the lighter orange region from $\mu^+ + \mu^- \to \mu^+ + \mu^- + \gamma$, $\mu^+ + \mu^- \to \tau^+ + \tau^- + \gamma$ and $\mu^+ + \mu^- \to \nu + \overline{\nu} + \gamma$. Indicated are the 2σ parameter space from $(g-2)_\mu$ in yellow, and the one for the LHCb B anomalies [132] is also plotted. Neutrino trident production limit is given as the green curve [176], and a recast LHC bound in purple [177]. The projection of LHC and ILC with different channels is given in three dashed black curves [178]. In the right panel, we choose $M_{Z'} = 1$ TeV and g' is taken to be 0.01, 0.05 and 0.1 (from outer to inner). The white cross is the prediction of $L_\mu - L_\tau$.

model or some other Z' model. This can be achieved by comparing the branching ratios. In the right panel of Fig. 3.6, we show for $M_{Z'} = 1$ TeV the 2σ allowed region for $\mathrm{Br}_{f\bar{f}}/\mathrm{Br}_{\mu^+\mu^-}$.

Thus, the parameter space above 100 GeV explaining the anomalous magnetic moment of the muon, as well as the B meson anomalies, is fully covered by the muon collider setup, adding further motivation to the facility. However, the processes considered here involves only leptons, for a decisive test of the B anomalies one has to include the quark sector. This is subject of the next section.

3.4 An Extension to the Quark Sector: The $R_{K^{(*)}}$ Anomaly

Finally, we discuss an extension to the quark sector. Here the motivation lies in long-standing anomalies in the B meson sector. The ratios R_K and R_{K^*} are defined as

$$R_K = \frac{\mathrm{BR}(B^+ \to K^+\mu^+\mu^-)}{\mathrm{BR}(B^+ \to K^+e^+e^-)}\,, \quad R_{K^\star} = \frac{\mathrm{BR}(B^0 \to K^{\star 0}\mu^+\mu^-)}{\mathrm{BR}(B^0 \to K^{\star 0}e^+e^-)}\,. \tag{3.32}$$

As many hadronic uncertainties are expected to cancel, the ratios are of particular interest as tests of lepton flavor universality. Results [179–182] on the ratios display a long-standing $> 3\sigma$ conflict with the SM prediction [183–186]. As the measurements are smaller than the SM expectation, one has the choice of of increasing $b \to se^+e^-$ decay or decreasing $b \to s\mu^+\mu^-$, the latter possibility being much more in agreement with other data [187].

An effective Lagrangian of the form

$$\mathcal{L}^{\mathrm{NP}}_{b\to s\mu\mu} \supset \frac{4G_\mathrm{F}}{\sqrt{2}} V_{tb}V_{ts}^* \left(C_9^\mu O_9^\mu + C_{10}^\mu O_{10}^\mu\right) + h.c., \tag{3.33}$$

with the CKM matrix V and operators

$$O_9^\mu = \frac{\alpha}{4\pi}\left(\bar{s}_\mathrm{L}\gamma_\mu b_\mathrm{L}\right)\left(\bar{\mu}\gamma^\mu\mu\right), \quad O_{10}^\mu = \frac{\alpha}{4\pi}\left(\bar{s}_\mathrm{L}\gamma_\mu b_\mathrm{L}\right)\left(\bar{\mu}\gamma^\mu\gamma_5\mu\right), \tag{3.34}$$

can explain the anomalies, where $C_9 = -C_{10} = -0.43$ [187, 188].

As a typical model [189–211], one introduces a Z' which dominantly couples to left-handed bs and $\mu^+\mu^-$ pairs:

$$\mathcal{L}_{Z'} \supset \left(\lambda^\mathrm{Q}_{23}\bar{b}_\mathrm{L}\gamma^\mu s_\mathrm{L} + \lambda^\mathrm{L}_{22}\bar{\mu}_L\gamma^\mu\mu_\mathrm{L}\right) Z'_\mu\,. \tag{3.35}$$

This interaction can, and is frequently being, obtained from $L_\mu - L_\tau$ models, in which necessary scalars and/or additional particles to break the symmetry generate a bs-coupling, see e.g. [99]. Integrating out the Z' field, the Wilson-coefficients at the scale $\mu = M_{Z'}$ are

$$C_9^\mu = -C_{10}^\mu = -\frac{\pi}{\sqrt{2}G_\mathrm{F}M_{Z'}^2\alpha}\left(\frac{\lambda^\mathrm{Q}_{23}\lambda^\mathrm{L}_{22}}{V_{tb}V_{ts}^*}\right). \tag{3.36}$$

Several limits on the scenario, see [212, 213], leave a narrow range of allowed parameters, as given in the yellow band in Fig. 3.7. LHC searches are not particularly relevant if only the two couplings λ^Q_{23} and λ^L_{22} are present, and this a muon collider is the definite machine to test this scenario in a definite manner [214].

The signal of interest is therefore $\mu\mu \to bs$. The bs signal is mimicked by SM dijet background from $\mu^+\mu^- \to jj$, where j can be any quark, except the top, whose b-momentum is always much smaller than $\sqrt{s}/2$. Efficiently tagging the b-jet and avoiding mistags of light

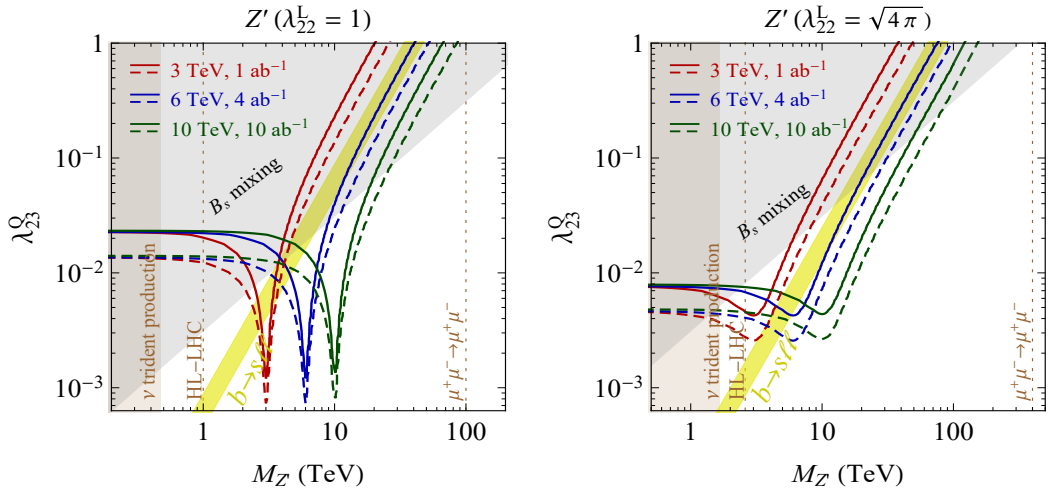

Figure 3.7: Sensitivity of a muon collider for a Z' coupling only to $\mu\mu$ and bs pairs. Assumed setups are $\sqrt{s} = 3$ TeV with $L = 1$ ab^{-1} (red curves), $\sqrt{s} = 6$ TeV with $L = 4$ ab^{-1} (blue), and $\sqrt{s} = 10$ TeV with $L = 10$ ab^{-1} (green). The 2σ parameter space to explain the B anomalies is in yellow [188]. Dashed (solid) lines are with (without) flavor tagging. Various other limits from B_s mixing [212], trident production [176], LHC dimuon resonance searches [223], as well as the projected sensitivity of HL-LHC [178] are also given. Taken from Ref. [214].

quarks as b quarks is thus necessary. Using $\epsilon_b = 70\%$ [215] and mistag rates $\epsilon_{uds} = 1\%$ as well as $\epsilon_c = 10\%$ for c quarks [216–218], we perform our analysis [214] with three collider setups with center-of-mass energies and luminosities, namely $(\sqrt{s}, L) = (3\text{ TeV}, 1\text{ ab}^{-1})$, $(6\text{ TeV}, 4\text{ ab}^{-1})$ and $(10\text{ TeV}, 10\text{ ab}^{-1})$. We apply `FeynCalc` [219–221] and `FeynArts` [222] for the numerical calculations of the scattering amplitudes. The statistical significance is measured in analogy to the previous section, the assumed systematic uncertainty is taken as 0.1% [158], and we will present results with and without flavor tagging.

The result is given in Fig. 3.7. There is a resonance near the center-of-mass energy, depending on $\Gamma = (2|\lambda^{\rm L}_{22}|^2 + 3|\lambda^{\rm Q}_{23}|^2)/(12\pi)$. Constraints from B_s mixing imply large $\lambda^{\rm L}_{22}$. For masses smaller than the center-of-mass energy there is no dependence on the mediator mass. With $L \propto s$, the event number is constant for $\sigma(s) \propto s^{-1}$ at large momentum transfer. In the regime of Z' masses much larger than $\sqrt{s}$ the results are valid for all realizations of the effective operators in Eq. (3.33). Recall that the dimuon signal from $\mu^+\mu^- \to \mu^+\mu^-$ is able to cover all values explaining the B anomalies [170], see the previous section. In this case, the inclusion of $\mu^+\mu^- \to b\bar{s}$ helps to clarify that the new physics is indeed what causes the B anomalies.

For $\lambda^{\rm L}_{22} = 1$ a window between HL-LHC and the muon collider setup with $\sqrt{s} = 3$ TeV may survive, which however will be covered by radiative return $\mu^+\mu^- \to bs\gamma$. For $\lambda^{\rm L}_{22} = \sqrt{4\pi}$, the muon collider with $\sqrt{s} = 6$ TeV will rule out most of the favored parameter space. Combining the HL-LHC and the muon collider sensitivities we observe that there is only a small corner of the parameter space left.

Chapter 4

Phenomenology of new Fermions

This section deals with new fermions related to neutrinos. The standard case of super-heavy see-saw neutrinos is well known and we have little to add. Instead, we will assume light new states that are accessible in low energy experiments like COHERENT and KATRIN. Moreover, as an extension to the quark sector we will introduce leptoquarks that couple to right-handed neutrinos, which are assumed to be dark matter particles.

4.1 Generics

New fermions are typically the most common new particles related to neutrino physics. The most obvious choice is a right-handed neutrino, for which a Majorana mass term M_R is allowed. Together with the Dirac mass term m_D from the L-Φ-N_R coupling, light neutrinos have a Majorana mass given by m_D^2/M_R and thus are universally suppressed for all three generations. This is the type I seesaw mechanism [12–16]. While naively for $m_D \sim v$ and $m_\nu \sim 0.1$ eV the new energy scale is $M_R \sim 10^{15}$ GeV, there are many ways around this argument. The new fermions do not need to be connected to neutrino mass, they may have masses much below the close-to-GUT scale, etc. "Motivated" scales are keV, where these singlets may be warm dark matter particles, or TeV, where they may be accessible at colliders or even be WIMPs (if made stable). The right-handed singlet neutrinos may even be Dirac particles. A summary of limits can be found in Fig. 4.1. Of course, the sterile neutrinos may be part of an UV-complete framework in which they couple to their own gauge sector. Examples are theories based on gauged $B - L$, or left-right symmetric theories.

In this chapter we will discuss three different mass scales, MeV, keV and TeV, and confront the scenarios with various limits in various processes.

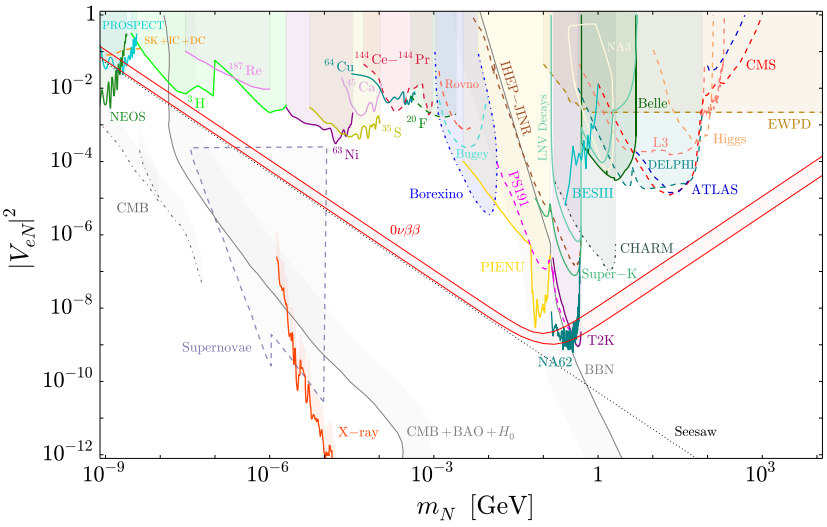

Figure 4.1: Constraints on the mass of a sterile neutrino and its mixing with electron neutrinos from a variety of astroparticle and particle physics searches. Taken from [224].

4.2 A new Fermion in Coherent Elastic Neutrino-Nucleus Scattering

Our first new fermion is called χ and is produced in CEνNS when a neutrino scatters with a nucleus N [225]:

$$\nu N \to \chi N \,.$$

To be produced, the mass of χ should not exceed the MeV-scale. The Lagrangian is

$$\mathcal{L} \supset y_\chi \bar{\chi} S \nu + y_N \bar{N} S N \,, \tag{4.1}$$

where y_χ, y_N are Yukawa constants and the mediator S is taken to be a scalar for definiteness [97]. In what follows we will discuss the constraints arising from CEνNS on the relevant parameters, and also investigate the role of χ in neutrino mass generation and in dark matter.

Let us first derive the CEνNS cross section: toward this end we need a relation between the recoil energy T and the angle of the outgoing nucleus with respect to the incoming neutrino:

$$\cos\theta = \frac{E_\nu T + MT + m_\chi^2/2}{E_\nu \sqrt{(M+T)^2 - M^2}} \,. \tag{4.2}$$

In Fig. 4.2 we plot the relation for some specific values of m_χ. The scattering angle lies within $\cos\theta_{\max} \leq \cos\theta \leq 1$, where

$$\cos\theta_{\max} = \frac{m_\chi \sqrt{4M\,(E_\nu + M) - m_\chi^2}}{2ME_\nu} \,, \qquad T_{\theta\max} = \frac{Mm_\chi^2}{2ME_\nu - m_\chi^2 + 2M^2} \,. \tag{4.3}$$

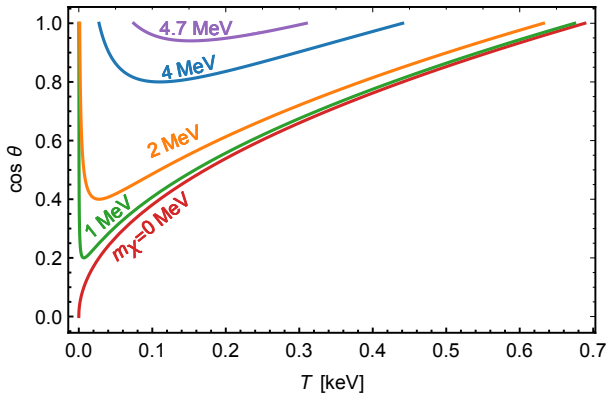

Figure 4.2: Relation between $\cos\theta$ and T and a Germanium target hit with a $E_\nu = 5$ MeV neutrino. The case $m_\chi = 0$ is the standard one. Taken from Ref. [225].

Given a mass of χ, the minimal amount of energy is

$$E_\nu^{\min} = m_\chi + \frac{m_\chi^2}{2M}\,. \tag{4.4}$$

The exchanged scalar S is assumed to be massive with its mass denoted by m_S. With the combined coupling constant $y^4 = y_\chi^2 y_N^2$, the dimensionless quantity

$$K = \left(1 + \frac{T}{2M}\right)\left(\frac{MT}{E_\nu^2} + \frac{m_\chi^2}{2E_\nu^2}\right), \tag{4.5}$$

the definition

$$\bar{y} \equiv \frac{y}{\sqrt{A}} \simeq \begin{cases} \sqrt{\left|(0.56y_n + 0.44y_p)y_\chi\right|} & \text{(for Ge target)}\,, \\ \sqrt{\left|(0.58y_n + 0.42y_p)y_\chi\right|} & \text{(for CsI target)}\,, \end{cases} \tag{4.6}$$

where the Yukawa couplings of the scalar S to neutrons and protons are denoted with y_n and y_p respectively, the differential cross section reads

$$\frac{d\sigma}{dT} = \frac{|i\mathcal{M}|^2}{32\pi M E_\nu^2} = \frac{M\bar{y}^4}{4\pi A^2\left(2MT + m_S^2\right)^2} K\,. \tag{4.7}$$

Continuing with the production of χ in CEνNS experiments we will focus again on COHERENT and CONUS, using the same approach as before in Sec. 2.5. In Fig. 4.3 we present the event excess spectrum for several choices of $(\bar{y},\ m_\chi,\ m_S)$. The kinks of the red and blue curves appearing in the right panel at $T \simeq 14$ keV are caused by the monochromatic muon-neutrino flux in COHERENT. Confronting with existing COHERENT and prospective CONUS data, in analogy to Sec. 2.5, results in Fig. 4.4. In Fig. 4.5, we show for an example value the sensitivities of future versions of the experiments together with their current ones. A discussion on other limits on the scenario can be found in Ref. [225]

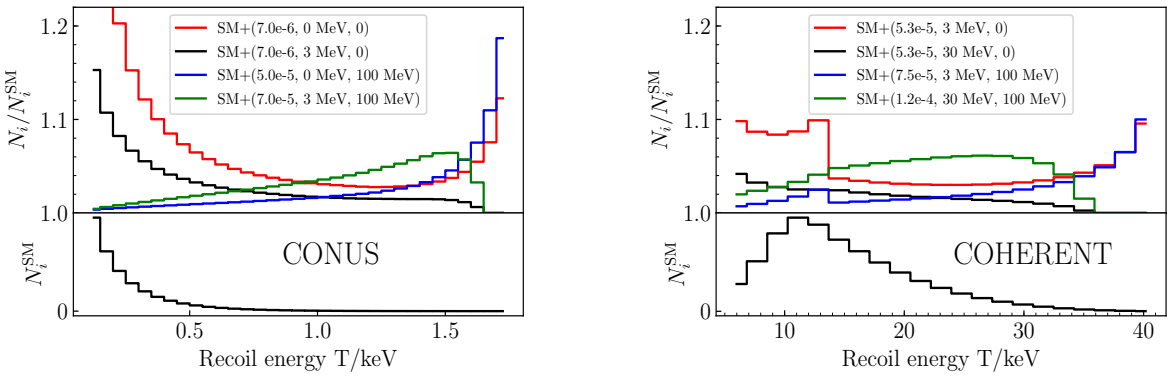

Figure 4.3: Event excess spectrum due to $\nu N \to \chi N$ in CONUS and COHERENT. Taken from Ref. [225].

(see also Sec. 2.5), it was found that sizable part of the parameter space is only reachable by coherent scattering.

Turning to neutrino mass generation, we can supplement the SM particle content with

$$\chi \sim (1,1,0)\,, \qquad N_R \sim (1,1,0)\,, \qquad S \sim (1,1,0)\,, \tag{4.8}$$

where our convention is $Q = I_3 + Y/2$, and χ and N_R are Majorana fermions and S is a real scalar. The relevant part of the Lagrangian reads

$$\mathcal{L} \supset y_1 \bar{N}_R \tilde{\Phi}^\dagger L + \frac{1}{2} M_N \bar{N}_R N_R^c + y_2\, \bar{\chi} \tilde{\Phi}^\dagger L + \frac{1}{2} m_\chi \bar{\chi}\, \chi^c + y_3\, \bar{\chi} S N_R^c + M_1 \bar{N}_R\, \chi^c + h.c.,$$

where y_i $(i = 1,2,3)$ are Yukawa couplings. After electroweak symmetry breaking, the neutral fermion mass matrix reads

$$\begin{pmatrix} \bar{\nu}_L^c & \bar{\chi} & \bar{N}_R \end{pmatrix} \begin{pmatrix} 0 & y_2 v & y_1 v \\ y_2 v & m_\chi & M_1 \\ y_1 v & M_1 & M_N \end{pmatrix} \begin{pmatrix} \nu_L \\ \chi^c \\ N_R^c \end{pmatrix}, \tag{4.9}$$

where $v \equiv \langle \Phi^0 \rangle = 174$ GeV and we assumed that S does not develop a non-vanishing vacuum expectation value. As demonstrated in Ref. [225], parameters that are compatible with all available laboratory constraints, and give an observable signal in coherent scattering, give a neutrino mass of order

$$\left(\frac{m_\nu}{0.1\,\text{eV}}\right) \simeq (1-x) \left(\frac{y_1}{10^{-7.25}}\right)^2 \left(\frac{\text{GeV}}{M_N}\right) + x \left(\frac{y_2}{10^{-8.75}}\right)^2 \left(\frac{\text{MeV}}{m_\chi}\right). \tag{4.10}$$

Here, $x \in [0,1]$ denotes relative contribution to the active neutrino mass from χ and N_R.

Finally, we can discuss dark matter in our framework. The MeV-scale for DM has recently gained considerable attention, see e.g. [226–231]. To cut the story short, eventually

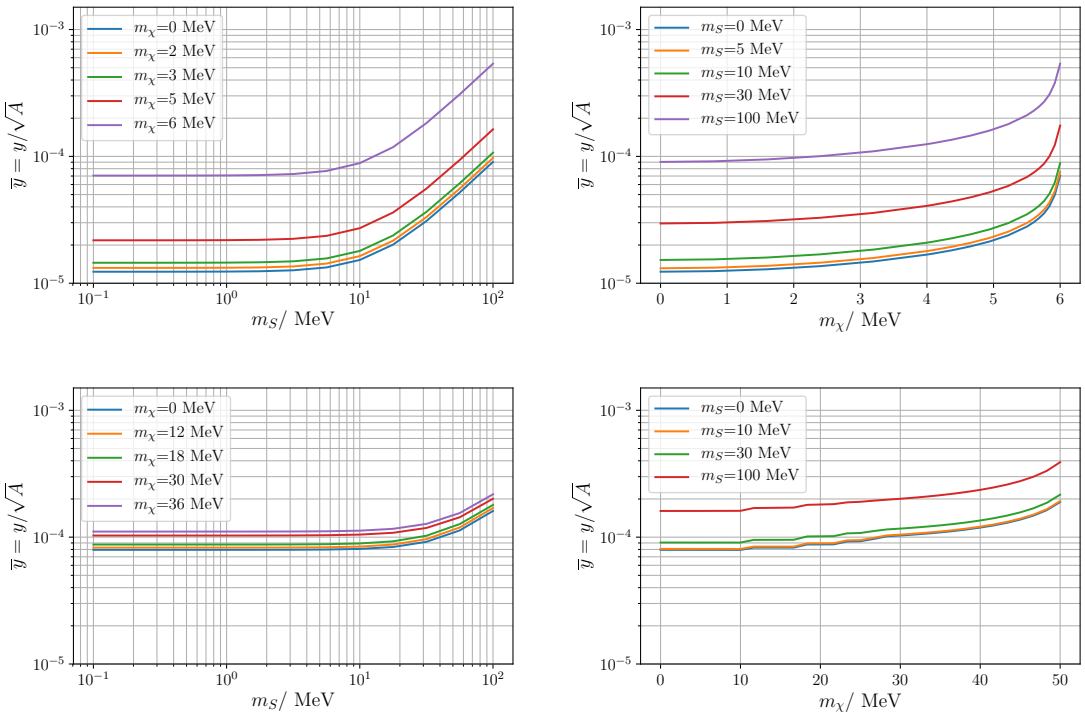

Figure 4.4: Constraints (with 90% C.L.) of CONUS (upper panels) and COHERENT (lower panels) in $\bar{y} - m_S$ (left panels) and $\bar{y} - m_\chi$ (right panels) parameter space. Taken from Ref. [225].

the parameter space leading to CEνNS would require a late-time entropy injection into the states in the thermal bath, for instance via decays of heavy scalars, in order not to overproduce the dark matter density.

To sum up, a new fermion coupling to light neutrinos can have interesting phenomenology in coherent scattering, contribute to neutrino mass and can have dark matter aspects.

4.3 Prospects for Finding Sterile Neutrino Dark Matter at KATRIN

Now we will focus on the fermionic DM at keV-scale. This DM candidate, produced from active neutrinos through oscillations and collisions, was suggested already in the 90s in the pioneering paper by Dodelson and Widrow [232]. Resonant conversion [233–235] in the presence of non-zero lepton asymmetries in the early Universe [236], was later suggested by Shi and Fuller. While the prime dark matter candidate is a WIMP, warm dark matter may solve some of the issues of cold dark matter scenario. A production of such a particle in the lab, in beta decay or electron capture, would obviously be of huge

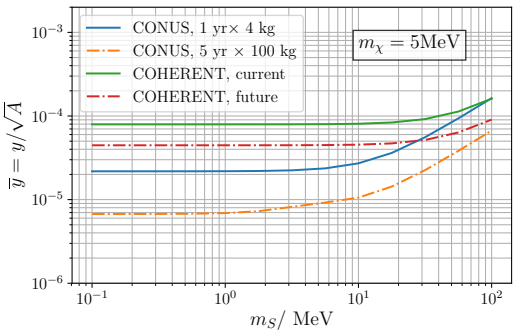

Figure 4.5: Future sensitivities of CONUS (5 yr × 100 kg exposure, 0.1 keV threshold) and COHERENT (statistics × 100) on the benchmark $m_\chi = 5$ MeV. Taken from Ref. [225].

interest. Making connection with the usual WIMP language, the production of sterile neutrinos is the analogue of collider searches. The direct detection analogue is probably too difficult a task as the cross section of non-relativistic sterile neutrinos in terrestrial detectors is tiny [248–251]. Indirect detection would be achieved by identifying their decay products, i.e. X-rays. We will not enter here the controversial discussion on the unidentified photon line at around 3.5 keV [237, 238], see e.g. Refs. [239–242], which can be interpreted as a decay signal of 7 keV sterile-neutrino dark matter.

In the Dodelson-Widrow scenario, one has [243]

$$\Omega_s h^2 \sim 0.12 \left(\frac{\sin^2 2\theta}{3.5 \cdot 10^{-9}} \right) \left(\frac{m_s}{7\,\text{keV}} \right), \tag{4.11}$$

where m_s and θ are the sterile neutrino mass and mixing angle, respectively. This has to be compared to future experimental sensitivities around $\sin^2 2\theta \sim 10^{-6}$ for a future setup of the KATRIN experiment. In its next stage, KATRIN will be equipped with a novel detector system, TRISTAN [244], which will look at the entire spectrum of the emitted electrons: in particular, if a keV sterile neutrino is produced in tritium decay, there will be a kink in the spectrum at an energy equal to the value of m_s. From Eq. (4.11), an observation in TRISTAN would mean that dark matter is overproduced. Moreover, strong astrophysical constraints [245–247] imply $\theta^2 \lesssim 10^{-10}$, leaving no chance for TRISTAN to observe anything. Our goal here is to avoid existing limits on keV-scale dark matter, as well as to push the mixing angle that generates the dark matter population up to the scale where future experiments are sensitive.

Starting with X-ray limits, those take advantage of the decay $\nu_s \to \nu\gamma$ and lead to limits around $\sin^2 2\theta \lesssim 10^{-10}$ for interesting sterile neutrino masses. We can reduce their strength by assuming keV-WDM is only part of the DM, the "cocktail" scenario. We can also diminish the rate of sterile neutrino decay. To demonstrate this, we introduce a scalar doublet $\Sigma = (\sigma^0, \sigma^-) \sim (1, 2, -1)$. The relevant part of the Lagrangian involving this state and ν_s reads

$$\mathcal{L} \supset \lambda\, \bar{\nu}_s \Sigma^\dagger L_e + \lambda'\, \bar{e}_R \tilde{\Sigma}^\dagger L_e + h.c., \tag{4.12}$$

where L_e is the electron lepton doublet. Those terms also imply $\nu_s \to \nu\gamma$ decays; complete cancellation between the SM and the Σ amplitude occurs when

$$\sin\theta = \left(\frac{-4\lambda\lambda'}{3g^2}\right)\frac{m_e}{m_s}\frac{m_{W_L}^2}{m_\Sigma^2}\left[\mathrm{Log}\left(\frac{m_e^2}{m_\Sigma^2}\right)+1\right]. \tag{4.13}$$

Taking $m_\Sigma \sim 1$ TeV and $\sin\theta \sim 10^{-4}$, which is in the ballpark of TRISTAN sensitivity, (4.13) yields $\lambda\lambda' \simeq 10^{-6}$ for $m_s \sim 1$ keV. If we do not want Σ to thermalize via coupling to ν_s and electrons, reheating should occur at sub-TeV temperatures. Such low-temperature reheating is consistent with our approach to be discussed next, namely that the production mechanism for sterile neutrinos stems from active to sterile neutrino oscillations at $T \lesssim 100$ MeV.

Another approach around strong X-ray limits is to decouple DM decay from beta decay [252]. Here, taking left-right symmetric models as an example, beta decay occurs predominantly via a heavy W_R boson. The decay of the keV-scale sterile neutrino DM can occur via small mixing θ, or via right-handed currents. When the dark matter particle is the lightest right-handed neutrino, only decays in active SM neutrinos are possible, which implies that the small mixing is dominant for the decay. DM decay and production in experiments are therefore decoupled.

Various structure formation, Lyman-α, 21-cm line and supernova bounds suffer from systematic effects and uncertainties, or do not apply due to the electron flavor we are interested in, hence only bounds from Milky Way satellite counts [253–255] will be added to the X-ray ones, see Ref. [256].

For the Dodelson-Widrow scenario the oscillation probability is

$$\langle P_m(\nu_\alpha \to \nu_s; p, t)\rangle = \frac{1}{2}\sin^2 2\theta_M\,, \tag{4.14}$$

where θ_M is the effective mixing angle in the thermal plasma [257]

$$\sin^2 2\theta_M = \frac{\Delta^2(p)\sin^2 2\theta}{\Delta^2(p)\sin^2 2\theta + D^2(p) + [\Delta(p)\cos 2\theta - V_T(p) - V_L(p)]^2}\,. \tag{4.15}$$

Here $\Delta(p) \simeq m_s^2/2p$, $D(p)$ quantifies loss of coherence due to collisions of ν_e in the plasma, and $V_T(p)$ is the thermal potential [254, 258]:

$$V_T(p,T) = \pm\sqrt{2}\,G_F\,\frac{2\,\zeta(3)\,T^3}{\pi^2}\frac{\eta_B}{4} - \frac{8\sqrt{2}\,G_F\,p}{3m_Z^2}(\rho_{\nu_e}+\rho_{\bar\nu_e}) - \frac{8\sqrt{2}\,G_F\,p}{3m_W^2}(\rho_{e^-}+\rho_{e^+})\,. \tag{4.16}$$

Here the upper (lower) sign holds for neutrinos (antineutrinos), $\zeta(x)$ is the Riemann ζ-function, $\eta_B = 6.05\times10^{-10}$ is the baryon asymmetry, ρ_x denotes the energy density of species x, m_Z and m_W are masses of weak gauge bosons and G_F is the Fermi constant. Finally, V_L is the potential related to the lepton asymmetry, which is vanishing for Dodelson-Widrow production. For the Shi-Fuller case it reads [257]

$$V_L = \frac{4\sqrt{2}\,\zeta(3)}{\pi^2}\,G_{\mathrm{F}}T^3\,L\,, \tag{4.17}$$

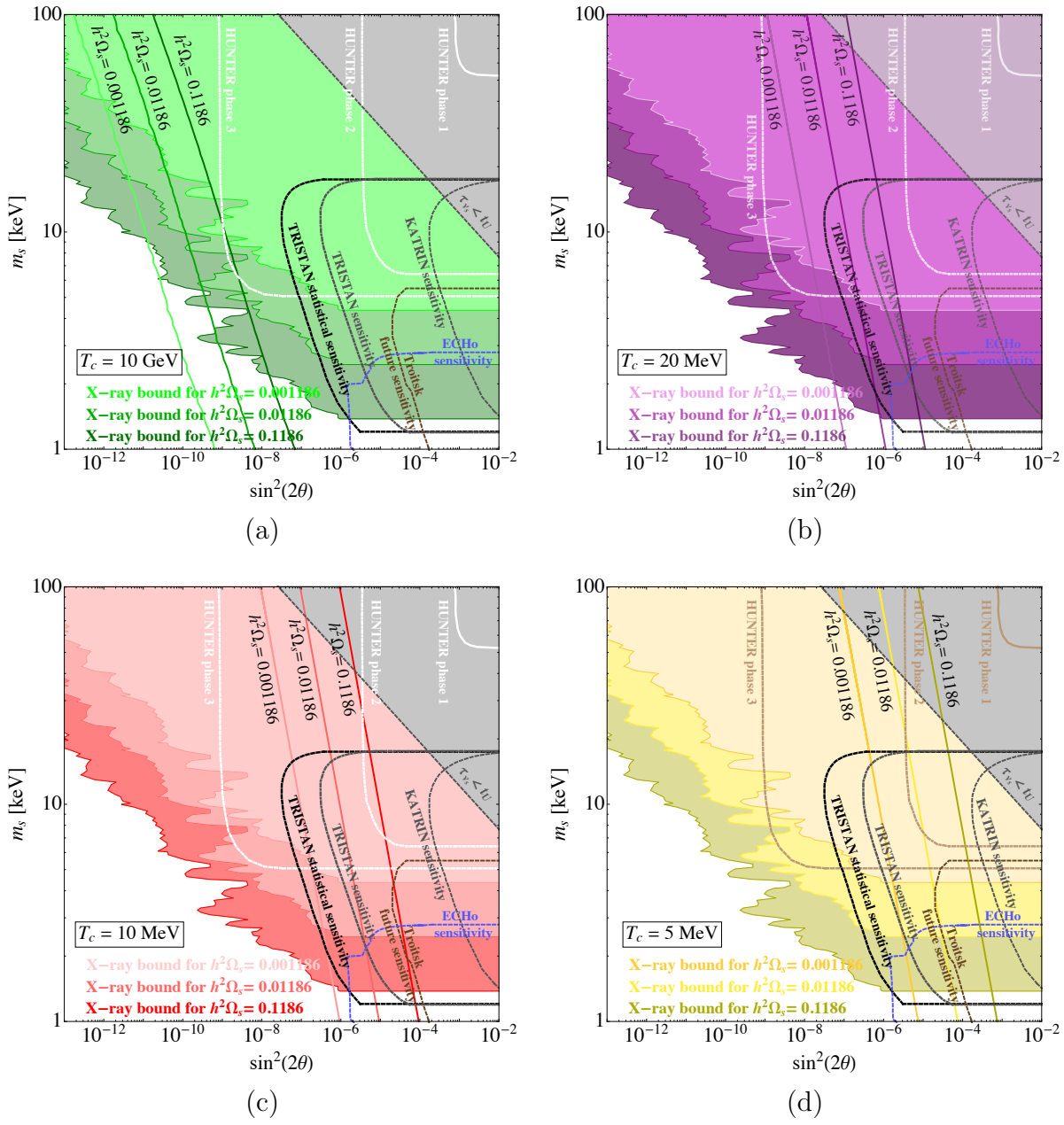

Figure 4.6: *Cocktail scenario*: X-ray constraints for sterile neutrinos being a subdominant DM contribution and different critical temperatures. The areas are compared to future terrestrial experiments. Taken from Ref. [256].

where the lepton asymmetry of number densities n_x is defined as $L = (n_\nu - n_{\overline{\nu}})/n_\gamma$. For calculating the sterile neutrino DM abundance we employ the `sterile-dm` code [259] that incorporates the effects of the QCD phase transition which occurs at temperatures where DM production peaks, appropriately treats the rapid change of relativistic degrees of freedom in this temperature range, and treats the evolution of asymmetries properly. The fact that `sterile-dm` does only deal with muon neutrinos is no issue, as the rates of

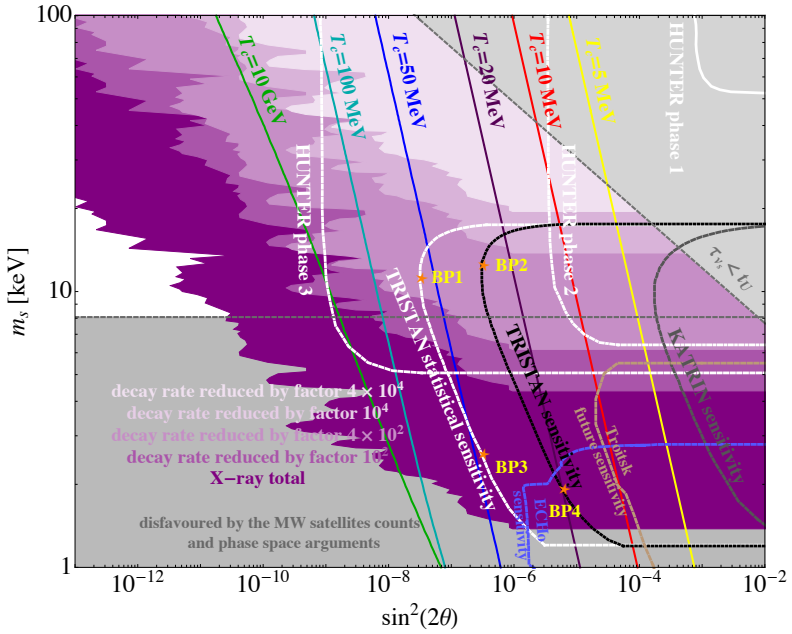

Figure 4.7: *X-ray suppression*: X-ray constraints for sterile neutrinos when the decay rate is reduced. The lines indicate the parameter space in which sterile neutrinos constitute the total DM abundance for the indicated values of T_c. Stars indicate four benchmark points, which lie in the future sensitivity region of TRISTAN. Taken from Ref. [256].

electron and muon neutrinos differ by less than 10% [254, 260].

As mentioned above, in order to allow TRISTAN to see a signal, we need to avoid X-ray limits and also avoid the overproduction of dark matter. For the latter necessity we note that the Dodelson-Widrow production has a peak at $T \simeq 133\,(m_s/\text{keV})^{1/3}$ MeV [257]. Hence, we could try to lower the temperature at which DM production starts, a scale we call *critical temperature* T_c. The obvious possibility is that it could simply be the reheating temperature $T_{\rm RH}$ [261, 262]. The lower limit on the reheating temperature stemming from BBN yields $T_{\rm RH} \gtrsim 4-5$ MeV [263, 264]. Another possibility not considered here is to arrange that via a phase transition the sterile neutrino mass at $T > T_c$ either vanishes or is very large [265]. In this case T_c can attain values smaller than the lower bound for $T_{\rm RH}$. Low values of T_c can be useful in e.g. left-right symmetric models [252, 266], in which sterile neutrinos decouple at high temperature due to their gauge interactions, leading to overclosure of the Universe.

Our analysis will confront the mass and mixing of sterile neutrinos with future constraints from Ref. [267]. "KATRIN sensitivity" denotes an expected measurement in the current version of KATRIN, "TRISTAN sensitivity" is the expectation for the TRISTAN project with 3 years data taking, and "statistical sensitivity" is what in principle would be possible. For comparison, we will also compare to the final sensitivity of the ECHo experiment [268], which will use electron capture. While the main focus is on KA-

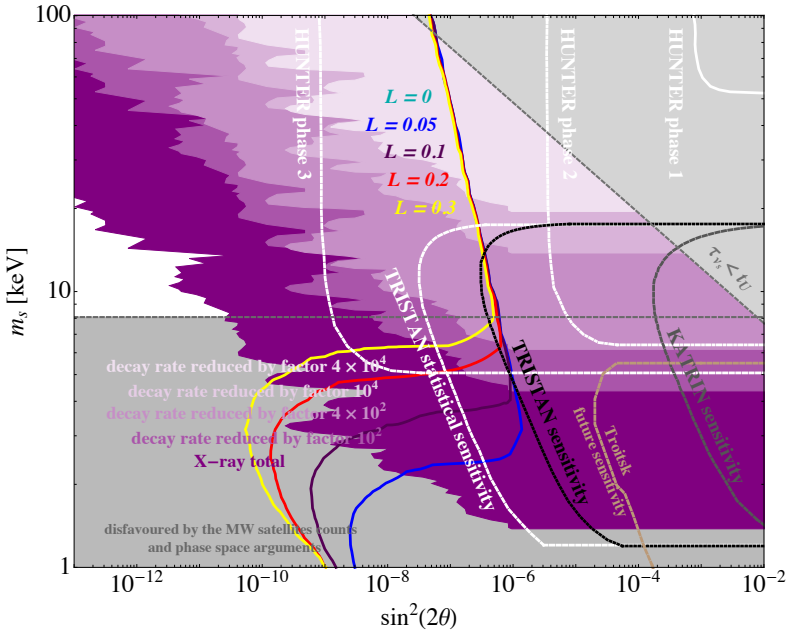

Figure 4.8: *Scenario with non-zero lepton asymmetries*: Sterile neutrino mass and mixing with $\Omega_s h^2 = 0.12$ for $T_c = 30$ MeV and several lepton asymmetries L. Taken from Ref. [256].

TRIN/TRISTAN, we display in addition the ambitious future HUNTER project [269], which will use electron capture of ^{137}Cs in a magneto-optical trap, and in general has much better prospects of finding keV-scale WDM, if realized.

The results on the sterile neutrino parameter space for reducing its contribution to dark matter and delaying its production are given in Fig. 4.6 for $T_c = 10$ GeV (that is, the standard Dodelson-Widrow scenario), as well as 20, 10, 5 MeV. TRISTAN could discover sterile neutrino DM if T_c is low enough. Effects of suppressing the X-ray limits due to a smaller decay rate leads to Fig. 4.7. In order to reach the full sensitivity region of TRISTAN, the sterile neutrino decay rate should be four orders of magnitude weaker.

Turning to lepton asymmetries, one notes that neutrinos and antineutrinos have an opposite sign of the lepton asymmetry potential Eq. (4.17). Therefore, one can arrange the sign of the asymmetry such that antineutrinos, relevant for KATRIN/TRISTAN, are the dominant DM component. Fig. 4.8 illustrates this option[1]. For this figure we always have sterile neutrinos contributing to all of dark matter. TRISTAN is still sensitive in the region where lines for $L \neq 0$ start departing from the Dodelson-Widrow line.

Thus, there can be compatibility of a terrestrial discovery of keV-scale sterile neutrinos

[1]Note that the final values of the asymmetry can in some regions in parameter space be at least a factor of a few times smaller in comparison to their initial values; this is a consequence of resonant transitions.

with their contribution to the DM density and constraints from X-ray searches. One can use a critical temperature above which production of DM is forbidden or heavily suppressed. Temperatures of $\mathcal{O}(10)$ MeV and a sterile neutrino contribution to DM of $1-10\%$ of the total DM abundance would make TRISTAN sensitive. Alternatively, sterile neutrino decay rates could be suppressed by four orders of magnitude in order get rid of X-ray limits, and to make TRISTAN find them, while at the same time sterile neutrinos could account for the total DM density.

4.4 An Extension to the Quark Sector: Leptoquarks and Fermion Singlets

This section deals with a method to couple right-handed singlet fermions to quarks by introducing leptoquarks. We focus on coupling to third-generation quarks, which avoids many constraints, and also allows, in contrast to many other models, a valid and consistent dark matter effective field theory (EFT) [270]. As sterile neutrinos of sizable mass are perfect WIMPs, we assume that they are stable enough to be DM, which can be realized by a $\mathbb{Z}_2$ symmetry. Therefore, the sterile neutrinos are, in absence of additional input, not involved in neutrino mass generation.

Leptoquarks are color-triplet bosons that carry both lepton and baryon numbers [271]; they have recently re-surfaced to explain flavor anomalies [272,273]. Here we only consider the scalar leptoquark $S_1'' \equiv S \sim (\bar{3}, 1, -\frac{4}{3})$ and the vector leptoquark $U_1'' \equiv U \sim (\bar{3}, 1, -\frac{2}{3})$, which only couple to the SM if there are sterile neutrinos. We will assume here baryon number violation, which rules out the coupling $\bar{d}d^c S$, which may lead to proton decay when combined with other couplings of S. We also ignore Higgs-portal-like terms of the form $XX^\dagger \Phi\Phi^\dagger$, where X is any of the leptoquarks. Moreover, as already mentioned, we want our leptoquarks to couple to third generation particles only.

Starting with the scalar S, the Lagrangian reads

$$\mathcal{L}_{\rm LQ} = -m_S^2 S^\dagger S + (D^\mu S)^\dagger D_\mu S + x_t\, \overline{t_R^c} N\, S + x_t^*\, (S)^\dagger \overline{N} t_R^c\,, \tag{4.18}$$

where the coupling to gluons is determined by

$$D_\mu = \partial_\mu + i g_s T^a G_\mu^a\,. \tag{4.19}$$

Since S has top-like quantum numbers, it behaves like a top squark [274]. We need to assume that S is odd under the stabilising $\mathbb{Z}_2$, because otherwise the Yukawa term in Eq. (4.18) is not allowed. The dark matter particles N could be either Dirac or Majorana, which has impact on the constraints. Fixing the coupling only to top quarks is not stable under RG effects, but it can be shown that up and charm quark couplings are at most of the order $10^{-7} x_t$ [275]. We continue by discussing the constraints on the scenario.

We implement the model via `FeynRules` [276] and calculate the DM relic density after freeze-out using `micrOMEGAs` [277–280]. In Fig. 4.9 we give for Dirac and Majorana singlets constraints on m_N and m_S, fixing at each point $|x_t|$ such that the observed DM relic density

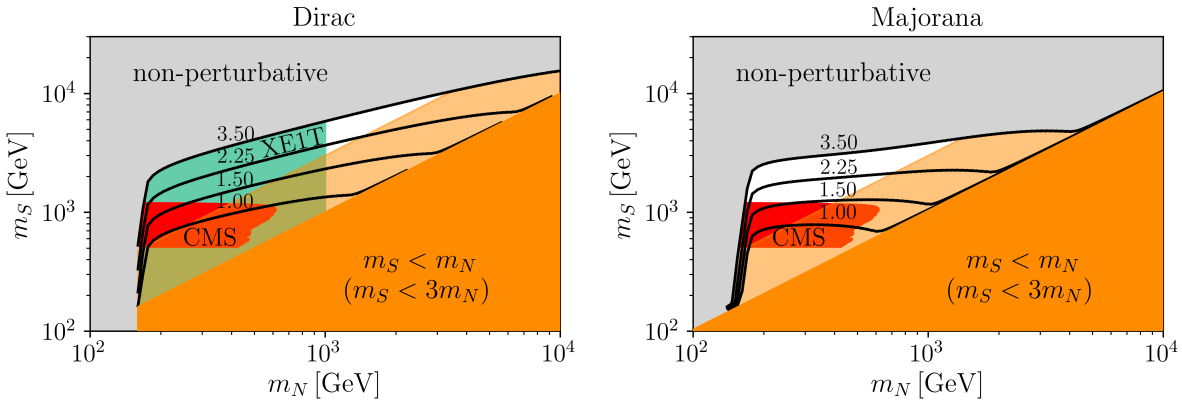

Figure 4.9: Contours of $|x_t|$ in the m_N-m_S-plane producing the correct relic abundance. Constraints from indirect and direct detection are very weak for Majorana neutrinos. In the case of Dirac neutrinos, direct detection limits from XENON1T are shown in teal. CMS limits are shown in red, perturbativity of the coupling and validity of the EFT description ($m_S < 3m_N$ in orange, $m_S < m_N$ in light orange) are also indicated.

is obtained. We find that as long as $m_S > m_N$, the freeze-out can be described by effective four-fermion operators. Other limits included are perturbativity $|x_t| > \sqrt{4\pi} \simeq 3.5$, and collider bounds from a CMS stop search [281] (see Ref. [282] for a very similar ATLAS search). While that analyses assume stop decays into neutralinos and tops, it applies to our case. As can be concluded from Ref. [283], current constraints from annihilation in dwarf spheroidal galaxies are consistent with the full DM mass range that we consider, if only annihilation into fermion pairs is considered. Regarding such indirect detection, gamma ray searches from DM annihilation in by Fermi-LAT [284] can be used, applying the spectra from [285] and J-factors from [286]. The result from Ref. [287] on annihilations into gluons, $NN \to gg$, are also relevant in the Majorana case for certain parameter configurations. The annihilation cross sections for $NN \to ff$ of Dirac (proportional to m_N^2) and Majorana neutrinos (proportional to m_f^2) are different, hence the indirect detection limits are different in Fig. 4.9. Regarding direct detection, note that we assume coupling to third generation particles only. At higher order, coupling to gluons or first generation particles is generated. As there is no vector current for Majoranas, only weak limits apply for this case. For Dirac, higher order limits generate a b-coupling dominating effects for protons, while in the scenario of t-coupling the neutron coupling dominates. Our scenarios also imply an effective $NN\Phi\Phi$ coupling; this Higgs-portal is constrained by direct detection constraints from XENON1T [288]. Gluon coupling $NNGG$ is another operator that may exist, but is is suppressed for heavy particles in the loop.

To briefly summarize, a neutral fermion singlet that couples via scalar leptoquarks to t-quarks can have masses as low as the weak scale, while the leptoquark mass should exceed the TeV-scale.

Turning to the vector leptoquark $U \equiv U_1'' \sim (3, 1, 2/3)$, the Lagrangian for its coupling

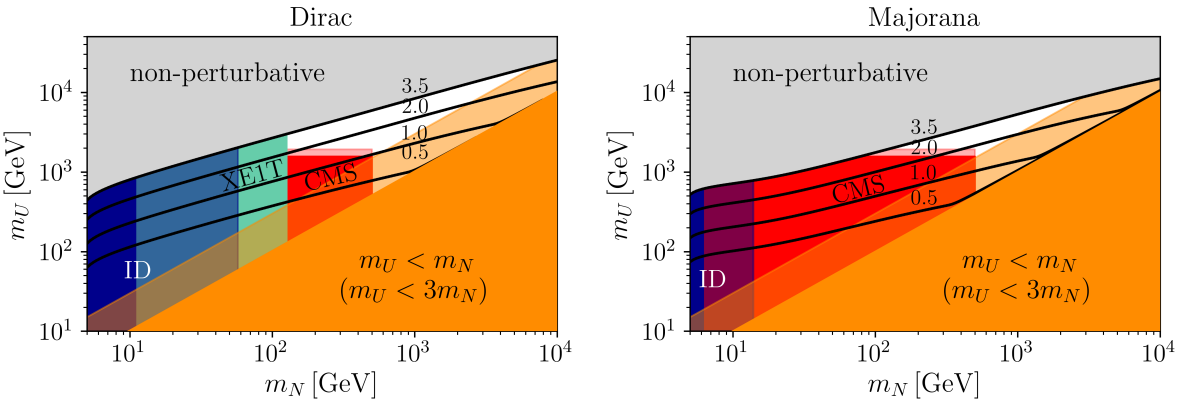

Figure 4.10: Contours of $|x_b|$ in the m_N-m_U-plane producing the correct relic abundance. Constraints from indirect and direct detection are very weak. CMS limits are shown in red, perturbativity of the coupling and validity of the EFT description ($m_S < 3m_N$ in orange, $m_S < m_N$ in light orange) are also indicated.

reads

$$\begin{aligned}\mathcal{L}_{\text{LQ}} = m_U^2 U_\mu^\dagger U^\mu - \frac{1}{2}(U^{\mu\nu})^\dagger U_{\mu\nu} - ig_S\kappa\, U_\mu^\dagger T^a U_\nu G^a_{\mu\nu} \\ + x_b\, \overline{b_R}\gamma_\mu N_R\, U^\mu + x_b^*\, U^{\dagger\mu}\overline{N_R}\gamma_\mu b_R\,,\end{aligned} \tag{4.20}$$

where again only the third generation is considered, and

$$U_{\mu\nu} = D_\mu U_\nu - D_\nu U_\mu \qquad \text{and} \qquad D_\mu = \partial_\mu + ig_s T^a G^a_\mu\,. \tag{4.21}$$

The origin of the leptoquark fixes the parameter κ to one or zero. As the scalar, we assume that U is also odd under the $\mathbb{Z}_2$ symmetry, otherwise the second line in Eq. (4.20) is not allowed. In Fig. 4.10 we plot the sterile neutrino mass m_N versus m_U, in analogy[2] to Fig. 4.9, fixing in particular at each point $|x_b|$ such that the observed DM relic density is obtained.

Again, we can summarize that there exists parameter space for a neutral fermion singlet that couples via vector leptoquarks to b-quarks, in which a consistent EFT description is possible. The sterile neutrino DM mass in the Majorana case needs to exceed 77 GeV for $\kappa = 0$ and 123 GeV for $\kappa = 1$.

[2]We apply a CMS vector-leptoquark search from Ref. [289], which however looks for decays into a massless neutrino and a bottom quark. We use the results of the scalar leptoquarks [281] as guiding principle to extend the curves to the case of massive N. A dedicated collider study of a vector leptoquark coupling to massive neutral fermions would be worthwhile.

Chapter 5

Summary

Neutrinos are special particles that are likely connected to new physics. While neutrino physics has entered the precision era, the values of all its standard parameters, its nature under self-conjugacy, the origin of its mass, its flavor distribution and its interactions with SM and BSM particles is far from settled or even completely unknown. This summary of some of my recent research work featured examples on new particles that couple to neutrinos: scalars, vectors and fermions. The constraints on these frameworks use existing, upcoming, intermediate and far future facilities and observations. Different flavors are used, and both low and high energy processes are crucial. The experiments or observations are either pure neutrino physics facilities, or the limits of interest are set as a byproduct; the experiments are also of large scale or small scale. This richness and broadness of phenomenology is connected to the richness and broadness of neutrino physics.

We have encountered tests and effects of new particles in cosmology, astroparticle, nuclear and particle physics. Motivation for the scalar, vector and fermionic particles that we considered can come from observational issues like the Hubble discrepancy, dark matter or neutrino mass considerations, the observed flavor content in the lepton sector, anomaly-free models, anomalies in meson decays or $g-2$, or by generic new particle content in in BSM scenarios. Unique properties of neutrinos allow to set unique limits from a variety of places. At the same time, the new interactions would have spectacular consequences in a variety of neutrino sources.

The limited amount of examples that could be given here is illustrative for the many new physics options of neutrinos. Other examples not discussed here are new charged particles coupling to neutrinos, electromagnetic features such as millicharge or magnetic moments, effective interactions in EFT language, extra-dimensional features, coupling to dark energy or ultralight dark matter, etc. Here another layer of tests and possibilities would enter.

The next decade will be crucial to test the various standard and non-standard neutrino features, and the results are very likely to help in developing our new picture of Nature.

Bibliography

[1] **GERDA**, M. Agostini *et al.*, "*Final Results of GERDA on the Search for Neutrinoless Double-β Decay*," Phys. Rev. Lett. **125** (2020) 252502, arXiv:2009.06079.

[2] **Majorana**, S. Alvis *et al.*, "*A Search for Neutrinoless Double-Beta Decay in ^{76}Ge with 26 kg-yr of Exposure from the MAJORANA DEMONSTRATOR*," Phys. Rev. C **100** (2019) no. 2, 025501, arXiv:1902.02299.

[3] **CUPID**, O. Azzolini *et al.*, "*Final result of CUPID-0 phase-I in the search for the ^{82}Se Neutrinoless Double-β Decay*," Phys. Rev. Lett. **123** (2019) no. 3, 032501, arXiv:1906.05001.

[4] **CUPID**, E. Armengaud *et al.*, "*New Limit for Neutrinoless Double-Beta Decay of ^{100}Mo from the CUPID-Mo Experiment*," Phys. Rev. Lett. **126** (2021) no. 18, 181802, arXiv:2011.13243.

[5] **CUORE**, D. Q. Adams *et al.*, "*High sensitivity neutrinoless double-beta decay search with one tonne-year of CUORE data*," arXiv:2104.06906.

[6] **KamLAND-Zen**, A. Gando *et al.*, "*Search for Majorana Neutrinos near the Inverted Mass Hierarchy Region with KamLAND-Zen*," Phys. Rev. Lett. **117** (2016) no. 8, 082503, arXiv:1605.02889. [Addendum: Phys. Rev. Lett.117,no.10,109903(2016)].

[7] **EXO-200**, G. Anton *et al.*, "*Search for Neutrinoless Double-β Decay with the Complete EXO-200 Dataset*," Phys. Rev. Lett. **123** (2019) no. 16, 161802, arXiv:1906.02723.

[8] M. Aker *et al.*, "*First direct neutrino-mass measurement with sub-eV sensitivity*," arXiv:2105.08533.

[9] **Planck**, N. Aghanim *et al.*, "*Planck 2018 results. VI. Cosmological parameters*," Astron. Astrophys. **641** (2020) A6, arXiv:1807.06209. [Erratum: Astron.Astrophys. 652, C4 (2021)].

[10] I. Esteban, M. C. Gonzalez-Garcia, M. Maltoni, T. Schwetz, and A. Zhou, "*The fate of hints: updated global analysis of three-flavor neutrino oscillations*," JHEP **09** (2020) 178, arXiv:2007.14792.

[11] Nufit, `http://www.nu-fit.org`.

[12] P. Minkowski, "$\mu \to e\gamma$ *at a Rate of One Out of* 10^9 *Muon Decays?*," Phys. Lett. **B67** (1977) 421–428.

[13] M. Gell-Mann, P. Ramond, and R. Slansky, "*Complex Spinors and Unified Theories*," Conf. Proc. **C790927** (1979) 315–321, `arXiv:1306.4669`.

[14] T. Yanagida, "*Horizontal Symmetry and Masses of Neutrinos*," Conf. Proc. **C7902131** (1979) 95–99.

[15] S. L. Glashow, "*The Future of Elementary Particle Physics*," NATO Sci. Ser. B **61** (1980) 687.

[16] R. N. Mohapatra and G. Senjanovic, "*Neutrino Mass and Spontaneous Parity Violation*," Phys. Rev. Lett. **44** (1980) 912.

[17] C. Wetterich, "*Neutrino Masses and the Scale of B-L Violation*," Nucl. Phys. **B187** (1981) 343–375.

[18] R. N. Mohapatra and R. Marshak, "*Local B-L Symmetry of Electroweak Interactions, Majorana Neutrinos and Neutron Oscillations*," Phys. Rev. Lett. **44** (1980) 1316–1319. [Erratum: Phys.Rev.Lett. 44, 1643 (1980)].

[19] R. Marshak and R. N. Mohapatra, "*Quark - Lepton Symmetry and B-L as the U(1) Generator of the Electroweak Symmetry Group*," Phys. Lett. B **91** (1980) 222–224.

[20] A. Masiero, J. Nieves, and T. Yanagida, "B^-l *Violating Proton Decay and Late Cosmological Baryon Production*," Phys. Lett. B **116** (1982) 11–15.

[21] R. N. Mohapatra and G. Senjanovic, "*Spontaneous Breaking of Global* B^-l *Symmetry and Matter - Antimatter Oscillations in Grand Unified Theories*," Phys. Rev. D **27** (1983) 254.

[22] W. Buchmuller, C. Greub, and P. Minkowski, "*Neutrino masses, neutral vector bosons and the scale of B-L breaking*," Phys. Lett. B **267** (1991) 395–399.

[23] J. C. Pati and A. Salam, "*Lepton Number as the Fourth Color*," Phys. Rev. D **10** (1974) 275–289. [Erratum: Phys.Rev.D 11, 703–703 (1975)].

[24] R. Mohapatra and J. C. Pati, "*A Natural Left-Right Symmetry*," Phys. Rev. D **11** (1975) 2558.

[25] R. N. Mohapatra and J. C. Pati, "*Left-Right Gauge Symmetry and an Isoconjugate Model of CP Violation*," Phys. Rev. D **11** (1975) 566–571.

[26] G. Senjanovic and R. N. Mohapatra, "*Exact Left-Right Symmetry and Spontaneous Violation of Parity*," Phys. Rev. D **12** (1975) 1502.

[27] G. Senjanovic, "*Spontaneous Breakdown of Parity in a Class of Gauge Theories*," Nucl. Phys. B **153** (1979) 334–364.

[28] R. N. Mohapatra and G. Senjanovic, "*Neutrino Masses and Mixings in Gauge Models with Spontaneous Parity Violation*," Phys. Rev. **D23** (1981) 165.

[29] X. He, G. C. Joshi, H. Lew, and R. Volkas, "*NEW Z-prime PHENOMENOLOGY*," Phys. Rev. D **43** (1991) 22–24.

[30] R. Foot, "*New Physics From Electric Charge Quantization?*," Mod. Phys. Lett. A **6** (1991) 527–530.

[31] X.-G. He, G. C. Joshi, H. Lew, and R. Volkas, "*Simplest Z-prime model*," Phys. Rev. D **44** (1991) 2118–2132.

[32] P. Binetruy, S. Lavignac, S. T. Petcov, and P. Ramond, "*Quasidegenerate neutrinos from an Abelian family symmetry*," Nucl. Phys. B **496** (1997) 3–23, arXiv:hep-ph/9610481.

[33] M. Magg and C. Wetterich, "*Neutrino Mass Problem and Gauge Hierarchy*," Phys. Lett. **B94** (1980) 61–64.

[34] J. Schechter and J. W. F. Valle, "*Neutrino Masses in $SU(2) \times U(1)$ Theories*," Phys. Rev. **D22** (1980) 2227.

[35] T. P. Cheng and L.-F. Li, "*Neutrino Masses, Mixings and Oscillations in $SU(2) \times U(1)$ Models of Electroweak Interactions*," Phys. Rev. **D22** (1980) 2860.

[36] G. Lazarides, Q. Shafi, and C. Wetterich, "*Proton Lifetime and Fermion Masses in an SO(10) Model*," Nucl. Phys. **B181** (1981) 287–300.

[37] R. Foot, H. Lew, X. G. He, and G. C. Joshi, "*Seesaw Neutrino Masses Induced by a Triplet of Leptons*," Z. Phys. **C44** (1989) 441.

[38] D. Wyler and L. Wolfenstein, "*Massless Neutrinos in Left-Right Symmetric Models*," Nucl. Phys. B **218** (1983) 205–214.

[39] R. Mohapatra, "*Mechanism for Understanding Small Neutrino Mass in Superstring Theories*," Phys. Rev. Lett. **56** (1986) 561–563.

[40] R. Mohapatra and J. Valle, "*Neutrino Mass and Baryon Number Nonconservation in Superstring Models*," Phys. Rev. D **34** (1986) 1642.

[41] E. K. Akhmedov, M. Lindner, E. Schnapka, and J. Valle, "*Dynamical left-right symmetry breaking*," Phys. Rev. D **53** (1996) 2752–2780, arXiv:hep-ph/9509255.

[42] S. Barr, "*A Different seesaw formula for neutrino masses*," Phys. Rev. Lett. **92** (2004) 101601, arXiv:hep-ph/0309152.

[43] M. Malinsky, J. Romao, and J. Valle, "*Novel supersymmetric SO(10) seesaw mechanism*," Phys. Rev. Lett. **95** (2005) 161801, arXiv:hep-ph/0506296.

[44] A. Zee, "*A Theory of Lepton Number Violation, Neutrino Majorana Mass, and Oscillation*," Phys. Lett. B **93** (1980) 389. [Erratum: Phys.Lett.B 95, 461 (1980)].

[45] E. Ma, "*Verifiable radiative seesaw mechanism of neutrino mass and dark matter*," Phys. Rev. D **73** (2006) 077301, arXiv:hep-ph/0601225.

[46] A. Zee, "*Quantum Numbers of Majorana Neutrino Masses*," Nucl. Phys. B **264** (1986) 99–110.

[47] K. Babu, "*Model of 'Calculable' Majorana Neutrino Masses*," Phys. Lett. B **203** (1988) 132–136.

[48] A. G. Riess *et al.*, "*A 2.4% Determination of the Local Value of the Hubble Constant*," Astrophys. J. **826** (2016) no. 1, 56, arXiv:1604.01424.

[49] T. Shanks, L. Hogarth, and N. Metcalfe, "*Gaia Cepheid parallaxes and 'Local Hole' relieve H_0 tension*," Mon. Not. Roy. Astron. Soc. **484** (2019) no. 1, L64–L68, arXiv:1810.02595.

[50] A. G. Riess, S. Casertano, D. Kenworthy, D. Scolnic, and L. Macri, "*Seven Problems with the Claims Related to the Hubble Tension in arXiv:1810.02595*," arXiv:1810.03526.

[51] **Planck**, N. Aghanim *et al.*, "*Planck 2018 results. VI. Cosmological parameters*," Astron. Astrophys. **641** (2020) A6, arXiv:1807.06209.

[52] A. G. Riess, S. Casertano, W. Yuan, L. M. Macri, and D. Scolnic, "*Large Magellanic Cloud Cepheid Standards Provide a 1% Foundation for the Determination of the Hubble Constant and Stronger Evidence for Physics beyond ΛCDM*," Astrophys. J. **876** (2019) no. 1, 85, arXiv:1903.07603.

[53] N. Schöneberg, G. Franco Abellán, A. Pérez Sánchez, S. J. Witte, V. Poulin, and J. Lesgourgues, "*The H_0 Olympics: A fair ranking of proposed models*," arXiv:2107.10291.

[54] L. Lancaster, F.-Y. Cyr-Racine, L. Knox, and Z. Pan, "*A tale of two modes: Neutrino free-streaming in the early universe*," JCAP **07** (2017) 033, arXiv:1704.06657.

[55] C. D. Kreisch, F.-Y. Cyr-Racine, and O. Doré, "*Neutrino puzzle: Anomalies, interactions, and cosmological tensions*," Phys. Rev. D **101** (2020) no. 12, 123505, arXiv:1902.00534.

[56] F.-Y. Cyr-Racine and K. Sigurdson, "*Limits on Neutrino-Neutrino Scattering in the Early Universe*," Phys. Rev. D **90** (2014) no. 12, 123533, arXiv:1306.1536.

[57] I. M. Oldengott, T. Tram, C. Rampf, and Y. Y. Y. Wong, "*Interacting neutrinos in cosmology: exact description and constraints*," JCAP **11** (2017) 027, arXiv:1706.02123.

[58] M. Park, C. D. Kreisch, J. Dunkley, B. Hadzhiyska, and F.-Y. Cyr-Racine, "Λ*CDM or self-interacting neutrinos: How CMB data can tell the two models apart*," Phys. Rev. **D100** (2019) no. 6, 063524, arXiv:1904.02625.

[59] J. Hasenkamp, "*Neutrino self-interactions*," Phys. Rev. **D93** (2016) no. 5, 055033, arXiv:1604.04742.

[60] G.-y. Huang, T. Ohlsson, and S. Zhou, "*Observational Constraints on Secret Neutrino Interactions from Big Bang Nucleosynthesis*," Phys. Rev. D **97** (2018) no. 7, 075009, arXiv:1712.04792.

[61] P. Bakhti, Y. Farzan, and M. Rajaee, "*Secret interactions of neutrinos with light gauge boson at the DUNE near detector*," Phys. Rev. **D99** (2019) no. 5, 055019, arXiv:1810.04441.

[62] N. Blinov, K. J. Kelly, G. Z. Krnjaic, and S. D. McDermott, "*Constraining the Self-Interacting Neutrino Interpretation of the Hubble Tension*," Phys. Rev. Lett. **123** (2019) no. 19, 191102, arXiv:1905.02727.

[63] A. De Gouva, M. Sen, W. Tangarife, and Y. Zhang, "*The Dodelson-Widrow Mechanism In the Presence of Self-Interacting Neutrinos*," arXiv:1910.04901.

[64] A. Das, A. Dighe, and M. Sen, "*New effects of non-standard self-interactions of neutrinos in a supernova*," JCAP **05** (2017) 051, arXiv:1705.00468.

[65] A. Dighe and M. Sen, "*Nonstandard neutrino self-interactions in a supernova and fast flavor conversions*," Phys. Rev. **D97** (2018) no. 4, 043011, arXiv:1709.06858.

[66] H. Ko *et al.*, "*Neutrino self-interaction and MSW effects on the supernova neutrino-process*," JPS Conf. Proc. **31** (2020) 011027, arXiv:1903.02086.

[67] S. Shalgar, I. Tamborra, and M. Bustamante, "*Core-collapse supernovae stymie secret neutrino interactions*," Phys. Rev. D **103** (2021) no. 12, 123008, arXiv:1912.09115.

[68] F. Forastieri, M. Lattanzi, and P. Natoli, "*Cosmological constraints on neutrino self-interactions with a light mediator*," Phys. Rev. D **100** (2019) no. 10, 103526, arXiv:1904.07810.

[69] K.-F. Lyu, E. Stamou, and L.-T. Wang, "*Self-interacting neutrinos: Solution to Hubble tension versus experimental constraints*," Phys. Rev. D **103** (2021) no. 1, 015004, arXiv:2004.10868.

[70] F. F. Deppisch, L. Graf, W. Rodejohann, and X.-J. Xu, "*Neutrino Self-Interactions and Double Beta Decay*," Phys. Rev. D **102** (2020) no. 5, 051701, arXiv:2004.11919.

[71] M. J. Dolinski, A. W. P. Poon, and W. Rodejohann, "*Neutrinoless Double-Beta Decay: Status and Prospects*," Ann. Rev. Nucl. Part. Sci. **69** (2019) 219–251, arXiv:1902.04097.

[72] J. Barea, J. Kotila, and F. Iachello, "*$0\nu\beta\beta$ and $2\nu\beta\beta$ nuclear matrix elements in the interacting boson model with isospin restoration*," Phys. Rev. **C91** (2015) no. 3, 034304, arXiv:1506.08530.

[73] J. Menendez, "*Neutrinoless $\beta\beta$ decay mediated by the exchange of light and heavy neutrinos: The role of nuclear structure correlations*," J. Phys. **G45** (2018) no. 1, 014003, arXiv:1804.02105.

[74] J. Hyvarinen and J. Suhonen, "*Nuclear matrix elements for $0\nu\beta\beta$ decays with light or heavy Majorana-neutrino exchange*," Phys. Rev. **C91** (2015) no. 2, 024613.

[75] T. Brune and H. Päs, "*Massive Majorons and constraints on the Majoron-neutrino coupling*," Phys. Rev. D **99** (2019) no. 9, 096005, arXiv:1808.08158.

[76] **NEMO-3**, R. Arnold *et al.*, "*Detailed studies of ^{100}Mo two-neutrino double beta decay in NEMO-3*," Eur. Phys. J. **C79** (2019) no. 5, 440, arXiv:1903.08084.

[77] C. Pitrou, A. Coc, J.-P. Uzan, and E. Vangioni, "*Precision big bang nucleosynthesis with improved Helium-4 predictions*," Phys. Rept. **754** (2018) 1–66, arXiv:1801.08023.

[78] G.-y. Huang and W. Rodejohann, "*Solving the Hubble tension without spoiling Big Bang Nucleosynthesis*," Phys. Rev. D **103** (2021) 123007, arXiv:2102.04280.

[79] A. Mazumdar, S. Mohanty, and P. Parashari, "*Flavour specific neutrino self-interaction: H_0 tension and IceCube*," arXiv:2011.13685.

[80] A. Arbey, "*AlterBBN: A program for calculating the BBN abundances of the elements in alternative cosmologies*," Comput. Phys. Commun. **183** (2012) 1822–1831, arXiv:1106.1363.

[81] A. Arbey, J. Auffinger, K. P. Hickerson, and E. S. Jenssen, "*AlterBBN v2: A public code for calculating Big-Bang nucleosynthesis constraints in alternative cosmologies*," Comput. Phys. Commun. **248** (2020) 106982, arXiv:1806.11095.

[82] V. Brdar, M. Lindner, S. Vogl, and X.-J. Xu, "*Revisiting neutrino self-interaction constraints from Z and τ decays*," Phys. Rev. D **101** (2020) no. 11, 115001, arXiv:2003.05339.

[83] M. Bustamante, C. Rosenstrøm, S. Shalgar, and I. Tamborra, "*Bounds on secret neutrino interactions from high-energy astrophysical neutrinos*," Phys. Rev. D **101** (2020) no. 12, 123024, arXiv:2001.04994.

[84] K. N. Abazajian and J. Heeck, "*Observing Dirac neutrinos in the cosmic microwave background*," Phys. Rev. D **100** (2019) 075027, arXiv:1908.03286.

[85] X. Luo, W. Rodejohann, and X.-J. Xu, "*Dirac neutrinos and $N_{\rm eff}$*," JCAP **06** (2020) 058, arXiv:2005.01629.

[86] L. Husdal, "*On Effective Degrees of Freedom in the Early Universe*," Galaxies **4** (2016) no. 4, 78, arXiv:1609.04979.

[87] X. Luo, W. Rodejohann, and X.-J. Xu, "*Dirac neutrinos and N_{eff}. Part II. The freeze-in case*," JCAP **03** (2021) 082, arXiv:2011.13059.

[88] **Planck**, Y. Akrami *et al.*, "*Planck 2018 results. I. Overview and the cosmological legacy of Planck*," arXiv:1807.06205.

[89] **Simons Observatory**, M. H. Abitbol *et al.*, "*The Simons Observatory: Astro2020 Decadal Project Whitepaper*," Bull. Am. Astron. Soc. **51** (2019) 147, arXiv:1907.08284.

[90] **SPT-3G**, B. Benson *et al.*, "*SPT-3G: A Next-Generation Cosmic Microwave Background Polarization Experiment on the South Pole Telescope*," Proc. SPIE Int. Soc. Opt. Eng. **9153** (2014) 91531P, arXiv:1407.2973.

[91] **CMB-S4**, K. N. Abazajian *et al.*, "*CMB-S4 Science Book, First Edition*," arXiv:1610.02743.

[92] K. Abazajian *et al.*, "*CMB-S4 Science Case, Reference Design, and Project Plan*," arXiv:1907.04473.

[93] D. Z. Freedman, "*Coherent Neutrino Nucleus Scattering as a Probe of the Weak Neutral Current*," Phys. Rev. **D9** (1974) 1389–1392.

[94] D. Z. Freedman, D. N. Schramm, and D. L. Tubbs, "*The Weak Neutral Current and Its Effects in Stellar Collapse*," Ann. Rev. Nucl. Part. Sci. **27** (1977) 167–207.

[95] D. K. Papoulias and T. S. Kosmas, "*Standard and Nonstandard Neutrino-Nucleus Reactions Cross Sections and Event Rates to Neutrino Detection Experiments*," Adv. High Energy Phys. **2015** (2015) 763648, arXiv:1502.02928.

[96] M. Lindner, W. Rodejohann, and X.-J. Xu, "*Coherent Neutrino-Nucleus Scattering and new Neutrino Interactions*," JHEP **03** (2017) 097, arXiv:1612.04150.

[97] Y. Farzan, M. Lindner, W. Rodejohann, and X.-J. Xu, "*Probing neutrino coupling to a light scalar with coherent neutrino scattering*," JHEP **05** (2018) 066, arXiv:1802.05171.

[98] G. Belanger, F. Boudjema, A. Pukhov, and A. Semenov, "*Dark matter direct detection rate in a generic model with micrOMEGAs 2.2*," Comput. Phys. Commun. **180** (2009) 747–767, arXiv:0803.2360.

[99] A. Crivellin, M. Hoferichter, and M. Procura, "*Accurate evaluation of hadronic uncertainties in spin-independent WIMP-nucleon scattering: Disentangling two- and three-flavor effects*," Phys. Rev. **D89** (2014) 054021, arXiv:1312.4951.

[100] M. Hoferichter, J. Ruiz de Elvira, B. Kubis, and U.-G. Meissner, "*High-Precision Determination of the Pion-Nucleon Term from Roy-Steiner Equations*," Phys. Rev. Lett. **115** (2015) 092301, arXiv:1506.04142.

[101] P. Junnarkar and A. Walker-Loud, "*Scalar strange content of the nucleon from lattice QCD*," Phys. Rev. **D87** (2013) 114510, arXiv:1301.1114.

[102] M. A. Shifman, A. I. Vainshtein, and V. I. Zakharov, "*Remarks on Higgs Boson Interactions with Nucleons*," Phys. Lett. **78B** (1978) 443–446.

[103] **Particle Data Group**, C. Patrignani *et al.*, "*Review of Particle Physics*," Chin. Phys. **C40** (2016) no. 10, 100001.

[104] **COHERENT**, D. Akimov *et al.*, "*Observation of Coherent Elastic Neutrino-Nucleus Scattering*," Science **357** (2017) no. 6356, 1123–1126, arXiv:1708.01294.

[105] D. Akimov *et al.*, "*Measurement of the Coherent Elastic Neutrino-Nucleus Scattering Cross Section on CsI by COHERENT*," arXiv:2110.07730.

[106] **COHERENT**, D. Akimov *et al.*, "*First Measurement of Coherent Elastic Neutrino-Nucleus Scattering on Argon*," Phys. Rev. Lett. **126** (2021) no. 1, 012002, arXiv:2003.10630.

[107] **CONUS**, H. Bonet *et al.*, "*Constraints on Elastic Neutrino Nucleus Scattering in the Fully Coherent Regime from the CONUS Experiment*," Phys. Rev. Lett. **126** (2021) no. 4, 041804, arXiv:2011.00210.

[108] **CONUS**, H. Bonet *et al.*, "*Novel constraints on neutrino physics beyond the standard model from the CONUS experiment*," arXiv:2110.02174.

[109] R. Strauss *et al.*, "*The ν-cleus experiment: A gram-scale fiducial-volume cryogenic detector for the first detection of coherent neutrino-nucleus scattering*," Eur. Phys. J. **C77** (2017) 506, arXiv:1704.04320.

[110] **CONNIE**, A. Aguilar-Arevalo *et al.*, "*The CONNIE experiment*," J. Phys. Conf. Ser. **761** (2016) no. 1, 012057, arXiv:1608.01565.

[111] **MINER**, G. Agnolet *et al.*, "*Background Studies for the MINER Coherent Neutrino Scattering Reactor Experiment*," Nucl. Instrum. Meth. A **853** (2017) 53–60, arXiv:1609.02066.

[112] H. T. Wong, "*Neutrino-nucleus coherent scattering and dark matter searches with sub-keV germanium detector*," Nucl. Phys. **A844** (2010) 229C–233C.

[113] V. Belov *et al.*, "*The νGeN experiment at the Kalinin Nuclear Power Plant*," JINST **10** (2015) no. 12, P12011.

[114] J. Billard *et al.*, "*Coherent Neutrino Scattering with Low Temperature Bolometers at Chooz Reactor Complex*," J. Phys. G **44** (2017) no. 10, 105101, arXiv:1612.09035.

[115] P. Galison and A. Manohar, "*Two Z's or not two Z's?*," Phys. Lett. **136B** (1984) 279–283.

[116] B. Holdom, "*Two $U(1)$'s and ϵ Charge Shifts*," Phys. Lett. **166B** (1986) 196–198.

[117] T. Araki, J. Heeck, and J. Kubo, "*Vanishing Minors in the Neutrino Mass Matrix from Abelian Gauge Symmetries*," JHEP **07** (2012) 083, arXiv:1203.4951.

[118] J. Heeck, *Neutrinos and Abelian Gauge Symmetries*. PhD thesis, Heidelberg U., 2014.

[119] L. N. Chang, O. Lebedev, W. Loinaz, and T. Takeuchi, "*Constraints on gauged $B-3L_\tau$ and related theories*," Phys. Rev. **D63** (2001) 074013, arXiv:hep-ph/0010118.

[120] M.-C. Chen, A. de Gouvêa, and B. A. Dobrescu, "*Gauge Trimming of Neutrino Masses*," Phys. Rev. **D75** (2007) 055009, arXiv:hep-ph/0612017.

[121] M.-C. Chen and J. Huang, "*TeV scale seesaw model and a flavorful Z' at the LHC*," Phys. Rev. **D81** (2010) 055007, arXiv:0910.5029.

[122] H.-S. Lee and E. Ma, "*Gauged $B-x_iL$ origin of R Parity and its implications*," Phys. Lett. **B688** (2010) 319–322, arXiv:1001.0768.

[123] E. Salvioni, A. Strumia, G. Villadoro, and F. Zwirner, "*Non-universal minimal Z' models: present bounds and early LHC reach*," JHEP **03** (2010) 010, arXiv:0911.1450.

[124] S. Choubey and W. Rodejohann, "*A Flavor symmetry for quasi-degenerate neutrinos: L(mu) - L(tau)*," Eur. Phys. J. C **40** (2005) 259–268, arXiv:hep-ph/0411190.

[125] J. Heeck and W. Rodejohann, "*Gauged L_mu - L_tau Symmetry at the Electroweak Scale*," Phys. Rev. D **84** (2011) 075007, arXiv:1107.5238.

[126] P. Athron, C. Balázs, D. H. Jacob, W. Kotlarski, D. Stöckinger, and H. Stöckinger-Kim, "*New physics explanations of a_μ in light of the FNAL muon $g-2$ measurement*," arXiv:2104.03691.

[127] **Muon g-2**, G. W. Bennett *et al.*, "*Final Report of the Muon E821 Anomalous Magnetic Moment Measurement at BNL*," Phys. Rev. D **73** (2006) 072003, arXiv:hep-ex/0602035.

[128] S. Borsanyi *et al.*, "*Leading hadronic contribution to the muon magnetic moment from lattice QCD*," Nature **593** (2021) no. 7857, 51–55, arXiv:2002.12347.

[129] P. Athron, C. Balázs, D. H. Jacob, W. Kotlarski, D. Stöckinger, and H. Stöckinger-Kim, "*New physics explanations of a_μ in light of the FNAL muon $g-2$ measurement*," arXiv:2104.03691.

[130] W. Altmannshofer, S. Gori, M. Pospelov, and I. Yavin, "*Quark flavor transitions in $L_\mu - L_\tau$ models*," Phys. Rev. D **89** (2014) 095033, arXiv:1403.1269.

[131] A. Crivellin, G. D'Ambrosio, and J. Heeck, "*Explaining $h \to \mu^\pm\tau^\mp$, $B \to K^*\mu^+\mu^-$ and $B \to K\mu^+\mu^-/B \to Ke^+e^-$ in a two-Higgs-doublet model with gauged $L_\mu - L_\tau$*," Phys. Rev. Lett. **114** (2015) 151801, arXiv:1501.00993.

[132] W. Altmannshofer, S. Gori, S. Profumo, and F. S. Queiroz, "*Explaining dark matter and B decay anomalies with an $L_\mu - L_\tau$ model*," JHEP **12** (2016) 106, arXiv:1609.04026.

[133] M. Masud, A. Chatterjee, and P. Mehta, "*Probing CP violation signal at DUNE in presence of non-standard neutrino interactions*," J. Phys. **G43** (2016) no. 9, 095005, arXiv:1510.08261.

[134] A. de Gouva and K. J. Kelly, "*Non-standard Neutrino Interactions at DUNE*," Nucl. Phys. **B908** (2016) 318–335, arXiv:1511.05562.

[135] M. Blennow, S. Choubey, T. Ohlsson, D. Pramanik, and S. K. Raut, "*A combined study of source, detector and matter non-standard neutrino interactions at DUNE*," JHEP **08** (2016) 090, arXiv:1606.08851.

[136] S. K. Agarwalla, S. S. Chatterjee, and A. Palazzo, "*Degeneracy between θ_{23} octant and neutrino non-standard interactions at DUNE*," Phys. Lett. **B762** (2016) 64–71, arXiv:1607.01745.

[137] P. Coloma, P. B. Denton, M. C. Gonzalez-Garcia, M. Maltoni, and T. Schwetz, "*Curtailing the Dark Side in Non-Standard Neutrino Interactions*," JHEP **04** (2017) 116, arXiv:1701.04828.

[138] K. N. Deepthi, S. Goswami, and N. Nath, "*Challenges posed by non-standard neutrino interactions in the determination of δ_{CP} at DUNE*," Nucl. Phys. **B936** (2018) 91–105, arXiv:1711.04840.

[139] P. B. Denton, Y. Farzan, and I. M. Shoemaker, "*A Plan to Rule out Large Non-Standard Neutrino Interactions After COHERENT Data*," JHEP **07** (2018) 037, arXiv:1804.03660.

[140] L. Wolfenstein, "*Neutrino Oscillations in Matter*," Phys. Rev. D **17** (1978) 2369–2374.

[141] M. M. Guzzo, A. Masiero, and S. T. Petcov, "*On the MSW effect with massless neutrinos and no mixing in the vacuum*," Phys. Lett. B **260** (1991) 154–160.

[142] T. Ohlsson, "*Status of non-standard neutrino interactions*," Rept. Prog. Phys. **76** (2013) 044201, arXiv:1209.2710.

[143] Y. Farzan and M. Tortola, "*Neutrino oscillations and Non-Standard Interactions*," Front. in Phys. **6** (2018) 10, arXiv:1710.09360.

[144] J. Heeck, M. Lindner, W. Rodejohann, and S. Vogl, "*Non-Standard Neutrino Interactions and Neutral Gauge Bosons*," SciPost Phys. **6** (2019) no. 3, 038, arXiv:1812.04067.

[145] I. Esteban, M. Gonzalez-Garcia, M. Maltoni, I. Martinez-Soler, and J. Salvado, "*Updated constraints on non-standard interactions from global analysis of oscillation data*," JHEP **08** (2018) 180, arXiv:1805.04530. [Addendum: JHEP 12, 152 (2020)].

[146] M. Lindner, F. S. Queiroz, W. Rodejohann, and X.-J. Xu, "*Neutrino-electron scattering: general constraints on Z' and dark photon models*," JHEP **05** (2018) 098, arXiv:1803.00060.

[147] M. Bauer, P. Foldenauer, and J. Jaeckel, "*Hunting All the Hidden Photons*," JHEP **18** (2020) 094, arXiv:1803.05466.

[148] Y. Farzan and J. Heeck, "*Neutrinophilic nonstandard interactions*," Phys. Rev. **D94** (2016) no. 5, 053010, arXiv:1607.07616.

[149] Y. Farzan, "*A model for large non-standard interactions of neutrinos leading to the LMA-Dark solution*," Phys. Lett. **B748** (2015) 311–315, arXiv:1505.06906.

[150] S. Bilmis, I. Turan, T. Aliev, M. Deniz, L. Singh, and H. Wong, "*Constraints on Dark Photon from Neutrino-Electron Scattering Experiments*," Phys. Rev. D **92** (2015) no. 3, 033009, arXiv:1502.07763.

[151] F. Tikhonin, "*On the effects at colliding mu meson beams*," arXiv:0805.3961.

[152] G. Budker, "*Accelerators and colliding beams*," Conf. Proc. C **690827** (1969) 33–39.

[153] J. P. Delahaye, M. Diemoz, K. Long, B. Mansoulié, N. Pastrone, L. Rivkin, D. Schulte, A. Skrinsky, and A. Wulzer, "*Muon Colliders*," arXiv:1901.06150.

[154] V. Shiltsev and F. Zimmermann, "*Modern and Future Colliders*," arXiv:2003.09084.

[155] M. Chiesa, F. Maltoni, L. Mantani, B. Mele, F. Piccinini, and X. Zhao, "*Measuring the quartic Higgs self-coupling at a multi-TeV muon collider*," JHEP **09** (2020) 098, arXiv:2003.13628.

[156] A. Costantini, F. De Lillo, F. Maltoni, L. Mantani, O. Mattelaer, R. Ruiz, and X. Zhao, "*Vector boson fusion at multi-TeV muon colliders*," JHEP **09** (2020) 080, arXiv:2005.10289.

[157] T. Han, D. Liu, I. Low, and X. Wang, "*Electroweak Couplings of the Higgs Boson at a Multi-TeV Muon Collider*," arXiv:2008.12204.

[158] T. Han, Z. Liu, L.-T. Wang, and X. Wang, "*WIMPs at High Energy Muon Colliders*," arXiv:2009.11287.

[159] P. Bandyopadhyay and A. Costantini, "*Obscure Higgs boson at Colliders*," Phys. Rev. D **103** (2021) no. 1, 015025, arXiv:2010.02597.

[160] J. Gu, L.-T. Wang, and C. Zhang, "*An unambiguous test of positivity at lepton colliders*," arXiv:2011.03055.

[161] R. Capdevilla, D. Curtin, Y. Kahn, and G. Krnjaic, "*Discovering the physics of $(g-2)_\mu$ at future muon colliders*," Phys. Rev. D **103** (2021) no. 7, 075028, arXiv:2006.16277.

[162] D. Buttazzo and P. Paradisi, "*Probing the muon g-2 anomaly at a Muon Collider*," arXiv:2012.02769.

[163] W. Yin and M. Yamaguchi, "*Muon $g-2$ at multi-TeV muon collider*," arXiv:2012.03928.

[164] "*Muon Collider Collaboration Meeting*,". https://indico.cern.ch/event/930508/.

[165] N. Chakrabarty, T. Han, Z. Liu, and B. Mukhopadhyaya, "*Radiative Return for Heavy Higgs Boson at a Muon Collider*," Phys. Rev. D **91** (2015) no. 1, 015008, arXiv:1408.5912.

[166] M. Karliner, M. Low, J. L. Rosner, and L.-T. Wang, "*Radiative return capabilities of a high-energy, high-luminosity e^+e^- collider*," Phys. Rev. D **92** (2015) no. 3, 035010, arXiv:1503.07209.

[167] A. Pukhov, E. Boos, M. Dubinin, V. Edneral, V. Ilyin, D. Kovalenko, A. Kryukov, V. Savrin, S. Shichanin, and A. Semenov, "*CompHEP: A Package for evaluation of Feynman diagrams and integration over multiparticle phase space*," arXiv:hep-ph/9908288.

[168] A. Pukhov, "*CalcHEP 2.3: MSSM, structure functions, event generation, batchs, and generation of matrix elements for other packages*," arXiv:hep-ph/0412191.

[169] A. Belyaev, N. D. Christensen, and A. Pukhov, "*CalcHEP 3.4 for collider physics within and beyond the Standard Model*," Comput. Phys. Commun. **184** (2013) 1729–1769, arXiv:1207.6082.

[170] G.-y. Huang, F. S. Queiroz, and W. Rodejohann, "*Gauged $L_\mu - L_\tau$ at a muon collider*," Phys. Rev. D **103** (2021) no. 9, 095005, arXiv:2101.04956.

[171] **CEPC Study Group**, M. Dong *et al.*, "*CEPC Conceptual Design Report: Volume 2 - Physics \& Detector*," arXiv:1811.10545.

[172] **CLICdp, CLIC**, T. Charles *et al.*, "*The Compact Linear Collider (CLIC) - 2018 Summary Report*," arXiv:1812.06018.

[173] D. Yu, M. Ruan, V. Boudry, H. Videau, J.-C. Brient, Z. Wu, Q. Ouyang, Y. Xu, and X. Chen, "*The measurement of the $H \to \tau\tau$ signal strength in the future e^+e^- Higgs factories*," Eur. Phys. J. C **80** (2020) no. 1, 7.

[174] A. Freitas, "*Weakly coupled neutral gauge bosons at future linear colliders*," Phys. Rev. D **70** (2004) 015008, arXiv:hep-ph/0403288.

[175] **CMS**, S. Chatrchyan *et al.*, "*The CMS Experiment at the CERN LHC*," JINST **3** (2008) S08004.

[176] W. Altmannshofer, S. Gori, M. Pospelov, and I. Yavin, "*Neutrino Trident Production: A Powerful Probe of New Physics with Neutrino Beams*," Phys. Rev. Lett. **113** (2014) 091801, arXiv:1406.2332.

[177] M. Drees, M. Shi, and Z. Zhang, "*Constraints on $U(1)_{L_\mu - L_\tau}$ from LHC Data*," Phys. Lett. B **791** (2019) 130–136, arXiv:1811.12446.

[178] F. del Aguila, M. Chala, J. Santiago, and Y. Yamamoto, "*Collider limits on leptophilic interactions*," JHEP **03** (2015) 059, arXiv:1411.7394.

[179] **LHCb**, R. Aaij *et al.*, "*Test of lepton universality with $B^0 \to K^{*0}\ell^+\ell^-$ decays*," JHEP **08** (2017) 055, arXiv:1705.05802.

[180] **LHCb**, R. Aaij *et al.*, "*Test of lepton universality in beauty-quark decays*," arXiv:2103.11769.

[181] **Belle**, A. Abdesselam *et al.*, "*Test of lepton flavor universality in $B \to K\ell^+\ell^-$ decays*," arXiv:1908.01848.

[182] **Belle**, A. Abdesselam *et al.*, "*Test of lepton flavor universality in $B \to K^*\ell^+\ell^-$ decays at Belle*," arXiv:1904.02440.

[183] C. Bobeth, G. Hiller, and G. Piranishvili, "*Angular distributions of $\bar{B} \to \bar{K}\ell^+\ell^-$ decays*," JHEP **12** (2007) 040, arXiv:0709.4174.

[184] M. Bordone, G. Isidori, and A. Pattori, "*On the Standard Model predictions for R_K and R_{K^*}*," Eur. Phys. J. C **76** (2016) no. 8, 440, arXiv:1605.07633.

[185] B. Capdevila, A. Crivellin, S. Descotes-Genon, J. Matias, and J. Virto, "*Patterns of New Physics in $b \to s\ell^+\ell^-$ transitions in the light of recent data*," JHEP **01** (2018) 093, arXiv:1704.05340.

[186] A. K. Alok, B. Bhattacharya, A. Datta, D. Kumar, J. Kumar, and D. London, "*New Physics in $b \to s\mu^+\mu^-$ after the Measurement of R_{K^*}*," Phys. Rev. D **96** (2017) no. 9, 095009, arXiv:1704.07397.

[187] J. Aebischer, W. Altmannshofer, D. Guadagnoli, M. Reboud, P. Stangl, and D. M. Straub, "*B-decay discrepancies after Moriond 2019*," Eur. Phys. J. C **80** (2020) no. 3, 252, arXiv:1903.10434.

[188] W. Altmannshofer and P. Stangl, "*New Physics in Rare B Decays after Moriond 2021*," arXiv:2103.13370.

[189] R. Gauld, F. Goertz, and U. Haisch, "*An explicit Z'-boson explanation of the $B \to K^*\mu^+\mu^-$ anomaly*," JHEP **01** (2014) 069, arXiv:1310.1082.

[190] A. J. Buras, F. De Fazio, and J. Girrbach, "*331 models facing new $b \to s\mu^+\mu^-$ data*," JHEP **02** (2014) 112, arXiv:1311.6729.

[191] W. Altmannshofer, S. Gori, M. Pospelov, and I. Yavin, "*Quark flavor transitions in $L_\mu - L_\tau$ models*," Phys. Rev. D **89** (2014) 095033, arXiv:1403.1269.

[192] A. Crivellin, G. D'Ambrosio, and J. Heeck, "*Explaining $h \to \mu^\pm\tau^\mp$, $B \to K^*\mu^+\mu^-$ and $B \to K\mu^+\mu^-/B \to Ke^+e^-$ in a two-Higgs-doublet model with gauged $L_\mu - L_\tau$*," Phys. Rev. Lett. **114** (2015) 151801, arXiv:1501.00993.

[193] A. Crivellin, G. D'Ambrosio, and J. Heeck, "*Addressing the LHC flavor anomalies with horizontal gauge symmetries*," Phys. Rev. D **91** (2015) no. 7, 075006, arXiv:1503.03477.

[194] C. Niehoff, P. Stangl, and D. M. Straub, "*Violation of lepton flavour universality in composite Higgs models*," Phys. Lett. B **747** (2015) 182–186, arXiv:1503.03865.

[195] A. Celis, J. Fuentes-Martin, M. Jung, and H. Serodio, "*Family nonuniversal Z' models with protected flavor-changing interactions*," Phys. Rev. D **92** (2015) no. 1, 015007, arXiv:1505.03079.

[196] A. Greljo, G. Isidori, and D. Marzocca, "*On the breaking of Lepton Flavor Universality in B decays*," JHEP **07** (2015) 142, arXiv:1506.01705.

[197] W. Altmannshofer and I. Yavin, "*Predictions for lepton flavor universality violation in rare B decays in models with gauged $L_\mu - L_\tau$*," Phys. Rev. D **92** (2015) no. 7, 075022, arXiv:1508.07009.

[198] A. Falkowski, M. Nardecchia, and R. Ziegler, "*Lepton Flavor Non-Universality in B-meson Decays from a U(2) Flavor Model*," JHEP **11** (2015) 173, arXiv:1509.01249.

[199] L. Calibbi, A. Crivellin, F. Kirk, C. A. Manzari, and L. Vernazza, "*Z' models with less-minimal flavour violation*," Phys. Rev. D **101** (2020) no. 9, 095003, arXiv:1910.00014.

[200] A. Carmona and F. Goertz, "*Lepton Flavor and Nonuniversality from Minimal Composite Higgs Setups*," Phys. Rev. Lett. **116** (2016) no. 25, 251801, arXiv:1510.07658.

[201] F. Goertz, J. F. Kamenik, A. Katz, and M. Nardecchia, "*Indirect Constraints on the Scalar Di-Photon Resonance at the LHC*," JHEP **05** (2016) 187, arXiv:1512.08500.

[202] C.-W. Chiang, X.-G. He, and G. Valencia, "*Z' model for $b \to s\ell\bar{\ell}$ flavor anomalies*," Phys. Rev. D **93** (2016) no. 7, 074003, arXiv:1601.07328.

[203] D. Bečirević, O. Sumensari, and R. Zukanovich Funchal, "*Lepton flavor violation in exclusive $b \to s$ decays*," Eur. Phys. J. C **76** (2016) no. 3, 134, arXiv:1602.00881.

[204] S. M. Boucenna, A. Celis, J. Fuentes-Martin, A. Vicente, and J. Virto, "*Non-abelian gauge extensions for B-decay anomalies*," Phys. Lett. B **760** (2016) 214–219, arXiv:1604.03088.

[205] S. M. Boucenna, A. Celis, J. Fuentes-Martin, A. Vicente, and J. Virto, "*Phenomenology of an $SU(2) \times SU(2) \times U(1)$ model with lepton-flavour non-universality*," JHEP **12** (2016) 059, arXiv:1608.01349.

[206] E. Megias, G. Panico, O. Pujolas, and M. Quiros, "*A Natural origin for the LHCb anomalies*," JHEP **09** (2016) 118, arXiv:1608.02362.

[207] I. Garcia Garcia, "*LHCb anomalies from a natural perspective*," JHEP **03** (2017) 040, arXiv:1611.03507.

[208] P. Ko, Y. Omura, Y. Shigekami, and C. Yu, "*LHCb anomaly and B physics in flavored Z' models with flavored Higgs doublets*," Phys. Rev. D **95** (2017) no. 11, 115040, arXiv:1702.08666.

[209] J. Kawamura, S. Raby, and A. Trautner, "*Complete vectorlike fourth family with U(1)' : A global analysis*," Phys. Rev. D **101** (2020) no. 3, 035026, arXiv:1911.11075.

[210] E. Megias, M. Quiros, and L. Salas, "*Lepton-flavor universality violation in R_K and $R_{D^{(*)}}$ from warped space*," JHEP **07** (2017) 102, arXiv:1703.06019.

[211] B. C. Allanach, "*$U(1)_{B_3-L_2}$ explanation of the neutral current $B-$anomalies*," Eur. Phys. J. C **81** (2021) no. 1, 56, arXiv:2009.02197.

[212] L. Di Luzio, M. Kirk, A. Lenz, and T. Rauh, "*ΔM_s theory precision confronts flavour anomalies*," JHEP **12** (2019) 009, arXiv:1909.11087.

[213] L. Di Luzio, M. Kirk, and A. Lenz, "*Updated B_s-mixing constraints on new physics models for $b \to s\ell^+\ell^-$ anomalies*," Phys. Rev. D **97** (2018) no. 9, 095035, arXiv:1712.06572.

[214] G.-Y. Huang, S. Jana, F. S. Queiroz, and W. Rodejohann, "*Probing the $R_{K^{(*)}}$ Anomaly at a Muon Collider*," arXiv:2103.01617.

[215] W. Liu and K.-P. Xie, "*Probing electroweak phase transition with multi-TeV muon colliders and gravitational waves*," arXiv:2101.10469.

[216] **ATLAS**, M. Aaboud *et al.*, "*Measurements of b-jet tagging efficiency with the ATLAS detector using $t\bar{t}$ events at $\sqrt{s} = 13$ TeV*," JHEP **08** (2018) 089, arXiv:1805.01845.

[217] B. Auerbach, S. Chekanov, J. Love, J. Proudfoot, and A. V. Kotwal, "*Sensitivity to new high-mass states decaying to $t\bar{t}$ at a 100 TeV collider*," Phys. Rev. D **91** (2015) no. 3, 034014, arXiv:1412.5951.

[218] C. Helsens, D. Jamin, M. L. Mangano, T. G. Rizzo, and M. Selvaggi, "*Heavy resonances at energy-frontier hadron colliders*," Eur. Phys. J. C **79** (2019) 569, arXiv:1902.11217.

[219] R. Mertig, M. Bohm, and A. Denner, "*FEYN CALC: Computer algebraic calculation of Feynman amplitudes*," Comput. Phys. Commun. **64** (1991) 345–359.

[220] V. Shtabovenko, R. Mertig, and F. Orellana, "*New Developments in FeynCalc 9.0*," Comput. Phys. Commun. **207** (2016) 432–444, arXiv:1601.01167.

[221] V. Shtabovenko, R. Mertig, and F. Orellana, "*FeynCalc 9.3: New features and improvements*," Comput. Phys. Commun. **256** (2020) 107478, arXiv:2001.04407.

[222] T. Hahn, "*Generating Feynman diagrams and amplitudes with FeynArts 3*," Comput. Phys. Commun. **140** (2001) 418–431, arXiv:hep-ph/0012260.

[223] B. Allanach, F. S. Queiroz, A. Strumia, and S. Sun, "*Z' models for the LHCb and $g-2$ muon anomalies*," Phys. Rev. D **93** (2016) no. 5, 055045, arXiv:1511.07447. [Erratum: Phys.Rev.D 95, 119902 (2017)].

[224] P. D. Bolton, F. F. Deppisch, L. Gráf, and F. Šimkovic, "*Two-Neutrino Double Beta Decay with Sterile Neutrinos*," Phys. Rev. D **103** (2021) no. 5, 055019, arXiv:2011.13387.

[225] V. Brdar, W. Rodejohann, and X.-J. Xu, "*Producing a new Fermion in Coherent Elastic Neutrino-Nucleus Scattering: from Neutrino Mass to Dark Matter*," JHEP **12** (2018) 024, arXiv:1810.03626.

[226] E. Bertuzzo, C. J. Caniu Barros, and G. Grilli di Cortona, "*MeV Dark Matter: Model Independent Bounds*," JHEP **09** (2017) 116, arXiv:1707.00725.

[227] Y. Hochberg, Y. Kahn, M. Lisanti, K. M. Zurek, A. G. Grushin, R. Ilan, S. M. Griffin, Z.-F. Liu, S. F. Weber, and J. B. Neaton, "*Detection of sub-MeV Dark Matter with Three-Dimensional Dirac Materials*," Phys. Rev. **D97** (2018) no. 1, 015004, arXiv:1708.08929.

[228] M. J. Dolan, F. Kahlhoefer, and C. McCabe, "*Directly detecting sub-GeV dark matter with electrons from nuclear scattering*," Phys. Rev. Lett. **121** (2018) no. 10, 101801, arXiv:1711.09906.

[229] M. Hufnagel, K. Schmidt-Hoberg, and S. Wild, "*BBN constraints on MeV-scale dark sectors. Part I. Sterile decays*," JCAP **1802** (2018) 044, arXiv:1712.03972.

[230] M. Dutra, M. Lindner, S. Profumo, F. S. Queiroz, W. Rodejohann, and C. Siqueira, "*MeV Dark Matter Complementarity and the Dark Photon Portal*," JCAP **1803** (2018) 037, arXiv:1801.05447.

[231] A. Berlin, D. Hooper, G. Krnjaic, and S. D. McDermott, "*Severely Constraining Dark Matter Interpretations of the 21-cm Anomaly*," Phys. Rev. Lett. **121** (2018) no. 1, 011102, arXiv:1803.02804.

[232] S. Dodelson and L. M. Widrow, "*Sterile-neutrinos as dark matter*," Phys. Rev. Lett. **72** (1994) 17–20, arXiv:hep-ph/9303287.

[233] L. Wolfenstein, "*Neutrino Oscillations in Matter*," Phys.Rev. **D17** (1978) 2369–2374.

[234] S. P. Mikheyev and A. Y. Smirnov, "*Resonance Amplification of Oscillations in Matter and Spectroscopy of Solar Neutrinos*," Sov. J. Nucl. Phys. **42** (1985) 913–917. [Yad. Fiz.42,1441(1985); ,305(1986)].

[235] S. P. Mikheev and A. Yu. Smirnov, "*Resonant amplification of neutrino oscillations in matter and solar neutrino spectroscopy*," Nuovo Cim. **C9** (1986) 17–26.

[236] X.-D. Shi and G. M. Fuller, "*A New dark matter candidate: Nonthermal sterile neutrinos*," Phys. Rev. Lett. **82** (1999) 2832–2835, arXiv:astro-ph/9810076.

[237] E. Bulbul, M. Markevitch, A. Foster, R. K. Smith, M. Loewenstein, and S. W. Randall, "*Detection of An Unidentified Emission Line in the Stacked X-ray spectrum of Galaxy Clusters*," Astrophys. J. **789** (2014) 13, arXiv:1402.2301.

[238] A. Boyarsky, O. Ruchayskiy, D. Iakubovskyi, and J. Franse, "*Unidentified Line in X-Ray Spectra of the Andromeda Galaxy and Perseus Galaxy Cluster*," Phys. Rev. Lett. **113** (2014) 251301, arXiv:1402.4119.

[239] N. Cappelluti, E. Bulbul, A. Foster, P. Natarajan, M. C. Urry, M. W. Bautz, F. Civano, E. Miller, and R. K. Smith, "*Searching for the 3.5 keV Line in the Deep Fields with Chandra: the 10 Ms observations*," Astrophys. J. **854** (2018) no. 2, 179, arXiv:1701.07932.

[240] T. E. Jeltema and S. Profumo, "*Discovery of a 3.5 keV line in the Galactic Centre and a critical look at the origin of the line across astronomical targets*," Mon. Not. Roy. Astron. Soc. **450** (2015) no. 2, 2143–2152, arXiv:1408.1699.

[241] E. Carlson, T. Jeltema, and S. Profumo, "*Where do the 3.5 keV photons come from? A morphological study of the Galactic Center and of Perseus*," JCAP **02** (2015) 009, arXiv:1411.1758.

[242] C. Shah, S. Dobrodey, S. Bernitt, R. Steinbrgge, J. R. C. Lpez-Urrutia, L. Gu, and J. Kaastra, "*Laboratory measurements compellingly support charge-exchange mechanism for the 'dark matter' ∼3.5 keV X-ray line*," Astrophys. J. **833** (2016) no. 1, 52, arXiv:1608.04751.

[243] A. Kusenko, "*Sterile neutrinos: The Dark side of the light fermions*," Phys. Rept. **481** (2009) 1–28, arXiv:0906.2968.

[244] T. Brunst *et al.*, "*Measurements with a TRISTAN prototype detector system at the "Troitsk nu-mass" experiment in integral and differential mode*," JINST **14** (2019) no. 11, P11013, arXiv:1909.02898.

[245] S. Horiuchi, P. J. Humphrey, J. Onorbe, K. N. Abazajian, M. Kaplinghat, and S. Garrison-Kimmel, "*Sterile neutrino dark matter bounds from galaxies of the Local Group*," Phys. Rev. **D89** (2014) no. 2, 025017, arXiv:1311.0282.

[246] K. Perez, K. C. Y. Ng, J. F. Beacom, C. Hersh, S. Horiuchi, and R. Krivonos, "*Almost closing the MSM sterile neutrino dark matter window with NuSTAR*," Phys. Rev. **D95** (2017) no. 12, 123002, arXiv:1609.00667.

[247] K. C. Y. Ng, B. M. Roach, K. Perez, J. F. Beacom, S. Horiuchi, R. Krivonos, and D. R. Wik, "*New Constraints on Sterile Neutrino Dark Matter from NuSTAR M31 Observations*," Phys. Rev. **D99** (2019) 083005, arXiv:1901.01262.

[248] S. Ando and A. Kusenko, "*Interactions of keV sterile neutrinos with matter*," Phys. Rev. **D81** (2010) 113006, arXiv:1001.5273.

[249] M. D. Campos and W. Rodejohann, "*Testing keV sterile neutrino dark matter in future direct detection experiments*," Phys. Rev. **D94** (2016) no. 9, 095010, arXiv:1605.02918.

[250] P. C. Divari and J. D. Vergados, "*Heavy sterile neutrino in dark matter searches*," Adv. High Energy Phys. **2018** (2018) 1479313, arXiv:1707.02550.

[251] Y. F. Li and Z.-z. Xing, "*Possible Capture of keV Sterile Neutrino Dark Matter on Radioactive β-decaying Nuclei*," Phys. Lett. **B695** (2011) 205–210, arXiv:1009.5870.

[252] J. Barry, J. Heeck, and W. Rodejohann, "*Sterile neutrinos and right-handed currents in KATRIN*," JHEP **07** (2014) 081, arXiv:1404.5955.

[253] A. Schneider, "*Astrophysical constraints on resonantly produced sterile neutrino dark matter*," JCAP **1604** (2016) no. 04, 059, arXiv:1601.07553.

[254] A. Merle, A. Schneider, and M. Totzauer, "*Dodelson-Widrow Production of Sterile Neutrino Dark Matter with Non-Trivial Initial Abundance*," JCAP **1604** (2016) no. 04, 003, arXiv:1512.05369.

[255] J. F. Cherry and S. Horiuchi, "*Closing in on Resonantly Produced Sterile Neutrino Dark Matter*," Phys. Rev. **D95** (2017) no. 8, 083015, arXiv:1701.07874.

[256] C. Benso, V. Brdar, M. Lindner, and W. Rodejohann, "*Prospects for Finding Sterile Neutrino Dark Matter at KATRIN*," Phys. Rev. D **100** (2019) no. 11, 115035, arXiv:1911.00328.

[257] K. Abazajian, G. M. Fuller, and M. Patel, "*Sterile neutrino hot, warm, and cold dark matter*," Phys. Rev. **D64** (2001) 023501, arXiv:astro-ph/0101524.

[258] D. Nötzold and G. Raffelt, "*Neutrino Dispersion at Finite Temperature and Density*," Nucl. Phys. **B307** (1988) 924–936.

[259] T. Venumadhav, F.-Y. Cyr-Racine, K. N. Abazajian, and C. M. Hirata, "*Sterile neutrino dark matter: Weak interactions in the strong coupling epoch*," Phys. Rev. **D94** (2016) no. 4, 043515, arXiv:1507.06655.

[260] T. Asaka, M. Laine, and M. Shaposhnikov, "*Lightest sterile neutrino abundance within the nuMSM*," JHEP **01** (2007) 091, arXiv:hep-ph/0612182. [Erratum: JHEP02,028(2015)].

[261] C. E. Yaguna, "*Sterile neutrino production in models with low reheating temperatures*," JHEP **06** (2007) 002, arXiv:0706.0178.

[262] G. Gelmini, S. Palomares-Ruiz, and S. Pascoli, "*Low reheating temperature and the visible sterile neutrino*," Phys. Rev. Lett. **93** (2004) 081302, arXiv:astro-ph/0403323.

[263] P. F. de Salas, M. Lattanzi, G. Mangano, G. Miele, S. Pastor, and O. Pisanti, "*Bounds on very low reheating scenarios after Planck*," Phys. Rev. **D92** (2015) no. 12, 123534, arXiv:1511.00672.

[264] T. Hasegawa, N. Hiroshima, K. Kohri, R. S. L. Hansen, T. Tram, and S. Hannestad, "*MeV-scale reheating temperature and thermalization of oscillating neutrinos by radiative and hadronic decays of massive particles*," JCAP **12** (2019) 012, arXiv:1908.10189.

[265] F. Bezrukov, A. Chudaykin, and D. Gorbunov, "*Hiding an elephant: heavy sterile neutrino with large mixing angle does not contradict cosmology*," JCAP **1706** (2017) no. 06, 051, arXiv:1705.02184.

[266] F. Bezrukov, H. Hettmansperger, and M. Lindner, "*keV sterile neutrino Dark Matter in gauge extensions of the Standard Model*," Phys. Rev. **D81** (2010) 085032, arXiv:0912.4415.

[267] **KATRIN**, S. Mertens *et al.*, "*A novel detector system for KATRIN to search for keV-scale sterile neutrinos*," J. Phys. G **46** (2019) no. 6, 065203, arXiv:1810.06711.

[268] K. Blaum *et al.*, "*The Electron Capture ^{163}Ho Experiment ECHo*," in *The Future of Neutrino Mass Measurements: Terrestrial, Astrophysical, and Cosmological Measurements in the Next Decade (NUMASS2013) Milano, Italy, February 4-7, 2013*. 2013. arXiv:1306.2655.

[269] P. F. Smith, "*Proposed experiments to detect keV range sterile neutrinos using energy-momentum reconstruction of beta decay or K-capture events*," New J. Phys. **21** (2019) no. 5, 053022, arXiv:1607.06876.

[270] I. Bischer, T. Plehn, and W. Rodejohann, "*Dark Matter EFT, the Third – Neutrino WIMPs*," SciPost Phys. **10** (2021) no. 2, 039, arXiv:2008.04718.

[271] I. Doršner, S. Fajfer, A. Greljo, J. Kamenik, and N. Košnik, "*Physics of leptoquarks in precision experiments and at particle colliders*," Phys. Rept. **641** (2016) 1–68, arXiv:1603.04993.

[272] M. Bauer and M. Neubert, "*Minimal Leptoquark Explanation for the $R_{D^{(*)}}$, R_K , and $(g-2)_g$ Anomalies*," Phys. Rev. Lett. **116** (2016) no. 14, 141802, arXiv:1511.01900.

[273] D. Buttazzo, A. Greljo, G. Isidori, and D. Marzocca, "*B-physics anomalies: a guide to combined explanations*," JHEP **11** (2017) 044, arXiv:1706.07808.

[274] T. Plehn, *Production of supersymmetric particles at high-energy colliders*. PhD thesis, Hamburg U., 1998. arXiv:hep-ph/9809319.

[275] M. Garny, J. Heisig, M. Hufnagel, and B. Llf, "*Top-philic dark matter within and beyond the WIMP paradigm*," Phys. Rev. **D97** (2018) no. 7, 075002, arXiv:1802.00814.

[276] A. Alloul, N. D. Christensen, C. Degrande, C. Duhr, and B. Fuks, "*FeynRules 2.0 - A complete toolbox for tree-level phenomenology*," Comput. Phys. Commun. **185** (2014) 2250–2300, arXiv:1310.1921.

[277] G. Belanger, F. Boudjema, A. Pukhov, and A. Semenov, "*micrOMEGAs_3: A program for calculating dark matter observables*," Comput. Phys. Commun. **185** (2014) 960–985, arXiv:1305.0237.

[278] G. Belanger, F. Boudjema, A. Pukhov, and A. Semenov, "*micrOMEGAs: A Tool for dark matter studies*," Nuovo Cim. C **033N2** (2010) 111–116, arXiv:1005.4133.

[279] G. Belanger, F. Boudjema, A. Pukhov, and A. Semenov, "*Dark matter direct detection rate in a generic model with micrOMEGAs 2.2*," Comput. Phys. Commun. **180** (2009) 747–767, arXiv:0803.2360.

[280] G. Belanger, F. Boudjema, A. Pukhov, and A. Semenov, "*MicrOMEGAs 2.0: A Program to calculate the relic density of dark matter in a generic model*," Comput. Phys. Commun. **176** (2007) 367–382, arXiv:hep-ph/0607059.

[281] **CMS**, A. M. Sirunyan *et al.*, "*Search for direct top squark pair production in events with one lepton, jets, and missing transverse momentum at 13 TeV with the CMS experiment*," JHEP **05** (2020) 032, arXiv:1912.08887.

[282] **ATLAS**, G. Aad *et al.*, "*Search for a scalar partner of the top quark in the all-hadronic $t\bar{t}$ plus missing transverse momentum final state at $\sqrt{s} = 13$ TeV with the ATLAS detector*," Eur. Phys. J. C **80** (2020) no. 8, 737, arXiv:2004.14060.

[283] I. Bischer and W. Rodejohann, "*General neutrino interactions from an effective field theory perspective*," Nucl. Phys. B **947** (2019) 114746, arXiv:1905.08699.

[284] **Fermi-LAT, DES**, A. Albert *et al.*, "*Searching for Dark Matter Annihilation in Recently Discovered Milky Way Satellites with Fermi-LAT*," Astrophys. J. **834** (2017) no. 2, 110, arXiv:1611.03184.

[285] M. Cirelli, G. Corcella, A. Hektor, G. Hutsi, M. Kadastik, P. Panci, M. Raidal, F. Sala, and A. Strumia, "*PPPC 4 DM ID: A Poor Particle Physicist Cookbook for Dark Matter Indirect Detection*," JCAP **03** (2011) 051, arXiv:1012.4515. [Erratum: JCAP 10, E01 (2012)].

[286] S. Ando, A. Geringer-Sameth, N. Hiroshima, S. Hoof, R. Trotta, and M. G. Walker, "*Structure formation models weaken limits on WIMP dark matter from dwarf spheroidal galaxies*," Phys. Rev. D **102** (2020) no. 6, 061302, arXiv:2002.11956.

[287] M. Garny, A. Ibarra, M. Pato, and S. Vogl, "*Internal bremsstrahlung signatures in light of direct dark matter searches*," JCAP **12** (2013) 046, arXiv:1306.6342.

[288] **XENON**, E. Aprile *et al.*, "*Dark Matter Search Results from a One Ton-Year Exposure of XENON1T*," Phys. Rev. Lett. **121** (2018) no. 11, 111302, arXiv:1805.12562.

[289] **CMS**, A. M. Sirunyan *et al.*, "*Searches for physics beyond the standard model with the M_{T2} variable in hadronic final states with and without disappearing tracks in proton-proton collisions at $\sqrt{s} = 13$ TeV*," Eur. Phys. J. C **80** (2020) no. 1, 3, arXiv:1909.03460.

Appendices

Appendix A

Main publications summarized in this work

1. G.-Y. Huang, S. Jana, F.S. Queiroz, and W. Rodejohann,
   Probing the $R_{K^{(*)}}$ Anomaly at a Muon Collider,
   arXiv:2103.01617 [hep-ph]

2. G.-Y. Huang, W. Rodejohann,
   Solving the Hubble tension without spoiling Big Bang Nucleosynthesis,
   Phys. Rev. D **103**, 123007 (2021) [arXiv:2102.04280 [hep-ph]]

3. G.-Y. Huang, F.S. Queiroz, and W. Rodejohann,
   Gauged $L_\mu - L_\tau$ at a muon collider,
   Phys. Rev. D **103**, 095005 (2021) [arXiv:2101.04956 [hep-ph]]

4. X. Luo, W. Rodejohann and X.-J. Xu,
   Dirac Neutrinos and $N_{\rm eff}$ II: the freeze-in case,
   JCAP **2103**, 082 (2021) [arXiv:2011.13059 [hep-ph]]

5. I. Bischer, T. Plehn and W. Rodejohann,
   Dark Matter EFT, the Third – Neutrino WIMPs,
   SciPost Phys. **10**, 039 (2021) [arXiv:2008.04718 [hep-ph]]

6. F.F. Deppisch, L. Graf, W. Rodejohann and X.-J. Xu,
   Neutrino Self-Interactions and Double Beta Decay,
   Phys. Rev. D **102**, 051701(R) (2020) [arXiv:2004.11919 [hep-ph]]

7. C. Benso, V. Brdar, M. Lindner and W. Rodejohann,
   Prospects for Finding Sterile Neutrino Dark Matter at KATRIN,
   Phys. Rev. D **100**, 115035 (2019) [arXiv:1911.00328 [hep-ph]]

8. J. Heeck, M. Lindner, W. Rodejohann and S. Vogl,
   Non-Standard Neutrino Interactions and Neutral Gauge Bosons,
   SciPost Phys. **6**, 038 (2019) [arXiv:1812.04067 [hep-ph]]

9. V. Brdar, W. Rodejohann and X.-J. Xu,
Producing a new Fermion in Coherent Elastic Neutrino-Nucleus Scattering: from Neutrino Mass to Dark Matter,
JHEP **1812**, 024 (2018) [arXiv:1810.03626 [hep-ph]]

10. Y. Farzan, M. Lindner, W. Rodejohann and X.-J. Xu,
Probing neutrino coupling to a light scalar with coherent neutrino scattering,
JHEP **1805**, 066 (2018) [arXiv:1802.05171 [hep-ph]]

Acknowledgments

First of all I would like to thank my long-time boss Manfred Lindner for trusting in me, and hiring me as a young clueless PostDoc in 2004. From that point on he continuously gave support and advice, be it in physics, administration, politics and many other things. I am also grateful to my Doktorvater Emmanuel Paschos for offering me a Phd position, and introducing me to the international and fascinating world of particle physics.

Of course, I never would be here without the continuous flow of brilliant students and PostDocs who luckily decided to work with me. My many coauthors from around the world gave me input and inspiration not only for the physics we did, but in general.

Finally, thank you Nina, for trying to understand why I work too much in this weird job, sticking with me, and raising two wonderful kids with me.